UNIVERSITI TEKNOLOGI MARA

FINITE ELEMENT SIMULATION MODEL FOR TENSILE PROPERTIES OF HYBRID REINFORCEMENT OF BANANA FIBER AND GLASS FIBER COMPOSITE

MUSTAFA BIN NORDIN

MSC

July 2026

UNIVERSITI TEKNOLOGI MARA

FINITE ELEMENT SIMULATION MODEL FOR TENSILE PROPERTIES OF HYBRID REINFORCEMENT OF BANANA FIBER AND GLASS FIBER COMPOSITE

MUSTAFA BIN NORDIN

Thesis submitted in fulfilment
of the requirements for the degree of
Master of Science
(Mechanical Engineering)

Faculty of Mechanical Engineering

July 2026

CONFIRMATION BY PANEL OF EXAMINERS

I certify that a Panel of Examiners has met on 15th February 2025 to conduct the final examination of Mustafa Bin Nordin on his Master of Science thesis entitled Finite Element Simulation Model for Tensile Properties of Hybrid Reinforcement of Banana Fiber and Glass Fiber Composites in accordance with Universiti Teknologi MARA Act 1976 (Akta 173). The Panel of Examiners recommends that the student be awarded the relevant degree. The Panel of Examiners was as follows:

Abdul Rahman Hemdi, PhD
Associate Professor
Faculty of Mechanical
Engineering
Universiti Teknologi MARA
(Chairman)

Ahmad Faiz Zubair, PhD
Senior Lecturer,
Faculty of Mechanical Engineering,
Universiti Teknologi MARA
(Internal Examiner)

Muhammad Najib Abdul Hamid, PhD
Senior Lecturer
Universiti Kuala Lumpur
(Enternal Examiner)

PROFESSOR DR HJH ZURAEDA IBRAHIM
Dean
Institute of Postgraduates Studies
Universiti Teknologi MARA
Date: 17 July 2026

AUTHOR'S DECLARATION

I declare that the work in this thesis was carried out in accordance with the regulations of Universiti Teknologi MARA. It is original and is the results of my own work, unless otherwise indicated or acknowledged as referenced work. This thesis has not been submitted to any other academic institution or non-academic institution for any degree or qualification.

I, hereby, acknowledge that I have been supplied with the Academic Rules and Regulations for Postgraduate, Universiti Teknologi MARA, regulating the conduct of my study and research.

Name of Student	:	Mustafa Bin Nordin
Student I.D. No	:	2022108177
Programme	:	Master of Science (Mechanical Engineering)
Faculty	:	Mechanical Engineering
Thesis Title	:	Finite Element Simulation Model for Tensile Properties of Hybrid Reinforcement of Banana Fiber and Glass Fiber Composites
Signature of Student	:	
Date	:	July 2026

ABSTRACT

Eco-friendly hybrid composites are increasingly important for achieving high mechanical performance. While fiberglass/epoxy composites are widely used, banana fiber hybrids remain underutilized despite their potential in aerospace and industrial applications. Previous studies show that simulation research on banana fiber reinforcement, alone or hybridized with fiberglass, remains limited. Therefore, this study aimed to fill this gap by simulating banana fiber reinforced with fiberglass composites. The first objective was to validate the tensile properties obtained from the experiment results with the simulation results. Second objective was to obtain the optimal tensile properties of glass fiber and banana fiber hybrid composites by varying the laminate configuration and fiber volume fraction across different configurations. To achieve this, both experimental and simulation approaches were employed to evaluate the tensile behavior of the composites. Six laminates were fabricated using the hand lay-up method: L1 (glass fiber), L2 (banana fiber), and L3–L5 (glass–banana fiber hybrid laminates). Tensile testing was conducted according to ASTM D638 at a constant crosshead speed of 1 mm/ min, while simulations were performed in Abaqus following a seven-step procedure, starting from model design until result extraction. The results compared between the experimental and simulation results was essential to validate the accuracy of the simulation model. An average percentage error of less than 9% was used as a guideline when comparing the Ultimate Load (kN) and Ultimate Stress (MPa). The values that the fiber and matrix volume fractions in each laminate configuration significantly influenced the tensile properties of the composites. Laminates with higher glass fiber content produced a higher fiber volume fraction, which contributed to improved mechanical performance. Laminate L1 exhibited the highest fiber volume fraction due to the presence of only glass fiber layers, resulting in superior tensile strength compared with the other configurations. In contrast, Laminate L2 showed the lowest fiber volume fraction because it consisted entirely of banana fiber, which has a lower density. This condition reduce fiber content and increased the matrix content and consequently reduced the tensile strength. Therefore, both objectives were successfully achieved by obtaining the validating and the agreement between the experimental and simulation results optimal tensile properties.

ACKNOWLEDGMENT

In the name of Allah, the Most Gracious and Most Merciful. Alhamdulillah, all praise is due to Allah SWT for blessing me with health, strength, and the opportunity to complete this master research project. By His grace and permission, I was able to accomplish this significant milestone.

I would like to extend my heartfelt gratitude to everyone who contributed to the successful completion of this project.First and foremost, my deepest appreciation goes to Ts. Dr. Mohd. Rozaiman Bin Aziz for his invaluable guidance, unwavering support, and encouragement throughout this study. His expertise and insights have played a vital role in shaping this work.

I am sincerely thankful to Universiti Teknologi MARA Pulau Pinang (UiTMPP) for providing the necessary facilities and resources that made this research possible.

Lastly, I would like to acknowledge the unwavering support of my family especially my mother, and my wife, Nur Amira Syahira Binti Adnan, whose understanding, encouragement, and belief in me have been a source of strength throughout this journey.

Thank you.

TABLE CONTENTS

	Page
CONFIRMATION BY PANEL OF EXAMINERS	**ii**
AUTHOR'S DECLARATION	**iii**
ABSTRACT	**iv**
ACKNOWLEDGMENT	**v**
TABLE CONTENTS	**vi**
LIST OF TABLES	**ix**
LIST OF FIGURES	**x**
LIST OF SYMBOL	**xiii**
LIST OF ABBREVIATIONS	**xiv**
LIST OF NOMENCLATURES	**xv**
CHAPTER 1 INTRODUCTION	**1**
1.1 Background of Study	1
1.2 Problem Statement	2
1.3 Research Objective	3
1.4 Scope of Study	3
1.5 Significance of the Study	4
CHAPTER 2 LITERATURE REVIEW	**5**
2.1 Introduction	5
2.2 Composite Applications	5
2.3 Application of Banana Fiber	6
2.4 Type of Material composite	7
2.4.1 Glass Fiber	9
2.4.2 Banana Fiber	11
2.4.3 Epoxy Resin	14
2.5 Experiment Approach of Glass Fiber and Banana Fiber	15
2.5.1 Composite Volume Fraction	16
2.5.2 Preparation for the Tensile Test Specimen	18

2.5.3 Configuration of Composite Laminate 21
2.5.4 Tensile Testing ASTM D638 Standard 23
2.6 Finite Element Analysis of Composite 24
2.6.1 Elastic Region for Composite 25
2.6.2 Damage Model of Composite 26
2.6.3 Material Properties for Simulation 26
2.6.4 Tensile Behavior Modeling and Simulation for Composite Material 28
2.7 Range of Ultimate Load and Ultimate Stress of Banana Fiber and Glass Fiber 30
2.8 Research Gap of Study 33

CHAPTER 3 RESEARCH METHODOLOGY 34
3.1 Introduction 34
3.2 Experimental Procedures 37
3.2.1 Design of Lamination Configuration 37
3.2.1 Fabrication of Specimens 38
3.2.4 Tensile Testing Based on ASTM D638 Standard 43
3.2.5 Composite Fibrous Structures 44
3.3 Finite Element Simulation 45
3.3.1 Create the Part of Specimen 45
3.3.2 Composite Material Property Simulation 47
3.3.3 Extraction Material Properties Simulation 48
3.3.4 Import Material Property of Banana Fiber and Glass Fiber 49
3.3.5 Set Layup Lamination 53
3.3.6 General Static Step 54
3.3.7 Meshing Model Structure 54
3.3.8 Setting Boundary Condition (BCs) 56

CHAPTER 4 RESULT AND DISCUSSION 57
4.1 Introduction 57
4.2 Finite Element Model Validation 57
4.3 Volume Fraction Analysis 61
4.4 Strength Analysis of Different Configurations 64
4.4.1 Laminate 1 (L1) 64
4.4.2 Laminate 2 (L2) 66

4.4.3 Laminate 3 (L3) 68
4.4.4 Laminate 4 (L4) 69
4.4.5 Laminate 5 (L5) 71
4.4.6 Laminate 6 (L6) 73
4.5 Comparison of the Composition Arrangement 75
4.6 Finding summary 80

CHAPTER 5 CONCLUSION **81**
5.1 Introduction 81
5.2 Conclusion 81
5.3 Recommendation 83

REFERENCE **85**
APPENDICES **90**
AUTHOR'S PROFILE **110**

LIST OF TABLES

Table	Title	Page
Table 2.1	Property Of Fibers (Kotla Rachana, 2020)	11
Table 2.2	Property Of Banana Fiber (Narayanan Et Al., 2019)	14
Table 2.3	Property Of Epoxy Resin (Kotla Rachana, 2020)	15
Table 2.4	Fiber Volume Fraction (Kureemun Et Al., 2018)	17
Table 2.5	Composite Specimen Layering Arrangements and Specimen ID (Santhanam Et Al., 2020)	21
Table 2.6	Lamina Engineering Constants of Pultruded GFRP Laminate (Xin Et Al., 2017)	27
Table 2.7	Lamina Ultimate Capacity of Pultruded GFRP Laminate (Xin Et Al., 2017)	27
Table 2.8	Lamina Orthotropic Properties for Each Unit Cell (Monzón Et Al., 2019)	28
Table 2.9	Range Of Tensile Property for Glass Fiber (Prem Chand Et Al., 2021)(Pillai Et Al., 2009)(Stanciu Et Al., 2021)	31
Table 2.10	Range Of Tensile Property For Banana Fiber (Monzón Et Al., 2019) (Sanjay Et Al., 2016)(Sampath Et Al., 2021)	31
Table 2.11	Tensile Test Result (Prem Chand Et Al., 2021)	32
Table 3.1	Design Of Composition Glass Fiber And Banana Fiber	37
Table 3.2	Property Of Density and Weight of Fiber and Matrix (Kotla Rachana, 2020), (Prabhu Et Al., 2021)	45
Table 3.3	Unit For Abaqus (Started & Edition, N.D.)	46
Table 3.4	Lamina Property (Monzón Et Al., 2019) (Morton, 2010)	48
Table 3.5	Hashin Property (Koloor Et Al., 2020)	49
Table 4.1	Volume Of Fraction Fiber and Matrix	63
Table 4.2	Result Experiment Versus Simulation	76
Table 7.1	Summary Of Density of Fiber	93
Table 7.2	Summary Of Density of Matrix	97
Table 7.3	Summary Of Weight of Fiber	101
Table 7.4	Summary Of Weight of Matrix	105

LIST OF FIGURES

Table	Title	Page
Figure 2.1	Composite Material in Jet (Quilter, 2019)	6
Figure 2.2	Classified Of Composition (William D. Callister, 2003)	8
Figure 2.3	Type Of Orientation Fiber Reinforce Composition. A) Continuous And Aligned, (B) Discontinuous and Aligned, And (C) Discontinuous and Randomly Oriented Fiber Reinforced Composites (William D. Callister, 2003)	8
Figure 2.4	Woven Roving (Kotla Rachana, 2020)	10
Figure 2.5	Extraction Of Banana Fiber (A) Banana Stem, (B) Manual Rolling of The Stem, (B) Rolled Stem, (D) Stem In Rotten Water, (E) Drying of Extracted Fiber, And (F) Extracted Fiber (Jubair Et Al., 2021)	12
Figure 2.6	The Layout of The Process (Al Rashid Et Al., 2020)	13
Figure 2.7	Methodology Flow Chart (Karthick Et Al., 2022)	16
Figure 2.8	Schematics Indicating the Stacking Sequences of Hybrid Flax-Carbon Epoxy Laminates (Karthick Et Al., 2022)	18
Figure 2.9	Hand Layup Process (Rajak Et Al., 2019)	19
Figure 2.10	Fabrication Of Composite (Reddy Et Al., 2020)	20
Figure 2.11	Sample Specimen Test in Meter (Sanjay Et Al., 2016)	21
Figure 2.12	Configurations Of Composite (LN: Flax; P: Banana Textile; PL: Plain; BK: Basket; TW: Twill) (Reddy Et Al., 2020)	22
Figure 2.13	Detailed Composition of The Composites (Al Rashid Et Al., 2020)	23
Figure 2.14	Computerized Universal Testing Machine (Sanjay Et Al., 2016)	24
Figure 2.15	Relation Between Lamina and Damage Initiation (Sanjay Et Al., 2016)	25
Figure 2.16	Element Stresses (Mpa): Direction X (Monzón Et Al., 2019)	29
Figure 2.17	Element Strains: Direction X (Monzón Et Al., 2019)	29
Figure 2.18	Typical Tensile Stress-Strain Curve (ASTM, 2014)	30

Figure 2.19	Stress-Strain Diagram for The Tensile Test (Jubair Et Al., 2021)	32
Figure 2.20	Tensile Test Results (Strength) (Jubair Et Al., 2021)	32
Figure 3.1	Flow Chart of The Overall Process	36
Figure 3.2	Cutting Glass Fiber	38
Figure 3.3	Cutting Banana Fiber	38
Figure 3.4	Treat Banana Fiber with Naoh	39
Figure 3.5	Wash And Dry Banana Fiber	39
Figure 3.6	A Laminate Banana Fiber Of 6g	39
Figure 3.7	Resin And Hardener	40
Figure 3.8	Weigh The Resin and Hardener With Ratio 10:1	40
Figure 3.9	Applied Wax on The Mat	41
Figure 3.10	Hand Layup Process	41
Figure 3.11	Curing Method	42
Figure 3.12	Design Of Tensile Test Specimen In Meter	42
Figure 3.13	Cutting Specimen as Per ASTM: D638 Standard	43
Figure 3.14	Tensile Test Testing in Uitmpp	44
Figure 3.15	Sketching Part	46
Figure 3.16	Saved Material Properties in Material Manager	50
Figure 3.17	Create Material Property	50
Figure 3.18	Input Lamina Property	51
Figure 3.19	Hashin Property	52
Figure 3.20	Damage Evaluation Property	52
Figure 3.21	Damage Stabilization Property	52
Figure 3.22	Nine Composite Layup	53
Figure 3.23	Step Manager	54
Figure 3.24	Meshing The Part With 5 Nodes	55
Figure 3.25	Convergence Analysis	55
Figure 3.26	Boundary Condition of Part In Top and Bottom	56
Figure 4.1	Specimen L1 After Tensile Test (A) Experiment (B) Simulation	59
Figure 4.2	Specimen L2 After Tensile Test (A) Experiment (B) Simulation	59

Figure 4.3	Specimen L3 After Tensile Test (A) Experiment (B) Simulation	60
Figure 4.4	Specimen L4 After Tensile Test (A) Experiment (B) Simulation	60
Figure 4.5	Specimen L5 After Tensile Test (A) Experiment (B) Simulation	60
Figure 4.6	Specimen L6 After Tensile Test (A) Experiment (B) Simulation	61
Figure 4.7	Load Vs Displacement Curve for L1	65
Figure 4.8	Stress Vs Strain Curve for L1	65
Figure 4.9	Load Vs Displacement Curve for L2	66
Figure 4.10	Stress Vs Strain Curve for L2	67
Figure 4.11	Load Vs Displacement Curve for L3	68
Figure 4.12	Simulation Stress Vs Strain Curve for L3	69
Figure 4.13	Load Vs Displacement Curve for L4	70
Figure 4.14	Stress Vs Strain Curve for L4	71
Figure 4.15	Load Vs Displacement Curve L5	72
Figure 4.16	Stress Vs Strain Curve for L5	73
Figure 4.17	Load Vs Displacement Curve for L6	74
Figure 4.18	Stress Vs Strain L6	75
Figure 4.19	Comparison Experiment and Simulation: Ultimate Load (Mpa)	79
Figure 4.20	Comparison Experiment and Simulation: Ultimate Stress (Mpa)	79

LIST OF SYMBOL

Symbol	
kN	Kilo Newton
m	Meter
mm	Milimeter
MPa	Mega Pascal
%	Percent
g	Gram
g/cm^3	Grams Per Cubic Centimeter

LIST OF ABBREVIATIONS

Abbreviations

BF	Banana Fiber
GF	Glass Fiber
L1	Laminate 1
L2	Laminate 2
L3	Laminate 3
L4	Laminate 4
L5	Laminate 5
L6	Laminate 6
VBF	Volume Banana Fiber
V_f	Volume Fiber
VGF	Volume Glass Fiber
V_m	Volume matrix

LIST OF NOMENCLATURES

Nomenclature

UiTMPP	Universiti Teknologi MARA

CHAPTER 1
INTRODUCTION

1.1 Background of Study

In the present day, the shift toward environmentally friendly materials has become an important factor in material selection. In addition to having good mechanical strength, these materials are widely used in various applications such as mechanical, construction, aerospace, automotive, biomedical, marine, and many other manufacturing industries. The development of composite material has become a major focus of research by combining the various beneficial properties of different constituent materials. Hence, hybrid composite of more than one fiber as composite offers the ability of the applications in aerospace manufacturing industries etc. (Rajak et al., 2019)

Many researchers have studied glass fiber as a base material for composite. S. K. Kotla Rachana (2020) stated that this glass fiber composite was used in aircraft and aerospace industries due it is lightweight and high stiffness property (Kotla Rachana, 2020). Moreover, to ensure efficient operation, this composite is corrosion resistance and has high strength. In the research was prepared by having different orientation of fibers in matrix with different thickness to determine their tensile strength, impact strength and Young's modulus of elasticity. Comparisons are made and the best one was picked up.

Various natural plant fibres, including sisal, bamboo, jute, pineapple, coconut, flax, hemp, and ramie, are widely used due to their sustainability and cost-effectiveness. Banana fiber is a natural fiber extracted from banana plants that is biodegradable, renewable, low cost, and easily available. In addition, it possesses good mechanical properties, such as high specific strength and stiffness, making it suitable as a reinforcement material in composite applications. In addition, banana fiber also has good mechanical properties, such as high specific strength and stiffness, which make it an attractive reinforcement material (Sivaranjana & Arumugaprabu, 2021). By combining the laminate of banana fiber with glass fiber, R. Prem Chand et al (2021) aimed to improve the laminate and its mechanical properties (Prem Chand et al., 2021).

Fiber-reinforced polymer composites (FRPs) boast superior strength. They are easier to fabricate and often come at a lower production cost. These combined benefits

make FRPs a popular choice for a wide range of applications. M. V. K. Reddy et al (2020) studied the effect to mechanical properties of tensile, flexural and impact composition of glass fiber and banana fiber in 5 difference configurations (Reddy et al., 2020). The test results demonstrated a significant influence of glass fiber on the tensile, flexural, and impact strength properties of banana fiber.

Natural fiber provides a benefit on cost-saving potential for various applications, and it has great strength and stiffness with little weight. For example, L. Karthick et al (2021) studied the glass fiber and banana fiber using hand layup method with different fiber volume fraction to get the best fiber (Karthick et al., 2022). By comparing fracture toughness, the best composite material for various automotive applications can be determined.

Monzón et al (2019), conducted a study on natural fibers which offers a reduced environmental impact due to their inherent renewability and lower energy requirements for production and processing(Monzón et al., 2019). Therefore, their research detailed the mechanical characterization of a newly developed technical textile utilizing enzyme-treated banana fiber and compared experimental outcomes with numerical simulations based on micromechanical unit cell definitions. The discrepancies in tensile strength and Young's modulus data experiment between the simulation results showed a 9% difference

1.2 Problem Statement

In automotive sector, car bumpers, dashboards and interior panels are commonly manufactured using glass fiber composites because of their strength and durability. However, these materials are costly and lack environmental sustainability. Replacing part of the glass fiber with banana fiber could make vehicles lighter, more affordable, and eco-friendlier. The challenge lies in ensuring that such hybrid composites can still deliver the required crash resistance and wear performance for safe, long-term use.

Unfortunately, studies focusing on the tensile performance of glass fiber-banana fiber hybrid composites remain limited. Although experimental studies have investigated banana fiber composites, few studies have focused on simulating banana-glass fiber hybrid composites with varying fiber volume fractions to predict their load-displacement behavior and stress-strain properties. Therefore, further investigation is required to evaluate the tensile properties of these hybrid composites and to determine

the optimal configuration that can improve mechanical performance while maintaining cost effectiveness.

1.3 Research Objective

1. To validate the tensile properties obtained from the experiment result with the simulation results.
2. To obtain the optimal tensile properties of glass fiber and banana fiber hybrid composites by varying the laminate configuration and fiber volume fraction in different configurations

1.4 Scope of Study

Banana fiber, glass fiber, and epoxy resin form the core components of this composite. The compositions for this study were divided into three categories: Glass Fiber + Epoxy Resin, Banana Fiber + Epoxy Resin, and Glass Fiber + Banana Fiber + Epoxy Resin. These specimens were laminated into nine layers with different configurations.

Glass fiber in the form as woven roving was selected from a local supplier, while banana fiber from Indonesia. As for the surface treatment, underwent NaOH to remove wax, hemicellulose, and residual lignin (Jubair et al., 2021). The epoxy matrix was prepared by mixing resin and hardener at a 10:1 ratio, and the hand lay-up method was used to fabricate the composites (Kotla Rachana, 2020). Meanwhile for the volume fractions, it were calculated to assess the mechanical properties and ensure an optimal fiber-to-resin ratio (Santhanam et al., 2020).

Tensile tests were conducted on the fabricated hybrid composites according to standardized testing methods ASTM D-638 under speed 1mm/min(Karthick et al., 2022)(Standard Test Method for Tensile Properties of Plastics 1, n.d.). The tensile properties were measured in Ultimate Load (kN) and Ultimate Stress (MPa) (Prem Chand et al., 2021).

Finite element analysis (FEA) was developed in Abaqus to simulate the tensile behavior of hybrid composites using 3D modeling, and convergence analysis was performed to ensure accuracy. The simulation models with experimental data were validated to ensure their accuracy and reliability with discrepancies below 9% (Monzón et al., 2019).

1.5 Significance of the Study

Banana fiber offers ecological advantages, but its tensile strength is usually lower than that of glass fiber. Because of this, the study explores combining banana and glass fibers to create composites with optimal configuration for the best performance. The hybrid composite of banana fiber and glass fiber give stronger composites that work better than those made with just one type of natural fiber (Batu & Lemu, 2020).

Furthermore, utilizing simulations to validate experimental results allows researchers to design and determine the optimal solution. This approach not only emphasizes the benefits of integrating natural and synthetic fibers but also helps reduce costs and minimize banana fiber waste. Additionally, banana fiber has the potential to serve as a sustainable alternative to synthetic fibers. The findings in this study suggest that adopting this design approach in textile manufacturing can lead to greater environmental and economic benefits while maintaining high performance, making it a valuable foundation for future research (Karthick et al., 2022), (Kisan et al., 2005).

CHAPTER 2
LITERATURE REVIEW

2.1 Introduction

This chapter provides a literature review for this research, emphasizing previous studies and identifying knowledge gaps related to glass fiber and banana fiber. It examines key studies investigating the tensile properties of glass and banana fiber composites in different configurations, with a focus on the methodologies, material compositions, testing procedures employed by various researchers to optimize these properties and the results achieved.

Additionally, recent advancements in both simulation and experimental techniques for validating tensile properties are discussed, with an in-depth comparison of simulated versus experimental results. By summarizing these advancements and pinpointing current gaps, this literature review establishes a foundation for further exploration and optimization of these composites for industrial applications.

2.2 Composite Applications

Composites are gradually replacing conventional materials in engineering applications such as mechanical, construction, aerospace, automotive, biomedical, marine, and many other manufacturing industries. They are extensively used in spacecraft due to their high specific strength, elevated modulus, low density, and superior wear resistance. Additionally, they reduce the overall weight of products while simultaneously lowering material costs(Rout & Satapathy, 2012).

Figure 2.1 illustrates an example of a composite material utilized in an aerospace application. Composite materials are highly significant as they are generally composed of relatively strong components (Quilter, 2019).

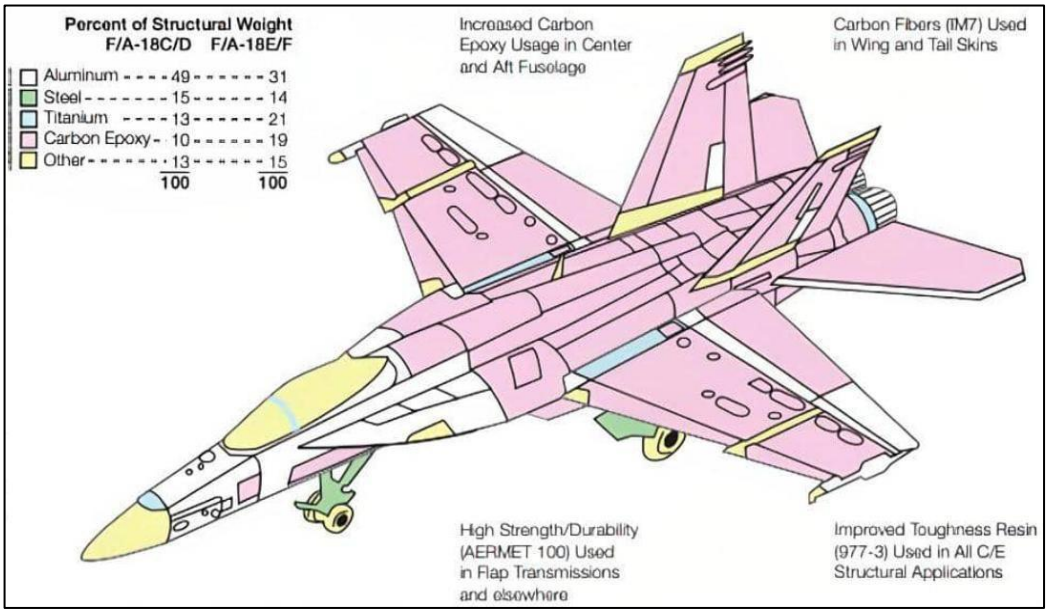

Figure 2.1 Composite material in jet (Quilter, 2019)

The material properties experienced a notable decline in several areas, such as tensile strength, flexural strength, impact strength, and hardness. This means that the material became less resistant to forces that could cause it to stretch, bend, fracture, or dent. A reduction in tensile strength indicates the material's diminished ability to withstand pulling or stretching forces, while a decrease in flexural strength shows it is less capable of resisting bending (Bisht & Gope, 2015).

2.3 Application of Banana Fiber

Al Rashid et al., 2020 (Al Rashid et al., 2020) study aimed to introduce new materials for field hockey equipment to reduce manufacturing costs and the environmental impact of synthetic materials without compromising the quality of the final product. The global sports industry has evolved into a major entertainment sector, driven by technological advancements and reaching billions worldwide. To ensure safety, sustainability, cost-effectiveness, durability, and recyclability of sports products, continuous innovation in materials and manufacturing processes is essential. Although countries such as China and India contribute to the fabrication and export of field hockey equipment, approximately 90% of the world’s hockey products are manufactured in Sialkot, Pakistan.

Synthetic fiber-reinforced polymer composites are widely used due to their high

mechanical strength; however, they present limitations such as high cost, high density, poor recyclability, and non-biodegradability. As a result, increasing attention has been given to natural fiber-reinforced composites, which offer advantages including low cost, low density, biodegradability, reusability, and recyclability. Common natural fibers include banana, coir, flax, hemp, jute, kenaf, and pineapple leaf fibers.

Despite these advantages, natural fiber composites often exhibit weak interfacial bonding between the fiber and polymer matrix. In particular, banana fibers are hydrophilic, resulting in poor compatibility with hydrophobic polymer matrices and consequently weak adhesion. To enhance interfacial bonding, surface modification techniques such as mechanical roughening and chemical treatment can be applied to reduce hydrophilicity and improve fiber–matrix adhesion.

2.4 Type of Material composite

The combination of properties in composites differs from those of metal alloys, ceramics, and polymeric materials. However, they are crucial for use in aerospace, underwater, and transportation applications. These fields require materials that are strong, stiff, resistant to abrasion and impact, and have a high resistance to corrosion (William D. Callister, 2003).

There are three classes of composite that are particle-reinforced, fiber-reinforced, and structural composition. Figure 2.2 shows the schematic classification of composition.

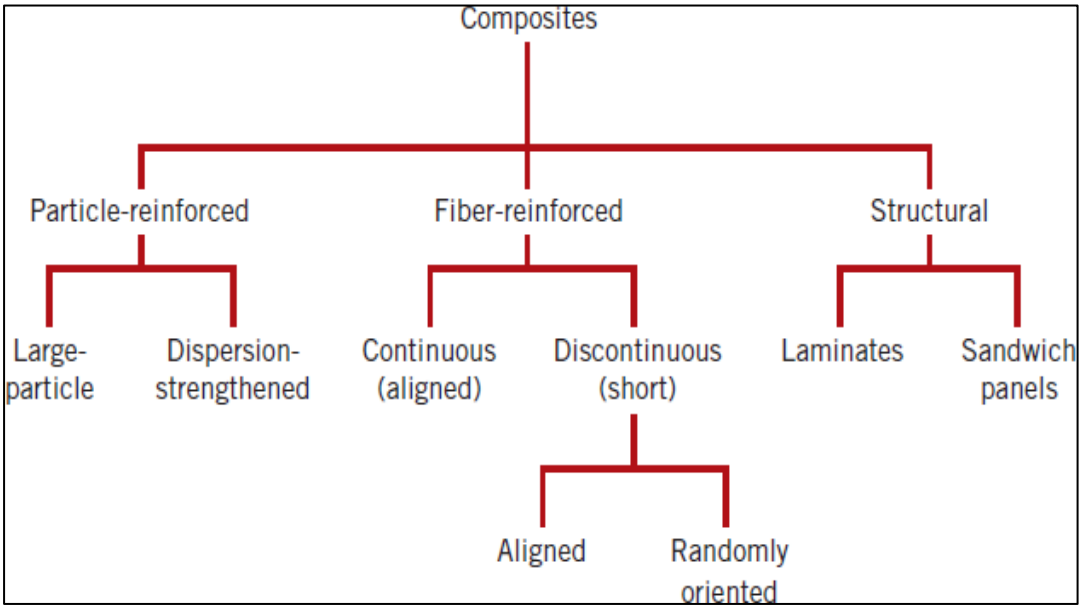

Figure 2.2 Classified of composition (William D. Callister, 2003)

Fiber-reinforced composites exhibit high specific strength and specific modulus properties, while also producing low-density fiber and matrix materials. The arrangement or orientation of fibers, as illustrated in Figure 2.3, can be classified into three types: continuous and aligned, discontinuous and aligned, and discontinuous with random orientation. (William D. Callister, 2003).

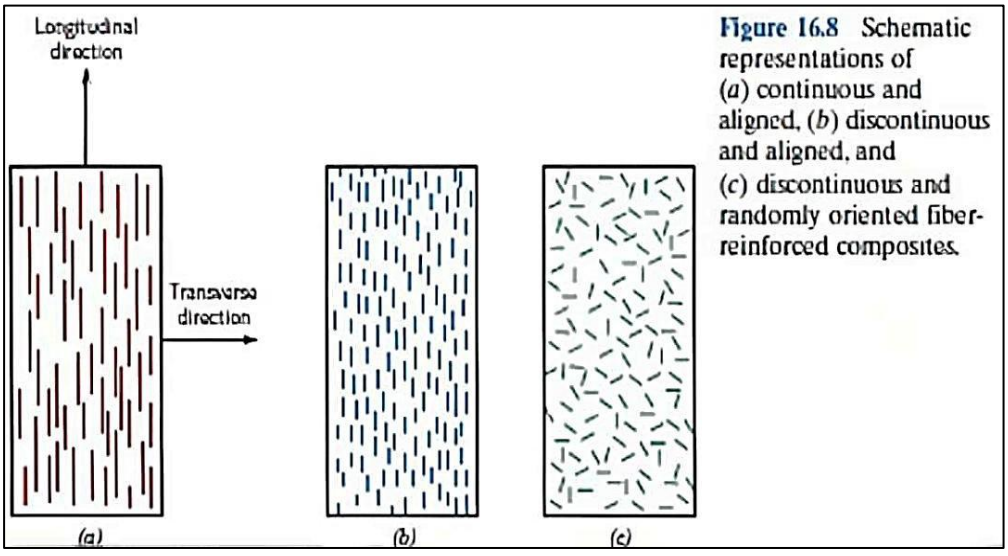

Figure 2.3 Type of orientation fiber reinforce composition. a) continuous and aligned, (b) discontinuous and aligned, and (c) discontinuous and randomly oriented fiber reinforced composites (William D. Callister, 2003)

Aligned fiber-reinforced composite materials exhibit highly orthotropic properties. The longitudinal tensile strength is significantly high, while the transverse tensile strength may be considerably lower, often falling below that of the matrix material. This variation depends on the properties of the fibers and matrix, the quality of the interfacial bond between them, and the presence of voids. In contrast, composites with random or discrete (chopped) fibers do not achieve the same strength levels as those with aligned fibers. However, a key advantage of this random orientation is that the material becomes isotropic and more cost-effective (*Fiber-Reinforced Composites*, n.d.).

2.6.1 Glass Fiber

Glass fiber is the commonly used reinforcement material and finds application in numerous fields, with the aerospace industry being a notable exception. It is lighter and less stiff compared to carbon fiber, allowing it to replace heavier metal components. One of its key features is its higher impact resistance and greater elongation-to-break. The properties and performance levels of glass fiber can vary significantly based on factors such as the type of glass, filament diameter, coating chemistry (known as "sizing"), and fiber form (By & Sloan, 2020).

As stated by S. K. Kotla Rachana (2020), glass fiber reinforcement is available in various forms, such as chopped strands, chopped strand mat, roving, and woven roving. As illustrated in Figure 2.4, woven roving consists of continuous roving woven into a fabric, which is commonly used for manufacturing flat laminates. The use of woven roving enables the integration of higher-quality fibers into the composite, resulting in improved specific strength. In this study, glass fiber reinforced plastic (GFRP) specimens were fabricated using a simple casting technique. Glass fiber was chosen as the reinforcement material due to its key advantages, including easy availability, high stiffness, flexibility in fiber placement, and economic feasibility (Kotla Rachana, 2020).



Figure 2.4 Woven roving (Kotla Rachana, 2020)

Table 2.1 compares the properties of E-glass, aramid, and Standard Modulus (SM) carbon fibers based on data obtained from S. K. Kotla Rachana (2020), highlighting their strengths and weaknesses for various applications. E-glass is the most affordable, with a relative cost of 1, while aramid is five times more expensive, and SM carbon is the costliest, with a relative cost of 10. In terms of density, E-glass is the heaviest at 2.5 g/cm³, aramid is the lightest at 1.4 g/cm³, and SM carbon falls in between at 1.8 g/cm³ (Kotla Rachana, 2020).

For stiffness, SM carbon is the strongest with a modulus of 210 GPa, followed by aramid at 100 GPa, and E-glass at 70 GPa. In tensile strength, SM carbon leads with 4000 MPa, aramid follows with 3000 MPa, and E-glass is lowest at 2400 MPa. E-glass, however, is the most flexible, with a strain of 4.5% at the breaking point, compared to 2.0% for aramid and 1.2% for SM carbon. In impact resistance, aramid is the best, E-glass is good, and SM carbon is fair. For fatigue resistance, SM carbon performs the best, E-glass is good, and aramid is the weakest.

In summary, E-glass is affordable and offers decent all-around performance but is less strong and stiff. Aramid is stronger and better for impacts but costs more and does not handle repeated stresses as well. SM carbon is the strongest and most durable but is expensive and less resistant to impacts. The right choice depends on whether cost, impact resistance, or high strength and durability are most important

Table 2.1

Property of fibers (Kotla Rachana, 2020)

Property	E-glass	Aramid	SM carbon
Relative cost of yarn	1	5	10
Density [g/cm³]	2.5	1.4	1.8
Modulus of elasticity [GPa]	70	100	210
Tensile strength [MPa]	2400	3000	4000
Strain at break point (%)	4.5	2.0	1.2
Impact strength	Good	Best	Fair
Fatigue resistance	Good	Weakest	Best

2.6.2 Banana Fiber

Banana fiber is a natural fiber that offers several advantages, including low cost per unit volume, high strength, and specific stiffness. Studies have shown that natural fiber composites demonstrate superior properties compared to traditional composites. Increasing the amount of banana fiber in the composite can enhance material properties, including stiffness and strength (Rajak et al., 2019).

Figure 2.5 outlines the fiber extraction process, where the banana plant's stem, resembling a trunk, has 60% of its water and lignin squeezed out, is submerged in stagnant water for 10 to 15 days to dissolve the lignin, then washed with clean water and dried in the open air at room temperature (Jubair et al., 2021).

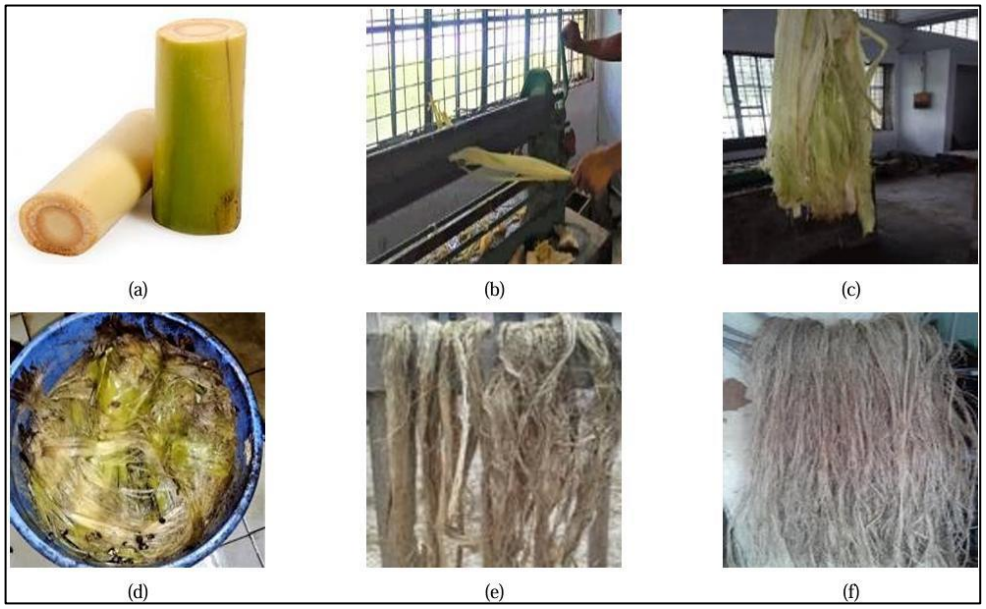

Figure 2.5 Extraction of banana fiber (a) banana stem, (b) manual rolling of the stem, (c) rolled stem, (d) stem in rotten water, (e) drying of extracted fiber, and (f) extracted fiber (Jubair et al., 2021)

The process layout, illustrated in Figure 2.6, outlines the steps involved in specimen preparation (Al Rashid et al., 2020). The banana fibers were initially treated in a solution of 5% NaOH and 95% distilled water (by volume) for 24 hours. After treatment, the fibers were trimmed to the desired dimensions and weighed. Meanwhile, the glass mold was cleaned with acetone, dried thoroughly, and coated with a mold release spray. Peel ply was then applied to the prepared mold surface.

Next, the fibers were carefully arranged on the glass mold, and epoxy resin was evenly applied using a brush. A roller was employed to ensure uniform distribution and to remove excess epoxy from the surface. Finally, a weight was placed on the setup to enhance curing. While this wet layup method produced functional laminates, minor variations in thickness were noted across different stacking sequences, highlighting the inherent limitations of this technique in achieving absolute precision.

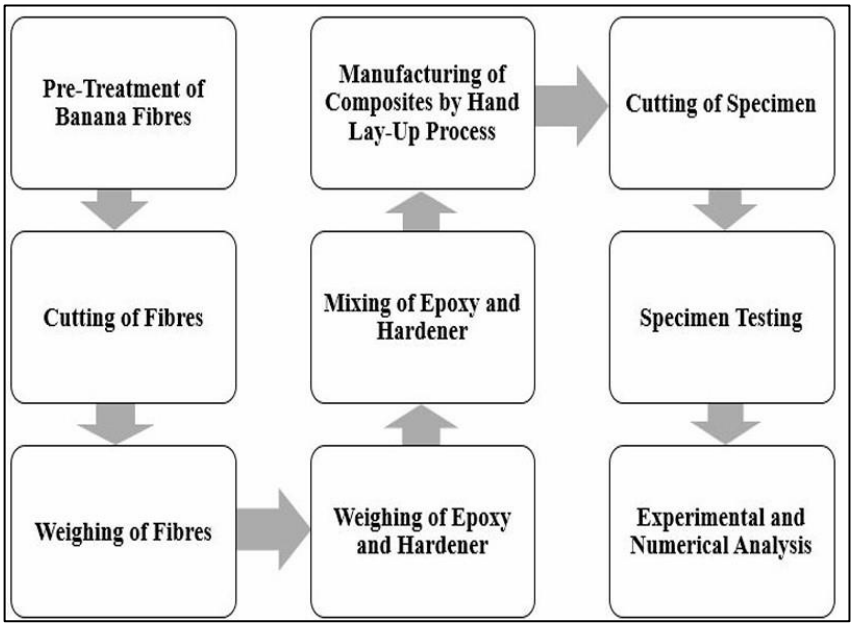

Figure 2.6 The layout of the process (Al Rashid et al., 2020)

Table 2.2 presents the material properties of banana fiber as utilized in the study conducted by P. Narayanan et al. (2019) to analyze its physical and mechanical characteristics (Narayanan et al., 2019). In their research, the banana fibers were sourced from Cherukupalli, a local village, ensuring their origin was consistent and representative of the region. The fibers were then processed to achieve a uniform length of 40 mm, which was accomplished using a specialized cutting machine to maintain precision and uniformity across samples. This uniform length was critical for ensuring reliable and consistent results in the subsequent analyses.

Table 2.2

Property of banana fiber (Narayanan et al., 2019)

Properties	Value
Density	1350 kg/m^3
Moisture content	11%
Tensile strength	56 MPa
Elongation at Break	2.60%
Young's modulus	3.5 MPa
Fineness	17.15

2.6.3 Epoxy Resin

Epoxy resin is the most widely used structural and engineering adhesive in various applications, providing high-performance bonding strength. It has been developed for a broad range of uses, including bonding metal, glass, and plastics. Epoxy resin can be formulated to be either rigid or flexible, transparent or opaque, and can cure quickly or slowly. Among common adhesives, epoxy resin stands out for its exceptional heat and chemical resistance. Generally, heat-cured epoxy resin offers greater heat and chemical resistance compared to room-temperature-cured epoxy resin. Some epoxies can also be cured through exposure to UV light, making them ideal for applications in optics, fiber optics, optoelectronics, and dentistry. Furthermore, the fundamental requirements for these epoxies used in die bonding include high transparency, low thermal stress, and a lower curing temperature (Fibers & Hodgkin, 2020).

Table 2.3 presents the properties of epoxy resin as reported by S. K. Kotla Rachana (2020). The resin used in the manufacturing process of glass epoxy composites is LY556, with the chemical formula ((CH)3C(C6H4OH)2), as described in their research (Kotla Rachana, 2020).

Table 2.3

Property of epoxy resin (Kotla Rachana, 2020)

Parameter	Value
Density	1.175 gm/cc
Rockwell hardness	80 M scale
Elastic modulus	2415 MPa
Flexural strength	>120 MPa
Tensile strength	>90 MPa
Impact strength	>20 Nm/m
Compressive strength	>173 MPa
Dielectric strength	300 V/mil
Thermal conductivity	0.188 W/m-oC
Dissipation factor	0.017
Elongation at break	3-9 %
Poisson's ratio	0.145

2.5 Experiment Approach of Glass Fiber and Banana Fiber

In order to compare and analyze the mechanical properties of glass fiber and banana fiber composites, Karthick (2022) provided a methodology flow chart, as shown in Figure 2.7 (Karthick et al., 2022). The banana fibers were manually extracted, sun-dried, and combined with glass fibers, polyester resin, and Methyl Ethyl Ketone Peroxide (MEKP) catalyst, sourced from a Tamil Nadu company, using the hand layup method to fabricate the composites. The resin and catalyst were mixed thoroughly, then layered with 5 mm chopped banana fiber and cured at room temperature for 24 hours. The same process was applied for glass fiber composites. Specimens for fracture toughness and tensile tests were prepared according to ASTM D5045 and D638-07 standards, respectively. Young's modulus, calculated from the tensile tests, was used in FRANC2D FEA software. The tests were performed using a 100Q Universal Testing Machine at a 1.5 mm/min crosshead speed, with a 7 mm pre-crack for the fracture toughness tests, and Kic values were determined.

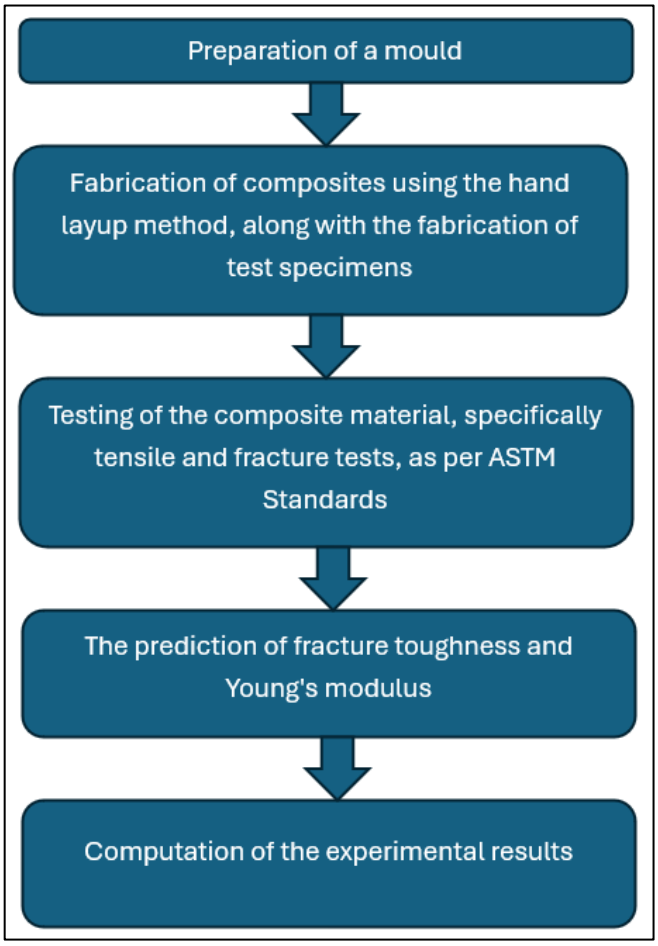

Figure 2.7 Methodology flow chart (Karthick et al., 2022)

2.6.1 Composite Volume Fraction

By referring to K. S. Pandya, C. et. al. (2019) The composite volume fraction is a key parameter used to describe the composition of a hybrid composite. It is defined as the ratio of the volume of a specific constituent material such as a reinforcement or matrix to the total volume of the hybrid composite. This parameter is essential for understanding the proportion of each constituent within the composite structure and plays a significant role in influencing the material's mechanical, thermal, and other physical properties (Pandya et al., 2011).

Table 2.4 shows the fiber volume fractions of various composite laminates get from U. Kureemun et. al (2018). The laminates are composed of two types of fibers: flax (F) and carbon (C). The table shows the average thickness of each laminate, the volume fraction of flax fibers (V_F), the volume fraction of carbon fibers (V_C), and the total fiber volume fraction (V_F+V_C). The arrangements of laminates FC1, FC2, FC3, FC4, and

FC5 differed as illustrated in Figure 2.8.

When dealing with hybrid composites containing multiple types of reinforcements, the volume fraction of a particular type of reinforcement is calculated as the ratio of the volume of that specific reinforcement to the total volume of all reinforcements within the composite. This ratio provides insight into the distribution and contribution of each reinforcement type in the overall performance of the composite material (Kureemun et al., 2018).

Table 2.4

Fiber volume fraction (Kureemun et al., 2018)

	Layup	Average Thickness	Fiber Volume Fraction (%)		
			Flax	Carbon	Flax+Carbon
Specimen	Number of Layup	mm	V_F	V_C	V_F+V_C
F1	4 Flex	4.23	29	0	29
FC1	2 Flex 2 Carbon	3.48	31	8	39
FC2	3 Flex 4 Carbon	3.8	29	14	43
FC3	3 Flex 4 Carbon	3.86	29	14	43
FC4	3 Flex 4 Carbon	3.73	31	15	46
FC5	3 Flex 4 Carbon	3.71	28	13	41
C2	13 Carbon	2.85	0	66	66

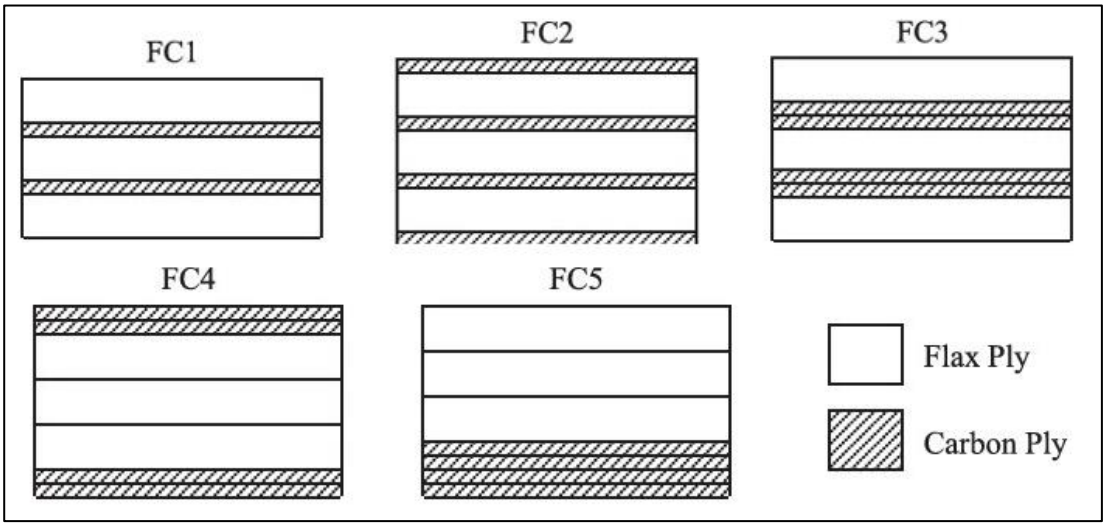

Figure 2.8 Schematics indicating the stacking sequences of hybrid flax-carbon epoxy laminates (Kureemun et al., 2018)

2.6.2 Preparation for the Tensile Test Specimen

The experimental investigation of composite materials involves examining mechanical properties with varying fiber types, fiber volume fractions, fiber lengths, and fiber orientation angles. Different types of composite laminate specimens were fabricated for tensile testing. The specimens were prepared in accordance with ASTM D-638 standard and subjected to tensile tests (Standard Test Method for Tensile Properties of Polymer Matrix Composite Materials, n.d.).

Figure 2.9 shows the hand layup, which is the most common and widely used open mold composite manufacturing process. Initially, fiber preforms were placed in a mold where a thin layer of antiadhesive coat is applied for easy extraction. The resin material was poured or applied using a brush on a reinforcement material. The roller was used to force the resin into the fabrics. This ensure an enhanced interaction between the successive layers of the reinforcement and the matrix materials [130–132]. Coat is applied for easy extraction (Rajak et al., 2019).

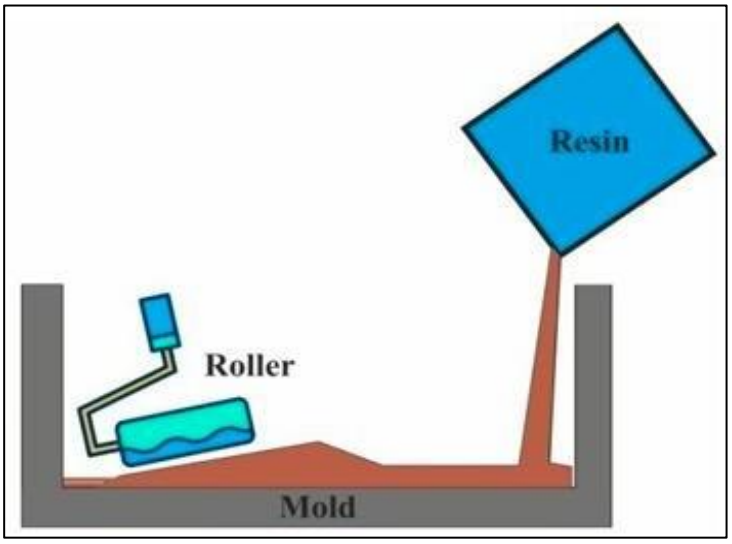

Figure 2.9: Hand layup process (Rajak et al., 2019)

The process of composite fabrication, as illustrated in Figure 2.10 and described by M. V. K. Reddy et al. (2020), involved the use of banana fibers collected from Eco Green Products Company and E-glass fibers procured from Sree Industrial Composite Products Ltd. These materials served as reinforcements in the composite, while epoxy resin obtained from Huntsman Ltd. acted as the matrix material. The epoxy resin and hardener were mixed in a 10:1 ratio (Reddy et al., 2020).

For casting the composite slabs, a mould with dimensions of 300 mm × 300 mm × 4 mm was used. In the case of chopped banana and glass fibers, the fibers were mixed with the epoxy resin using simple mechanical stirring. This method facilitated the preparation of composites with five different compositions based on the varying glass fiber content. For mat-type banana and glass fibers, the mats were directly placed in the mould, and the epoxy-hardener mixture was poured between the layers according to the specified proportions.

Each cast composite was subjected to a load of approximately 20 kg for 24 hours before being removed from the mould. Subsequently, the composites were post-cured in air for another 24 hours. Finally, specimens of appropriate dimensions were cut from the composites for mechanical testing.

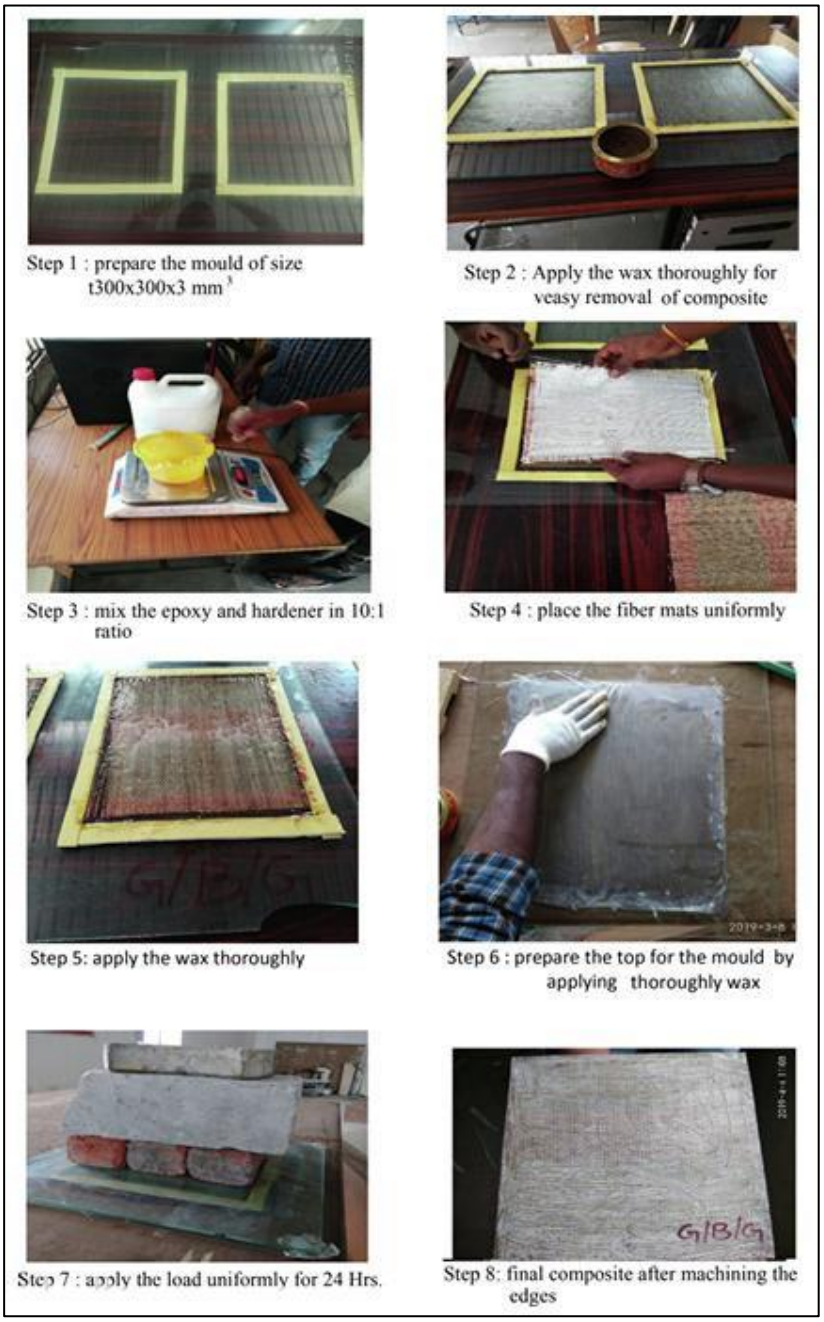

Figure 2.10 Fabrication of composite (Reddy et al., 2020)

The tensile test specimen was designed based on ASTM D-638 standards, which set guidelines for the shape and size of the sample used to test the strength of materials (Kisan et al., 2005). The specimen is typically shaped like a dog bone, with specific dimensions to ensure uniform stress distribution during the test. These dimensions include the gauge length (where the material is stretched), the narrow section (where it breaks), and the overall length.

For composite materials like glass fiber and banana fiber, the specimen was adjusted

to fit the thickness and properties of the material. Figure 2.11 shows a diagram of the specimen's shape and dimensions, following the ASTM D-638 guidelines (Sanjay et al., 2016).

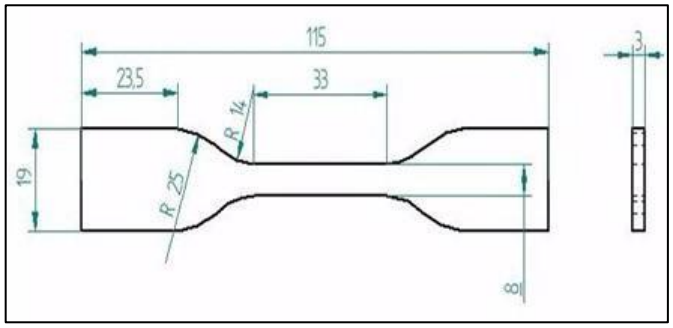

Figure 2.11 Sample specimen test in meter (Sanjay et al., 2016)

2.6.3 Configuration of Composite Laminate

The composite specimens were fabricated using the hand layup method, followed by a compression molding technique. Five different stacking sequences were designed, incorporating both banana and glass fiber fabrics. This resulted in six distinct specimens, produced by varying the arrangement of the woven fabrics as illustrated in Table 2.5, adapted from V. Santhanam et. al. (2020) (Santhanam et al., 2020). To evaluate the influence on mechanical properties, the banana fibers underwent chemical treatment with a 2% Sodium Hydroxide (NaOH) solution.

Table 2.5
Composite specimen layering arrangements and specimen ID (Santhanam et al., 2020)

Specimen ID	Layering arrangement (B- Banana, G-Glass)
A	B-B-B-B-B
B	G-B-B-B-G
C	B-G-B-G-B
D	B-G-G-G-B
E	G-B-G-B-G
F	G-G-G-G-G

Figure 2.12 illustrates the natural fiber composite fabricated through compression molding, utilizing an innovative technical textile with various configurations derived from the study by M. D. Monzón et al (2019) (Monzón et al., 2019). The coding system used in the figure denotes the materials and weave patterns: "LN" refers to flax textile (Lineo), "P" indicates banana textile, and "PL," "BK," and "TW" represent plain, basket, and twill weaves, respectively. Each configuration employed either 1, 2, or 3 layers of textile, combined with 1 or 2 polypropylene sheets, each having a uniform thickness of 1 mm. These variations in material and layering were designed to explore the mechanical and structural properties of the composites.

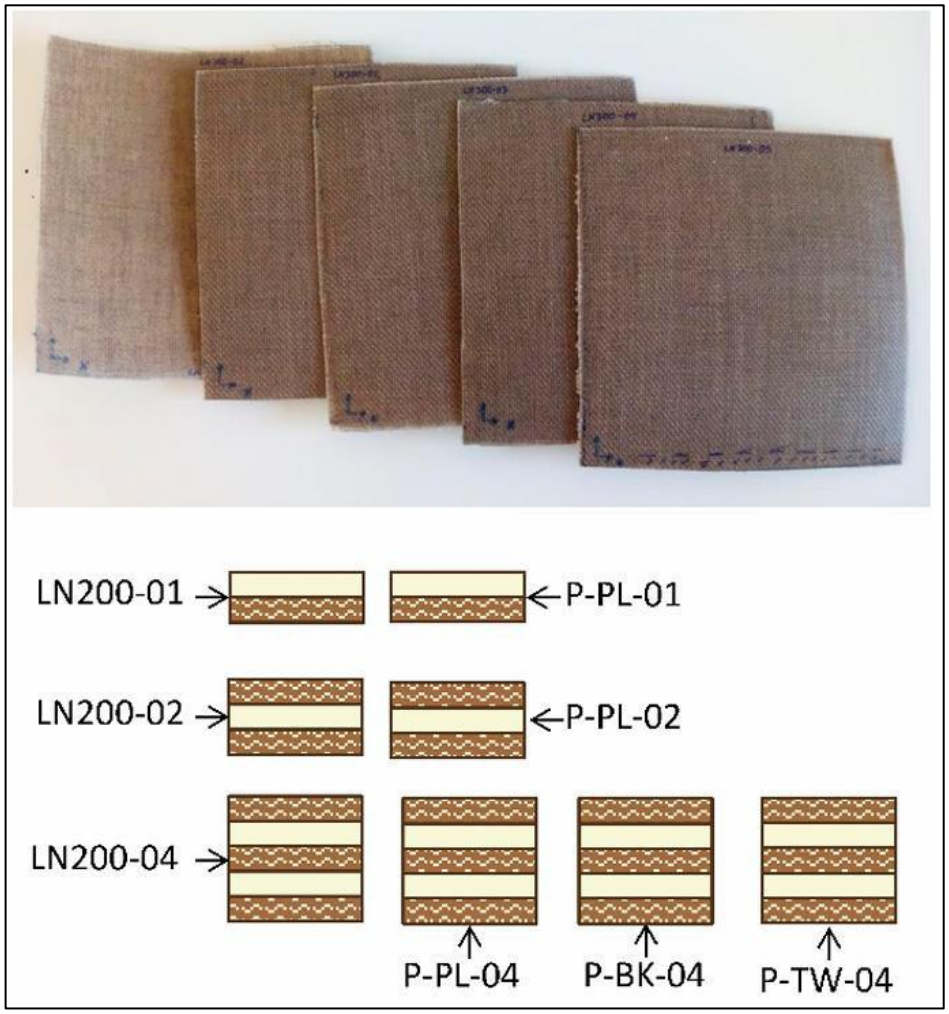

Figure 2.12 Configurations of composite (LN: flax; P: banana textile; PL: plain; BK: basket; TW: twill) (Monzón et al., 2019)

A. Al Rashid et al. (2019) provide details on the stacking sequence, sample numbers, specimen weights, and material descriptions, as illustrated in Figure 2.13 (Al Rashid et al., 2020). The table summarizes composite materials made by combining E-glass and banana fibers, emphasizing the stacking sequences, the number of samples tested for each configuration, their weights in grams, and the descriptions of the fiber arrangements.

The stacking sequence column indicates the order of fiber layers, such as "G8," representing eight layers of E-glass fibers, or "G4B1G3," denoting four layers of E-glass, followed by one layer of banana fiber, and then three more layers of E-glass. The samples column lists multiple samples for each configuration (e.g., G8-1, G8-2, G8-3) to assess variability. The weight (g) column records the weight of each sample in grams. Lastly, the Description column offers a textual representation of the fiber arrangement, mirroring the information in the stacking sequence.

Stacking Sequence	Samples	Weight (g)	Description
G8	G8-1	21.96	8 layers of E-glass fibers.
	G8-2	21.88	
	G8-3	21.93	
G4B1G3 (G7B1)	G4B1G3-1	21.68	4 layers of E-glass fibers, 1 layer of banana fibers, and then 3 layers of E-glass fibers.
	G4B1G3-2	21.72	
	G4B1G3-3	21.66	
G3B2G3 (G6B2)	G3B2G3-1	19.10	3 layers of E-glass fibers, 2 layers of banana fibers, and then 3 layers of E-glass fibers.
	G3B2G3-2	19.07	
	G3B2G3-3	19.11	
G3B3G2 (G5B3)	G3B3G2-1	17.31	3 layers of E-glass fibers, 3 layers of banana fibers, and then 2 layers of E-glass fibers.
	G3B3G2-2	17.25	
	G3B3G2-3	17.29	

Figure 2.13 Detailed composition of the composites (Al Rashid et al., 2020)

2.6.4 Tensile Testing ASTM D638 Standard

The tensile behaviour of banana fiber and glass fiber was evaluated by conducting a tensile test in accordance with ASTM D638 standards. A universal testing machine (UTM), specifically the Instron 3366 model with a maximum load capacity of 10 kN, as depicted in Figure 2.14, was used for testing. The test was performed on flat, dog-bone-shaped specimens, which were secured in the grips of the UTM. A gradually increasing load was applied until the specimen fractured, and the corresponding break load and ultimate tensile strength were recorded. Additionally, tensile stress and strain data were captured, and load versus displacement graphs were generated (Sanjay et al., 2016).



Figure 2.14 Computerized Universal Testing Machine (Sanjay et al., 2016)

According to Karthick et al. (2022), tensile properties of composite specimens composed of glass fiber and banana fiber with varying volume fractions were evaluated. The tests were performed using a 100Q Universal Testing Machine, adhering to the ASTM D638 standard to ensure consistency and reliability of the results (Karthick et al., 2022). During the testing process, the crosshead speed was carefully maintained at 1.5 mm/min, allowing for accurate measurement of the material's tensile behaviour under standardized conditions.

2.6 Finite Element Analysis of Composite

Finite Element Analysis is used to model composites in order to predict their behaviour under load until they fail. It is ideal for complex calculations. To be subjected to FEA modelling, the material property must be identified and clearly selected. The model for composite used ‘Lamina Damage Model’. Loading and support rollers were modeled as rigid bodies and discretized using rigid (Koloor et al., 2020).

Composite structures are made of multidirectional (MD) fiber-reinforced polymer (FRP) composite laminates, which fail due to multiple damages in matrix, interface, and fiber constituents at different scales.

The yield point of a unidirectional FRP composite is assumed as the lamina strength limit representing the damage initiation phenomena, while yielding of MD composites in structural applications are not quantified due to the complexity of the sequence of damage evolutions in different laminas dependent on their angle and specification.

The response of the FRP composite laminates to applied load such that yielding of

the material is achieved is predicted in this study, based on the damage mechanics approach.

A composite material possesses two critical mechanical properties: elastic and damage resistance. Figure 2.15 illustrates the elastic-damage behaviour of a composite lamina with stress-displacement in various modes. Under elastic conditions, it follows the classical lamina theory; however, under damage conditions, it follows the damage mode (Koloor et al., 2020).

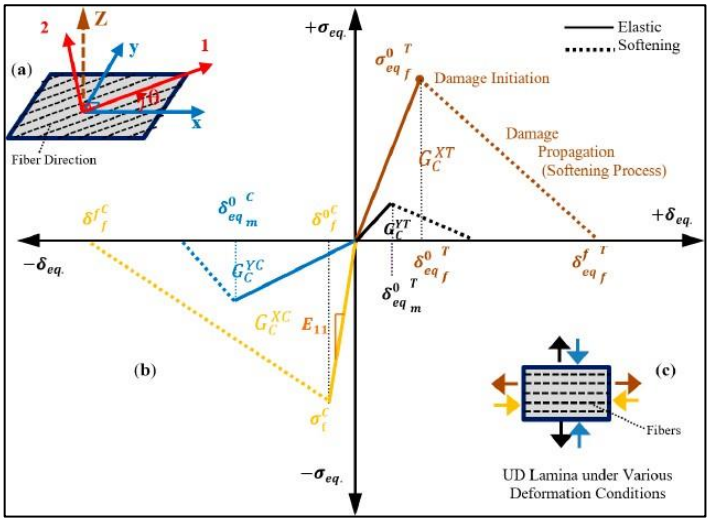

Figure 2.15 Relation between lamina and damage initiation (Koloor et al., 2020)

2.6.1 Elastic Region for Composite

The elastic region is defined as a lamina, where it is assumed to exhibit orthotropic properties, with a stiffer response along the fiber direction and a softer behavior in the matrix (Abaqus, 2006). A lamina serves as the fundamental geometric unit for a composite before undergoing further analysis (Monzón et al., 2019). This region is characterized by properties such as E_1, E_2, V_{12}, G_{12}, G_{13}, and G_{23}, where;

E_1 - axial stiffness of composite ply, Pa, E_2 - transverse stiffness of composite ply, Pa, v_{12} - Poisson ratio, G_{12} - Shear stiffness of composite ply acting in 1 direction on a plane with normal in 2 direction, Pa, G_{13} - Shear stiffness of composite ply acting in 1 direction on a plane with normal in 3 direction, Pa, G_{23} - Shear stiffness of composite ply acting in 2 direction on a plane with normal in 3 direction, Pa

2.6.2 Damage Model of Composite

The damage mode of the lamina was assessed using Hashin's quadratic stress-based failure model. Since no plastic deformation was observed in the FRP composite, the process was considered to represent damage evolution. Initially, this stage was referred to as "damage initiation," as it involves six material properties: X_T, X_C, Y_T, Y_C, S_L, and S_T (Xin et al., 2017).

X_T - longitudinal tensile strength, X_C - longitudinal compressive strength, Y_T - transverse tensile strength, Y_C - transverse compressive strength, S_L - longitudinal shear strength, S_T - transverse shear strength.

As illustrated in Figure 2.15, the progression of the initially damaged composite through a softening process is referred to as "damage propagation." In this phase, the composite releases fracture energy, denoted as G_C, which is fully dissipated, leading to failure characterized by G_{XT}, G_{XC}, G_{YT}, and G_{YC} [30]. Below is a description of these properties:

G_{XT} - longitudinal tensile fracture energy, G_{XC} - longitudinal compressive fracture energy, G_{YT} - transverse tensile fracture energy and G_{YC} - transverse compressive fracture energy.

2.6.3 Material Properties for Simulation

By referring to the work of Xin et al. (2017), the experimental and simulation analysis of pultruded glass fiber reinforced polymer (GFRP) laminates was studied, emphasizing their significance and practical applications in designing and constructing GFRP structures for bridge engineering (Xin et al., 2017). They proposed a continuum damage model that incorporated lamina shear nonlinearity, damage along the thickness direction, innovative damage evaluation methods, a loading/unloading strategy, and viscous methods to overcome convergence difficulties. This model was implemented using a user material subroutine. Three types of pultruded GFRP laminates were fabricated, and their material properties were tested to validate the

numerical and theoretical models. The finite element simulation results correlated well with experimental data, offering a valuable reference for GFRP structural design and construction. The simulation used predicted lamina engineering constants based on material properties listed in Table 2.6 and Table 2.7.

Table 2.6

Lamina engineering constants of pultruded GFRP laminate (Xin et al., 2017)

Mechanical Properties	**GF800**	**GF700**	**GF600**
E_1 (GPa)	45.95	39.63	36.87
E_2 (GPa)	14.56	11.67	10.64
E_3 (GPa)	14.56	11.67	10.64
G_{12} (GPa)	4.50	3.59	3.27
G_{13} (GPa)	4.50	3.59	3.27
G_{23} (GPa)	5.51	4.34	3.93
V_{12}	0.25	0.27	0.28
V_{13}	0.25	0.27	0.28
V_{23}	0.30	0.32	0.33

Table 2.7

Lamina ultimate capacity of pultruded GFRP laminate (Xin et al., 2017)

Mechanical Properties	**GF800**	**GF700**	**GF600**
X_T (MPa)	1341.2	1158.9	988.8
Y_T (MPa)	47.8	48.9	49.6
Z_T (MPa)	47.8	48.9	49.6
X_C (MPa)	1048.4	908.2	837.7
Y_C (MPa)	100.1	96.9	95.3
Z_C (MPa)	100.1	96.9	95.3
S_{xy} (MPa)	65.5	64.8	64.9
S_{xz} (MPa)	65.5	64.8	64.9
S_{xz} (MPa)	65.5	64.8	64.9

Monzón et al. (2019) conducted a numerical simulation of a novel technical textile-reinforced composite made from banana fiber, achieving a global average error of 9% compared to experimental results (Monzón et al., 2019). This confirmed the suitability of predictive modeling based on the multiscale method for designing such composites. Table 2.8 presents the lamina orthotropic parameters for three configurations studied: plane fabric with banana threads and a polypropylene matrix P-PL-04, twill fabric with banana threads and a polypropylene matrix P-TW-04, and basket fabric with banana threads and a polypropylene matrix P-BK-04.

Table 2.8

Lamina orthotropic properties for each unit cell (Monzón et al., 2019)

Parameters	**P-PL**	**P-TW**	**P-BK**
E11(MPa)	1286.7	1283.9	1294.2
E22(MPa)	1288.8	1286.4	1295.6
E33(MPa)	1245.4	1238.1	1227.4
V12	0.384	0.383	0.388
V23	0.384	0.383	0.388
V31	0.371	0.369	0.361
G12(MPa)	453.2	451.6	454.7
G23(MPa)	449.1	447	438.9
G31(MPa)	449.2	447.1	438.8

2.6.4 Tensile Behavior Modeling and Simulation for Composite Material

Monzón et. al. (2019) performed tensile tests on banana fiber-reinforced composites, which were modelled according to ISO 527-2:2012 using previously determined unit cell properties for each material (Monzón et al., 2019). The boundary conditions included fixing one end of the sample as the stationary clamp and applying a longitudinal displacement at the opposite end as the mobile clamp. Following the simulation, stresses and strains along the X-axis were evaluated in the central section of the sample, with the results for stress and strain presented in Figure 2.16 and Figure 2.17, respectively. To compare the simulation with experimental data, average stress and strain values were calculated, as the results showed minimal variation.

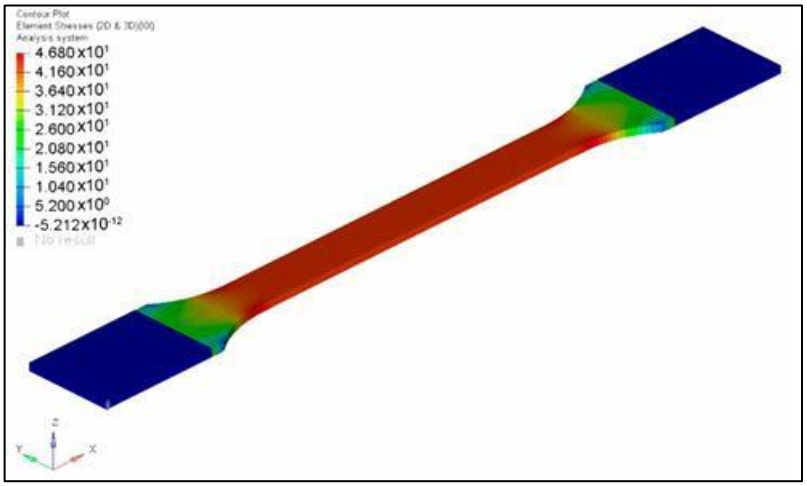

Figure 2.16 Element stresses (MPa): Direction X (Monzón et al., 2019)

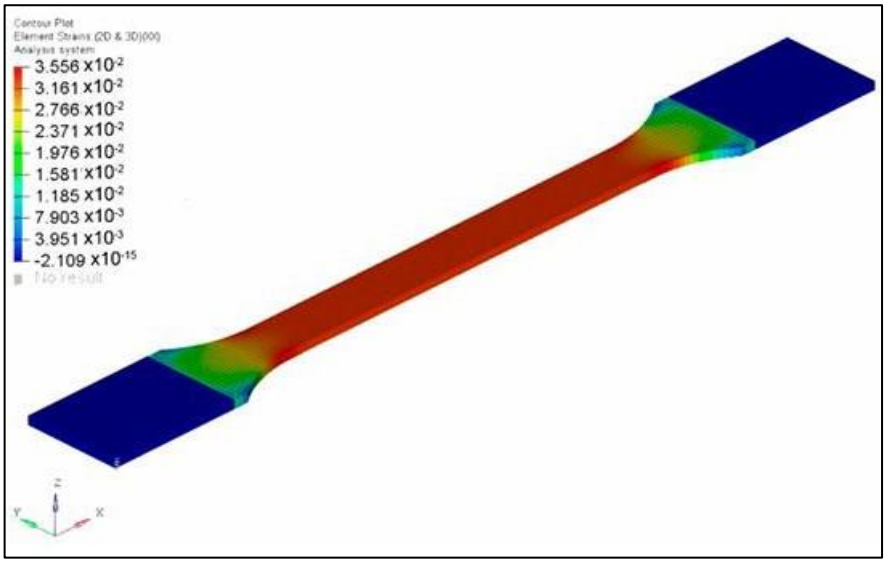

Figure 2.17 Element strains: Direction X (Monzón et al., 2019)

2.7 Range of Ultimate Load and Ultimate Stress of Banana Fiber and Glass Fiber

The load versus displacement graph was converted into a stress versus strain graph. From this, yield stress, Young's modulus (E), and the fracture point were determined [16]. The stress-strain graph for the composite material is shown in Figure 2.18. The relationship between yield stress and Young's modulus reflects the amount of load required to deform the material in its elastic region. Yield stress represents the maximum stress the material can endure, while Young's modulus quantifies the stress-strain behaviour within this elastic region(ASTM, 2014)

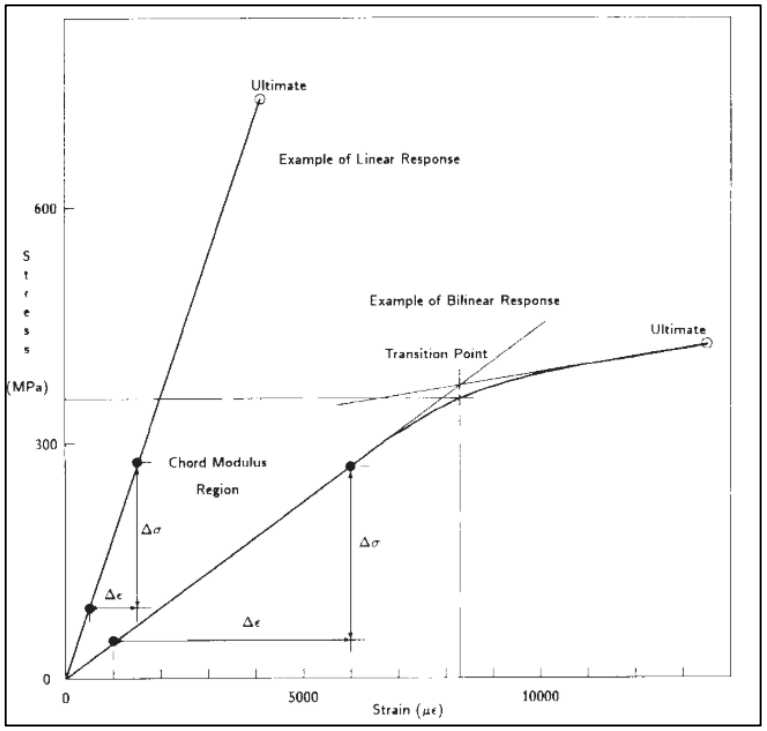

Figure 2.18 Typical tensile stress-strain curve (ASTM, 2014)

To justify the acceptability of the results of glass fiber, several journals were reviewed to establish a range for ultimate load and ultimate stress values as tabulated in Table 2.9. The lowest recorded break load was reported by Prem Chand et al. (2021) (Prem Chand et al., 2021) at 5.68 kN, resulting in a low ultimate stress of approximately 120 MPa. In contrast, the highest ultimate load was documented by Pillai et al (2009) (Pillai et al., 2009) at 11.58 kN, while the highest ultimate stress was reported by Stanciu, et al (2021) (Stanciu et al., 2021)at 228 MPa.

Table 2.9

Range of tensile property for glass fiber (Prem Chand et al., 2021)(Pillai et al., 2009)(Stanciu et al., 2021)

Level	Ultimate Load Experiment (kN)	Ultimate Stress Experiment (MPa)
Low	5.68	120.00
Middle	5.74	190.07
High	11.58	228.00

The table presents in Figure 2.10 show the results of an experiment on banana fiber conducted to evaluate the ultimate load and ultimate stress of a material from another source. The material was tested under three different conditions: Low, Middle, and High. At the Low level, the material sustained a maximum load of 0.53 kN before failure, while the maximum stress recorded was 6.45 MPa (Sanjay et al., 2016) At the Middle level, the maximum load increased to 0.91 kN (Sampath et al., 2021), with the ultimate stress reaching 10 MPa (Moon et al., 2024). At the High level, the material withstood an ultimate load of 1.11 kN (Monzón et al., 2019), while the stress experienced rose significantly to 45 MPa (Moon et al., 2024).

Table 2.10

Range of tensile property for banana fiber (Monzón et al., 2019) (Sanjay et al., 2016)(Sampath et al., 2021)(Moon et al., 2024)

Level	Ultimate Load Experiment (kN)	Ultimate Stress Experiment (MPa)
Low	0.53	6.45
Middle	0.91	10
Heigh	1.11	45

In Prem Chand et al. (2021) works, their study focused on banana and E-glass fiber-reinforced hybrid epoxy composites (Prem Chand et al., 2021). Tensile tests were conducted on banana E-glass laminates to evaluate mechanical properties such as tensile strength (σ) and Young's modulus (E) under load, as presented in Table 2.11 (Prem Chand et al., 2021).

Table 2.11

Tensile test result (Prem Chand et al., 2021)

Ultimate load (P) in N	Cross sectional area (A) in mm^2	Ultimate tensile strength (σ) in MPa	Young's modulus (E) in MPa
5680	47.33	120	1481.48

Jubair et al. (2021) investigated the mechanical properties of banana-glass fiber-reinforced hybrid composites (Jubair et al., 2021). The results are presented in stress-strain curves for four composites in Figure 2.19, showing banana fiber with the lowest maximum stress and glass fiber with the highest. Figure 2.20, a bar chart, illustrates banana fiber's tensile strength as the lowest at 35.86 MPa, glass fiber as the highest, and hybrids 1 and 2 at 42.83 MPa and 69.28 MPa, respectively, with 19.44% and 93.20% improvements over banana fiber.

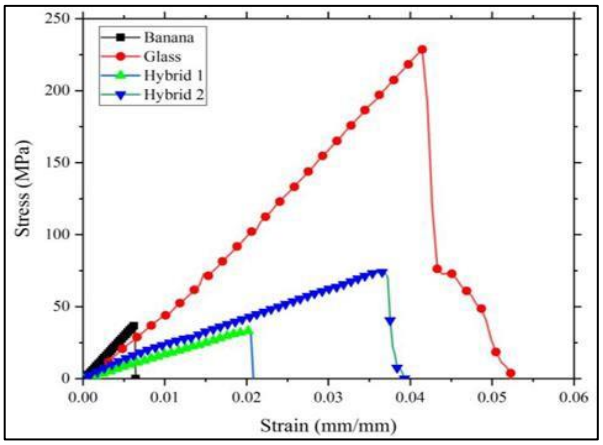

Figure 2.19 Stress-strain diagram for the tensile test (Jubair et al., 2021)

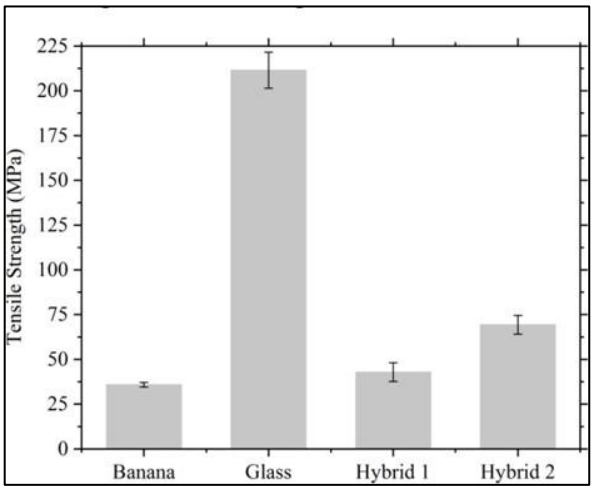

Figure 2.20: Tensile test results (strength) (Jubair et al., 2021)

2.8 Research Gap of Study

Based on the literature review, composite materials are widely used in spacecraft applications due to their high specific strength, high modulus, low density, and excellent wear resistance. In addition, the use of composites helps reduce the overall weight of products while lowering material costs (Rout & Satapathy, 2012). In another study, banana fiber was investigated for field hockey equipment to reduce manufacturing costs and minimize the environmental impact of synthetic materials without compromising product quality (Al Rashid et al., 2020).

Previous studies have examined the mechanical properties of glass fiber, banana fiber, and their hybrid composites through experimental approaches. Meanwhile, numerical studies using finite element analysis (FEA) have primarily focused on glass fiber and natural fiber composites individually (Santhanam et al., 2020). However, limited research has integrated both experimental and simulation approaches to investigate hybrid composites consisting of glass fiber and banana fiber. Furthermore, the optimisation of stacking sequence configurations and the comparison between experimental results and FEA predictions, particularly in terms of tensile strength and stress distribution, have not been widely discussed (Prem Chand et al., 2021) (Koloor et al., 2020).

Therefore, a clear research gap exists in analysing several laminate configurations, evaluating their tensile performance, and comparing the ultimate stress values obtained from experimental testing and simulation to assess the accuracy and reliability of the modelling approach (Jubair et al., 2021). This study aims to address this gap by understanding the tensile behaviour of hybrid glass–banana fiber laminates with different configurations, as well as in validating simulation predictions against experimental results while verifying the volume fraction composition of the hybrid composite (Kureemun et al., 2018) (Sanjay et al., 2016).

CHAPTER 3
RESEARCH METHODOLOGY

3.1 Introduction

The flow chart illustrates the overall research methodology used to determine the optimal laminate arrangement of the hybrid composite through both experimental testing and numerical simulation. The process began with the start of the study, followed by the experimental procedure. First, the materials were prepared by arranging the reinforcement fibers and resin matrix to ensure proper bonding during fabrication. After the material preparation stage, the composite specimens were fabricated according to the required laminate configuration and tensile specimen standards. The fabricated specimens were then subjected to a tensile test to evaluate their mechanical properties, such as tensile strength, deformation behaviour, and failure characteristics.

After completing the tensile test, a decision point (Yes/No) was implemented. If the tensile test results met the specifications reported in previous studies (Yes), the process proceeded to the comparison stage. If the results did not meet the required standards (No), the process reverted to the material preparation and specimen fabrication stages to enhance specimen quality before repeating the tensile test.

In parallel with the experimental work, a numerical simulation was performed using Abaqus software. The simulation began by designing the tensile specimen model based on the geometry used in the experimental test. Next, the material properties of the lamina and resin were defined in the simulation environment. The analysis settings were then established using static general analysis with the required output parameters.

Subsequently, the boundary conditions were applied by creating sets at the top and bottom surfaces of the specimen, where one end was fixed while the tensile load or displacement was applied to the opposite end to replicate the experimental loading condition. After defining the loading conditions, the specimen model was divided into smaller finite elements through a meshing process to enable accurate numerical analysis.

Once the mesh was generated, the simulation job was executed in Abaqus to obtain stress and strain distributions within the composite specimen. A convergence analysis

was then performed to ensure the accuracy and stability of the simulation results. If the convergence criteria were satisfied (Yes), the simulation results were accepted, and the process proceeded to the comparison stage. However, if the results did not converge (No), the mesh was refined and the simulation job was repeated until convergence was achieved.

Finally, the results obtained from the experimental tensile test and the Abaqus simulation were compared to evaluate the accuracy of the numerical model and the mechanical performance of the composite material. If the results were not satisfactory (No), the process returned to the input stage to revise the lamina properties and Hashin failure criteria before repeating the analysis. However, if the experimental data and simulation results were valid and in good agreement (Yes), the optimal laminate arrangement of the hybrid composite was determined. Once the best laminate configuration was identified, the research process reached the final stage.

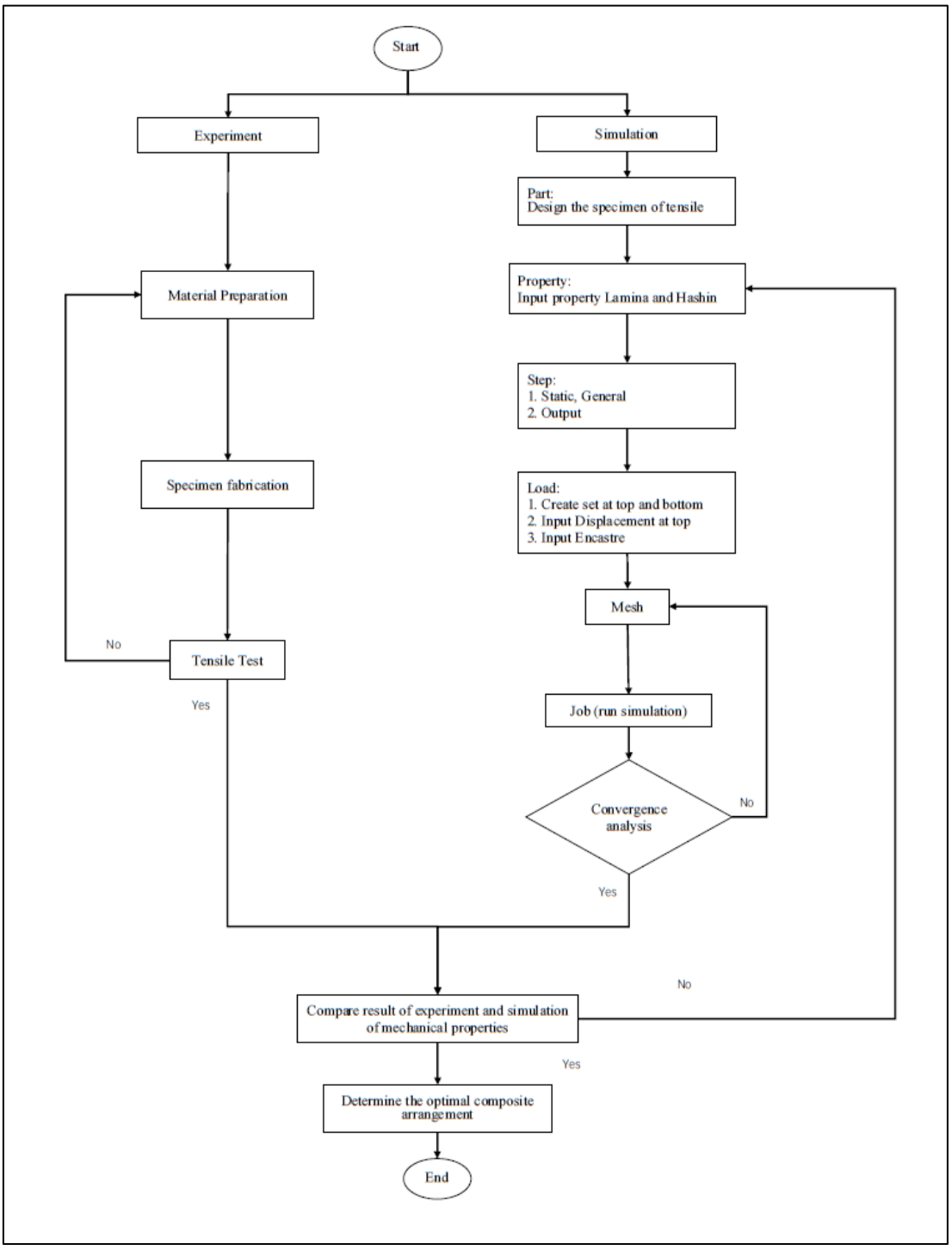

Figure 3.1 Flow chart of the overall process

3.2 Experimental Procedures

This study employed six laminates composed of glass fiber and banana fiber in various configurations. The hand layup method was employed for the fabrication of composite specimens. According to ASTM D-638, tensile tests were conducted on all specimens at a rate of 1 mm/min.

3.2.1 Design of Lamination Configuration

The specimens were meticulously arranged using the hand layup method, each layer was placed one by one to form the composite structure. Six different types of specimens were prepared, each with distinct configurations, to undergo tensile tests. As indicated in Table 3.1, the configuration labelled L1 consists of glass fiber combined with epoxy resin, while L2 is composed of banana fiber with epoxy resin. Configurations L3 through L6 are hybrid composites, incorporating layers of both glass fiber and banana fiber embedded in epoxy resin. This arrangement allows for a comprehensive evaluation of the tensile properties of various fiber combinations followed by Sanjay et al. (2016) (Sanjay et al., 2016). The specimens were tested using three samples for each laminate configuration until the results were validated through comparison with previous journal studies and simulation results. Only one specimen was used for the results discussion, as the previous study also conducted the analysis using a single sample (Santhanam et al., 2020).

Table 3.1

Design of composition glass fiber and banana fiber

Laminate	**Designations**	**Layer**	
		Banana	**Glass Fiber**
L1	G+G+G+G+G+G+G+G+G	00	09
L2	B+B+B+B+B+B+B+B+B	09	00
L3	B+G+B+G+B+G+B+G+B	05	04
L4	G+B+G+B+G+B+G+B+G	04	05
L5	B+B+G+B+G+B+G+B+B	06	03
L6	G+G+B+G+B+G+B+G+G	03	06

3.2.2 Fabrication of Specimens

The glass fiber and banana fiber were cut into pieces measuring 210mm x 210mm, as illustrated in Figure 3.2 and Figure 3.3. Sharp scissor was used to cut both fibers (Sivaranjana & Arumugaprabu, 2021).

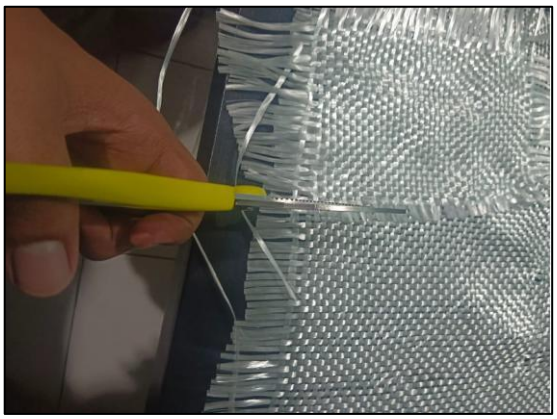

Figure 3.2 Cutting glass fiber



Figure 3.3 Cutting banana fiber

The banana fibers were then treated with NaOH for approximately 2 hours, as shown in Figure 3.4. This treatment removed the wax, hemicellulose, and lignin that obscure the fiber surface. Consequently, it improved adhesion at the interface and facilitated the infiltration of the matrix resin into the fibers (Sivaranjana & Arumugaprabu, 2021).

Following the NaOH treatment as illustrated in Figure 3.5, the banana fibers were thoroughly washed with water to remove any residual chemicals. After they were completely dried, approximately 6 grams of banana fiber were weighed out for each laminate, as illustrated in Figure 3.6.



Figure 3.4 Treat banana fiber with NaOH



Figure 3.5 Wash and dry banana fiber



Figure 3.6 A laminate banana fiber of 6g

Next the fiber layup sequence outlined in Table 3.1, each laminate's individual fiber layers was carefully positioned on the work surface. This ensured a well-organized and planned laminate structure before proceeding with resin preparation.

Following a 10:1 weight ratio as recommended by Kotla Rachana (2020) (Kotla Rachana, 2020) studies, the resin and hardener were carefully measured and mixed to form the matrix as in Figure 3.7. As shown in Figure 3.8, 60 grams of resin and 6 grams of hardener were weighed out using a digital scale. The mixture was then thoroughly stirred in a cup to ensure proper homogenization.



Figure 3.7 Resin and hardener

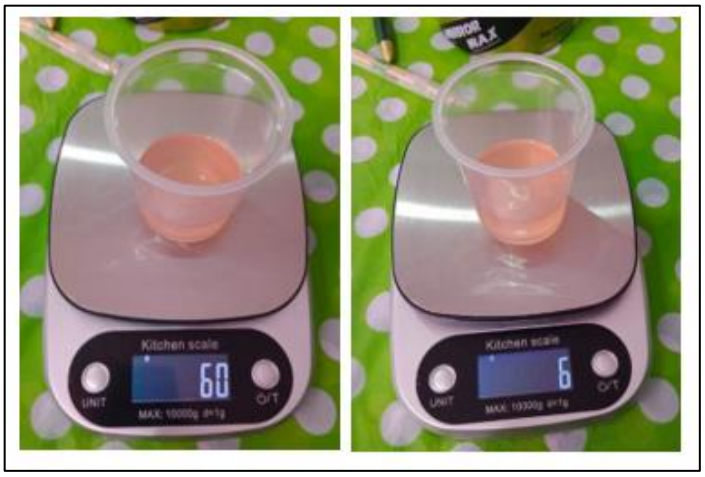

Figure 3.8 Weigh the resin and hardener with ratio 10:1

Wax was applied to the surface of the board as illustrated in Figure 3.9, which served as a releasing agent. This wax layer facilitated the easy removal of the composite material from the board once the curing process completed. The wax prevented the composite from adhering to the board, ensuring that the final product can be separated without damage or difficulty.



Figure 3.9 Applied wax on the mat

A straightforward layup technique was employed to layer nine sheets of glass fiber (Jubair et al., 2021)(Kotla Rachana, 2020).The matrix was poured onto the mat and evenly distributed with a brush as depicted in in Figure 3.10. The first piece of glass fiber laminate was positioned onto the wet board and the matrix was applied uniformly using a brush. Rollers were applied on the wet laminate surfaces to eliminate air bubbles and ensure a strong bond with the gel coat. This procedure was repeated for all nine layers of fiber in each laminate, as outlined in Table 3.1.



Figure 3.10 Hand layup process

Based on the method described by Reddy et al. (2020), the curing process involved subjecting each composite cast to a load of approximately 20 kg for 24 hours to ensure proper consolidation and solidification, as illustrated in Figure 3.11 (Reddy et al., 2020). Following this initial curing stage, the cast was carefully detached from the board and allowed to undergo post-curing in ambient air for an additional 24 hours. This post-curing step was essential for releasing any residual stress and ensuring the composite achieved its optimal mechanical properties.



Figure 3.11 Curing method

After the initial 24-hour curing period, the composite was carefully removed along with the board. The composite was then cut according to the ASTM D638 standard, which specifies dimensions and procedures for tensile testing of plastics as shown in Figure 3.12. ASTM D-638 (Raheem, 2019) was selected due to this test method covers the determination of the tensile properties test specimens when tested under defined conditions of pretreatment, temperature, humidity, and testing machine speed. The thickness for this study was 5.1mm to 13.5mm.

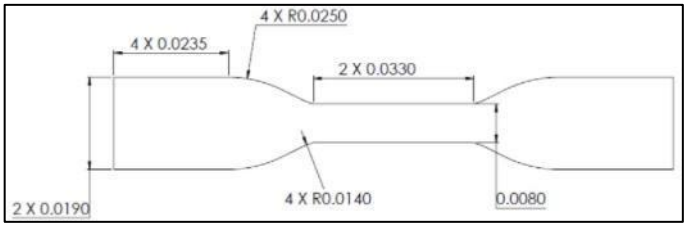

Figure 3.12 Geometry of tensile test specimen in meter

Subsequently, specimens were cut to the appropriate dimensions before conducting the tensile tests. This cutting process, as illustrated in Figure 3.13, was performed using a hand saw to ensure precision and adherence to the specified standards. The hand saw allowed for controlled and accurate cutting of the composite material into test specimens of the required size and shape for subsequent physical and mechanical evaluations (Karthick et al., 2022) (Raheem, 2019) .

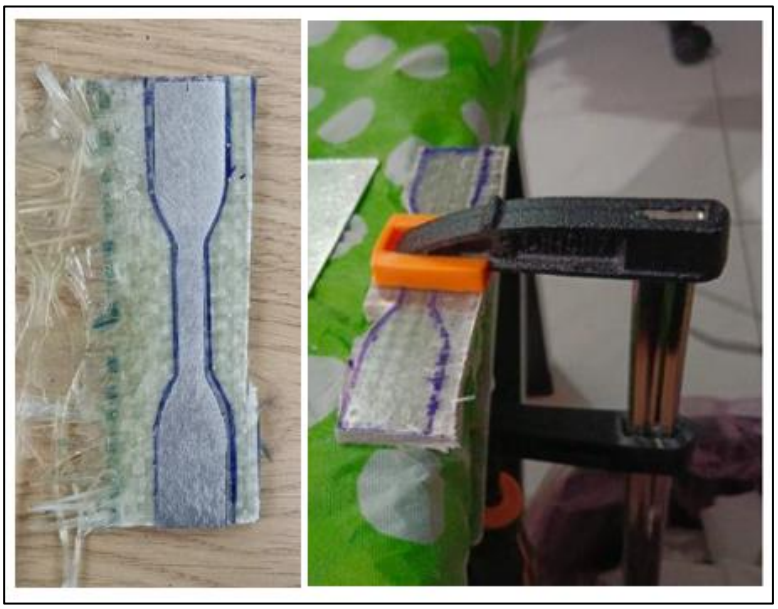

Figure 3.13 Cutting specimen as per ASTM: D638 standard

3.2.3 Tensile Testing Based on ASTM D638 Standard

Figure 3.14 Figure 3.14 shows the Universal Testing Machine (UTM) located in the Civil Engineering Laboratory for Strength Testing at Universiti Teknologi MARA (UiTM) Pulau Pinang, Malaysia. The Universal Testing Machine was used to determine the tensile properties of the composite specimens, including the ultimate tensile strength, maximum load, and elongation at break.

The tensile test was conducted in accordance with ASTM D638, which specifies the procedure for evaluating the tensile behavior of polymer and composite materials. The test was performed under displacement-controlled conditions with a constant crosshead speed of 1 mm/min at room temperature (≈ 25°C). Three specimens were tested for each laminate configuration to ensure repeatability and reliability of the data.

During the test, the specimen was subjected to a uniaxial tensile load until failure occurred. The applied load and corresponding displacement were continuously recorded by the machine's data acquisition system to generate the load–displacement curve. From this recorded data, the tensile stress–strain behaviour, ultimate tensile strength, and failure characteristics of the specimens were determined.



Figure 3.14 Tensile test testing in UiTMPP

3.2.4 Composite Fibrous Structures

The fiber volume fraction of both glass fiber and banana fiber was calculated by using Equation 3.1 following the guidelines outlined in ASTM D2584. This calculation determined the composite volume fraction as the ratio of the volume of a specific constituent to the total volume of the hybrid composite. It indicated the amounts of resin and fiber in the material and described in Section 2.4.1. This was crucial for assessing mechanical properties and achieving the desired fiber-to-resin ratio in composite materials (Messiry, 2013) (Ciprian et al., 2015).

$$V_f = [\rho_m \cdot w_f/(\rho_m \cdot w_f + \rho_f \cdot w_m)] \quad (3.1)$$

$$V_m = [1 - V_f] \quad (3.2)$$

where V_f volume fraction of fibers, w_f weight of fibers, w_m weight of matrix, ρ_f density of fibers, ρ_m density of matrix, V_m volume fraction of matrix.

Table 3.2 presents the density property of glass fiber (ρ_{gf}) obtained from S. K. Kotla Rachana (2020) (Kotla Rachana, 2020), while the densities of banana fiber (ρ_{bf}) and matrix (ρ_m) were sourced from L. Prabhu et al. (2021)(Prabhu et al., 2021). The weight of glass fiber (w_{mbf}), banana fiber (w_{mbf}), and the matrix was determined for each layer of the fiber specimen, and these weights were utilized for every layer of glass fiber and banana fiber. These properties were used in Equation 3.1 and Equation 3.2. These data were obtained from previous studies because the manufacturer did not provide the datasheet.

Table 3.2
Property of density and weight of fiber and matrix (Kotla Rachana, 2020), (Prabhu et al., 2021)

Property	Value	Unit
Density Glass Fiber (ρ_{gf})	2.5	g/cm^3
Weight of Glass Fiber (w_{gf})	1.086	g
Density of Banana Fiber (ρ_{bf})	1.250	g/cm^3
Weight of Banana Fiber (w_{bf})	0.466	g
Density of Matrix (ρ_m)	1.1	g/cm^3
Weight of matrix for glass fiber (w_{mgf})	0.854	g
Weight of matrix for banana fiber (w_{mbf})	2.561	g

3.3 Finite Element Simulation

This study employed Abaqus finite element (FE) software for simulating tensile tests. Abaqus offers a comprehensive suite of features ideally suited for this analysis, including a vast material library, contact surface definition tools, diverse element selection, various meshing options, and advanced load application methods.

3.3.1 Create the Part of Specimen

The part was sketched as illustrated in Figure 3.15, adhering to the dimensions and shape of the specimen described in Section 3.2.2. A 3D deformable shell planar component was then generated, utilizing the sketched 2D shape along with a

conventional shell section to represent the part's thickness.

The model was developed using the 'SI (mm)' unit system, as indicated in Table 3.3. This means that all measurements and calculations throughout the modeling process, from the initial creation of parts to the final results by referring to the International System of Units (SI) (Started & Edition, n.d.), specifically using millimeters for length. By standardizing the SI unit system, consistency and accuracy are maintained across all stages of the modeling and simulation process. This approach ensures that all dimensions, material properties, and other relevant parameters are correctly scaled and interpreted, leading to reliable and precise outcomes.

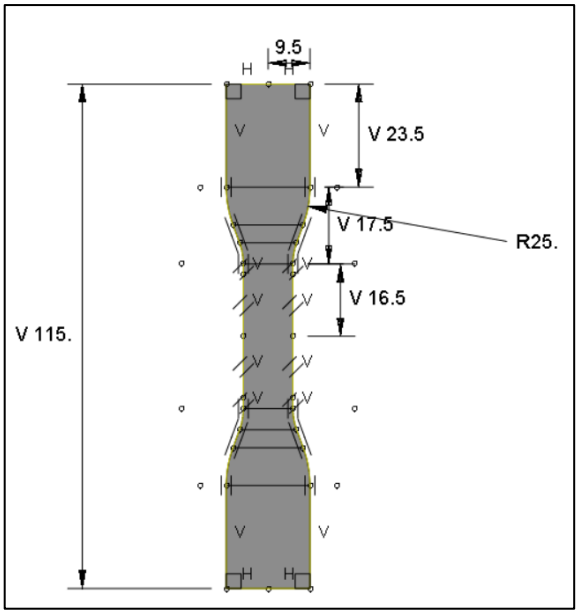

Figure 3.15 Sketching part

Table 3.3

Unit for Abaqus (Started & Edition, n.d.)

Quantity	SI	SI (mm)	US Unit (ft)	US Unit (inch)
Length	m	mm	ft	in
Force	N	N	lbf	lbf
Mass	kg	tonne (10^3 kg)	slug	lbf·s²/ft
Time	s	s	s	s
Stress	Pa (N/m²)	MPa (N/mm²)	lbf/ft²	psi (lbf/in²)
Energy	J	mJ (10^{-3} J)	ft·lbf	in·lbf
Density	kg/m³	tonne/mm³	slug/ft³	lbf·s²/in⁴

3.3.2 Composite Material Property Simulation

To ensure accurate modeling simulations, it was essential to import data sets from reliable sources such Monzón et al. (2019)(Monzón et al., 2019) and Koloor et al. (2020) (Koloor et al., 2020). By meticulously importing and defining these data sets, the simulation reflected real-world behavior more closely, leading to a more reliable and valid results. This careful preparation was a critical step in the simulation process, as it formed the foundation for generating a realistic and accurate simulation, ensuring that the final model accurately represented the intended design and operational conditions.

It was assumed that both glass fiber epoxy and banana fiber epoxy materials exhibited anisotropic and orthotropic characteristics(Abaqus, 2006). Anisotropic materials have directionally dependent properties, meaning their mechanical or physical properties vary based on the direction of the applied forces. In this case, the elastic properties of these materials, such as Young's modulus, shear modulus, and Poisson's ratio, differ along different axes, indicating their anisotropic nature.

Elastic behaviour in Abaqus is the ‘lamina property’ and requires six composite properties: E_1, E_2, V_{12}, G_{12}, G_{13}, and G_{23} (Started & Edition, n.d.).
E_1 - axial stiffness of the composite, E_2 - transverse stiffness of the composite, V_{12} - Poison’s ratio of the composite, G_{12} - axial shear stiffness, G_{13} - shear stiffness (stress) acting in the 1 direction on a plane with a normal in the 3 direction, G_{23} - shear stiffness (stress) acting in the 2 direction on a plane with a normal in the 3 direction.

Conversely, orthotropic materials have three mutually perpendicular planes of symmetry, where properties differ along each axis but remain uniform within each plane. For glass fiber epoxy and banana fiber epoxy, the behavior related to damage initiation (the point at which damage begins) and damage evolution (how the damage progresses) was considered orthotropic. This implied that the way these materials initiated and propagated damage varies along the three principal material directions but were consistent within each directional plane.

‘Damage initiation and evaluation behaviour’ in Abaqus was set to ‘Hashin’ property. There are having ten composite properties: X_T, X_C, Y_T, Y_C, S_L, S_T, G_{XT}, G_{XC}, G_{YT} and G_{YC} (Koloor et al., 2020).

X_T – longitudinal tensile strength, X_C – longitudinal compressive strength, Y_T – transverse tensile strength, Y_C - transverse compressive strength, S_L - longitudinal shear strength, S_T - transverse shear strength, G_{XT} - longitudinal tensile fracture energy, G_{XC} - longitudinal compressive fracture energy, G_{YT} - transverse tensile fracture energy and G_{YC} - transverse compressive fracture energy.

3.3.3 Extraction Material Properties Simulation

The 'Lamina Property' and 'Hashin Property' were used to model the specimens accurately. These properties defined the behavior and characteristics of the composite materials under different conditions. To generate a realistic simulation model, these material properties were meticulously extracted from several credible sources. By integrating these properties into the simulation, it became possible to predict how the composite materials would respond to various stresses and strains, thereby providing valuable insights into their tensile properties and overall mechanical behaviour.

Table 3.4 shows that the lamina properties for banana fiber + resin and glass fiber + resin which were referred from Monzón et al. (2019) (Monzón et al., 2019) and Morton (2010) (Morton, 2010), respectively. Meanwhile, Table 3.5 presented the Hashin material properties for glass fiber + resin, which were derived from Koloor et al. (2020) (Koloor et al., 2020). However, as material properties for banana fiber + epoxy were limited in previous study, this study utilized the Hashin material properties from Koloor et al. (2020) (Koloor et al., 2020; Monzón et al., 2019).

Table 3.4
Lamina property(Monzón et al., 2019) (Morton, 2010)

Property	Unit	Banana Fiber + Resin	Glass Fiber + Resin
E_{11}	MPa	1286.7	27380
E_{22}	MPa	1288.8	3005
V_{12}	NA	0.384	0.272
G_{12}	MPa	453.2	1090
G_{23}	MPa	449.1	1090
G_{31}	MPa	449.2	1141

Table 3.5

Hashin property (Koloor et al., 2020)

Property	Unit	Banana Fiber + Resin	Glass Fiber + Resin
X_T	MPa	1340	820
X_C	MPa	1192	500
Y_T	MPa	19.6	80.6
Y_C	MPa	92.3	322
S_L	MPa	51	54.5
S_T	MPa	23	161.2
G_{XT}	N/mm	48.4	32
G_{XC}	N/mm	60.5	20
G_{YC}	N/mm	4.5	4.5
G_{YC}	N/mm	8.5	4.5

3.3.4 Import Material Property of Banana Fiber and Glass Fiber

Firstly, the material properties for both banana fiber and glass fiber were created in the material manager as shown in Figure 3.16. As detailed in section 3.3.3, on the extraction of material properties, the properties for Lamina and Hashin should be imported, as referenced in Table 3.4 and Table 3.5. This involved using specific values for tensile strength, elasticity, and other mechanical properties derived from the cited studies. The density of the specimens in the simulation was set same as the experimental density measurements to maintain consistency and accuracy. By accurately inputting these properties, the simulation closely reflected the real behaviour of the composite materials.

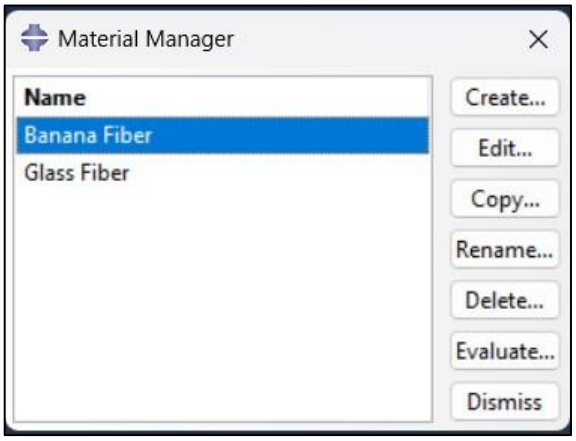

Figure 3.16 Saved material properties in material manager

Access the elastic region by opened Mechanical > Elasticity in Figure 3.17 of the Material Manager. Then, 'Lamina' was chosen and key in the material properties (E_1, E_2), Poisson's ratio (V_{12}), and shear modulus (G_{12}, G_{13}, G_{23}).as shown Figure 3.18.

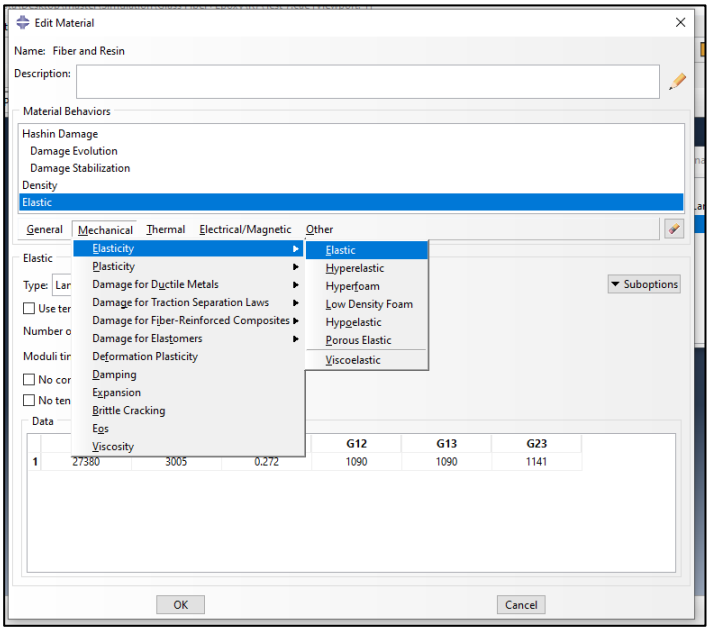

Figure 3.17 Create material property

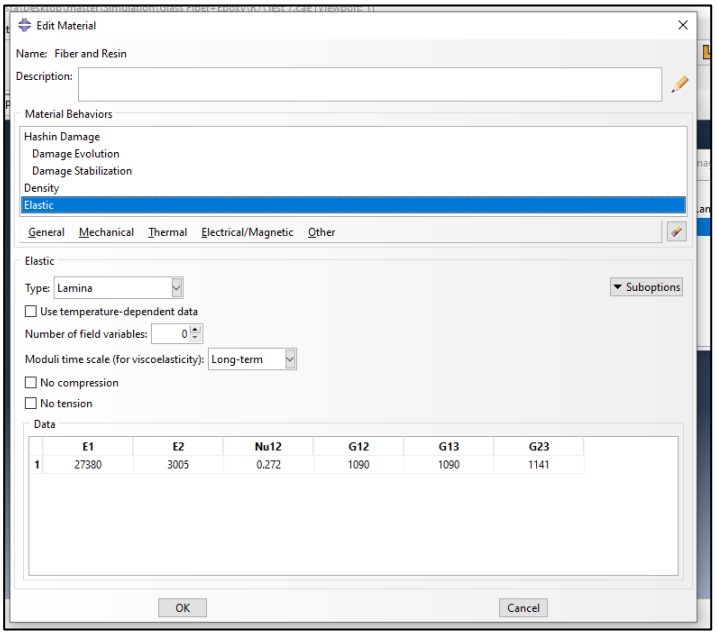

Figure 3.18 Input lamina property

For the plastic region, Hashin mode was selected as the property model. Choose 'Damage for Fiber-Reinforced Composites' and select Hashin Damage. After that, material properties X_T (tensile strength in the fiber direction), X_C (compressive strength in the fiber direction), Y_T (tensile strength in the transverse direction), Y_C (compressive strength in the transverse direction), S_L (shear strength in the longitudinal direction), and S_T (shear strength in the transverse direction) as indicated in Figure 3.19 were key in. This step defined that the material behaves under plastic deformation according to the Hashin damage model.

To perform damage evaluation, input the parameters G_{XT}, G_{XC}, G_{YT}, and G_{YC} was input as illustrated in Figure 3.20. These parameters represented the shear strength of the material under different loading conditions: G_{XT} is the shear strength in the X direction under tension, G_{XC} is the shear strength in the X direction under compression, G_{YT} is the shear strength in the Y direction under tension, and G_{YC} is the shear strength in the Y direction under compression.

Next, was to input the damage stabilization property as depicted in Figure 3.21. This step involved techniques to stabilize the damage, which could include stress redistribution, material hardening, or applying repair methods such as patching or reinforcing the damaged area. These steps ensured that the material or structure remained stable and maintained its integrity despite the damage.

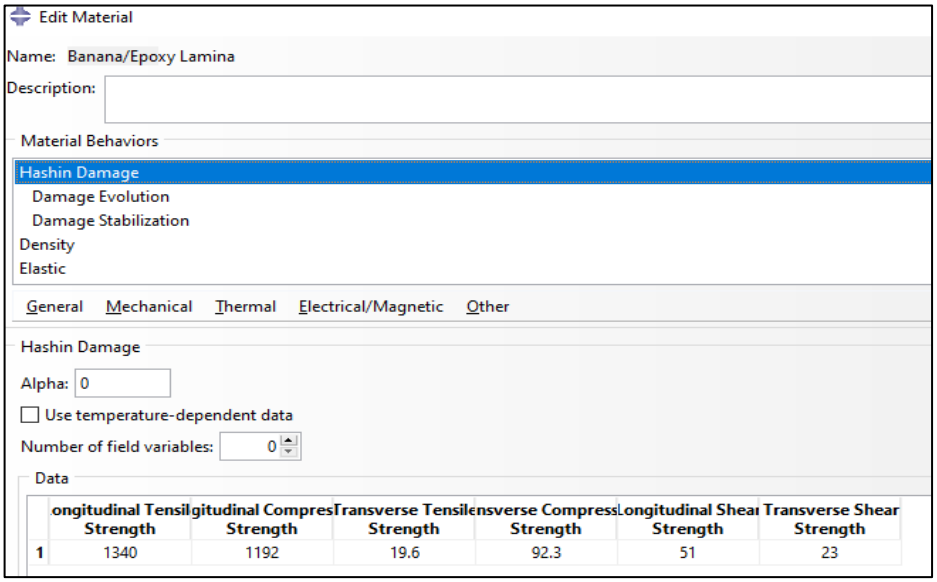

Figure 3.19 Hashin property

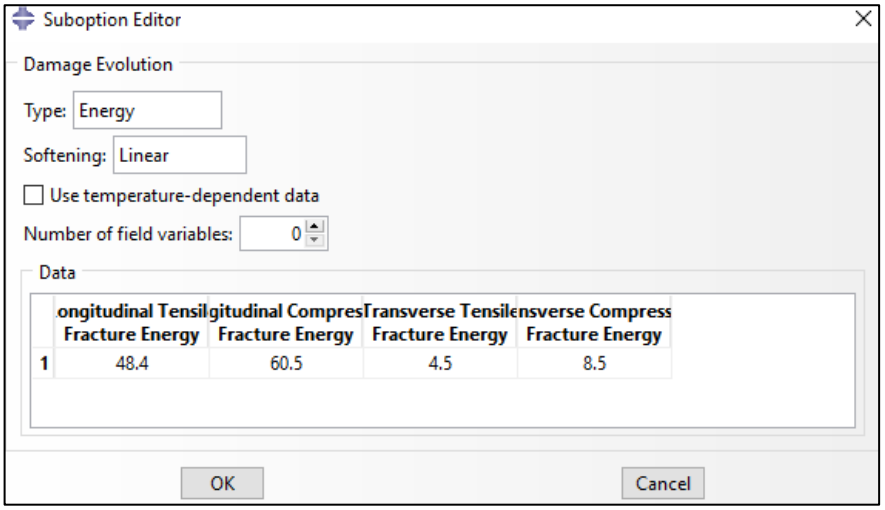

Figure 3.20 Damage evaluation property

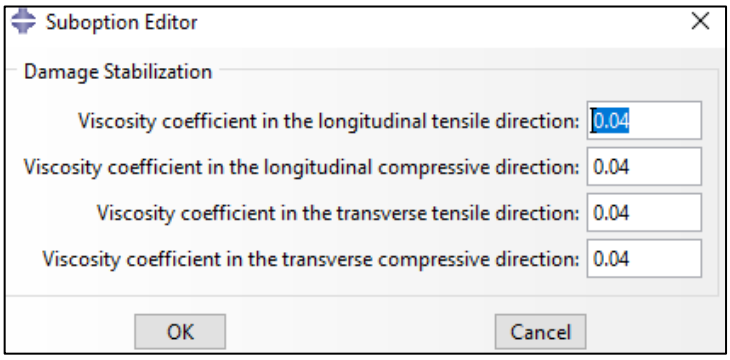

Figure 3.21 Damage stabilization property

3.3.5 Set Layup Lamination

Figure 3.22 shows the arrangement of banana fiber and glass fiber in a composite layup with 9 plies, using the saved properties described in section 3.3.4. This served as an example for creating Laminate 3 (L3).

This process involved organizing the layers of composite materials in a specific sequence to achieve the desired mechanical characteristics based on experimental data and as detailed in Table 3.4. The ply layup consists of 9 individual plies, each representing a single layer of material and using 0° angles.

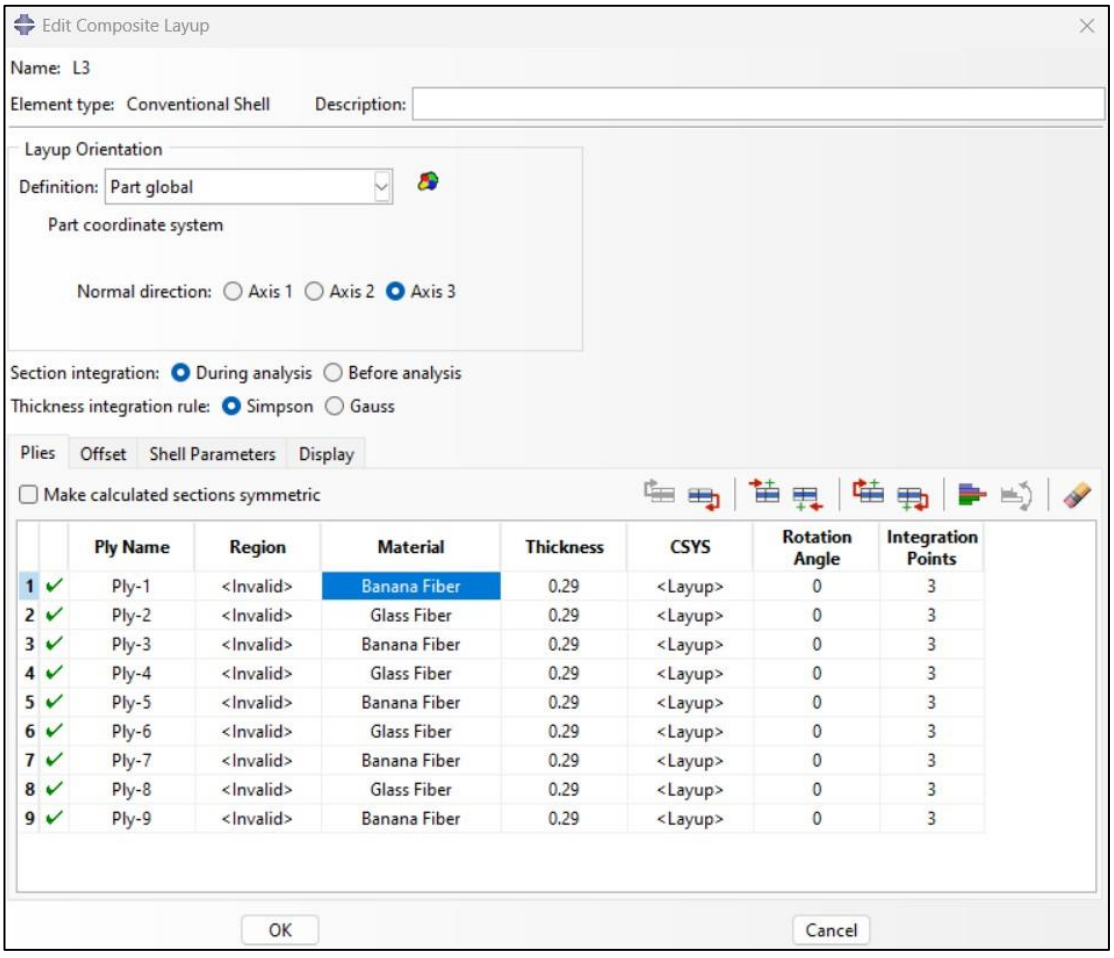

Figure 3.22 Nine composite layup

3.3.6 General Static Step

As shown in Figure 3.23, the simulation step chosen for this study was 'General Static' because it is suited to the nonlinear analysis required for composite materials. The composite material under study exhibited complex, nonlinear behavior, making nonlinear analysis essential to accurately capture its stress-strain relationship and failure mechanisms. 'General Static' analysis is designed to handle static loading conditions and can account for large deformations and material nonlinearities, providing a robust method for investigating the performance of composite materials under various loading scenarios. This method ensured a balance between computational efficiency and accuracy, which was crucial for obtaining detailed insights into the material's behaviour without excessively long computation times (Abaqus, 2006).

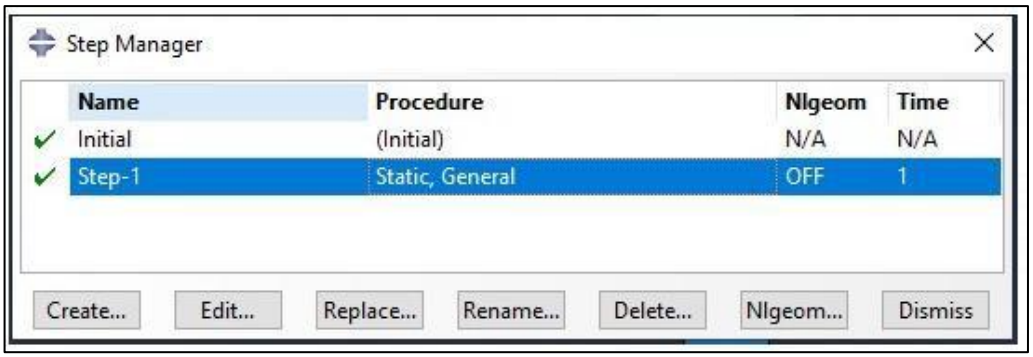

Figure 3.23 Step manager

3.3.7 Meshing Model Structure

The mesh structure of the model was designed using only quadrilateral (quad) elements, specifically quad shell elements, to ensure accurate and efficient simulation results. Quadrilateral elements were chosen due to their superior performance in capturing geometry and stress distribution. As illustrated in Figure 3.24, the mesh was structured with five nodes along the length of the part, which was essential for accurately applying boundary conditions later in the 'Load' step. The "edge by number" process was employed to seed the top and bottom edges of the part, ensuring the creation of the correct number of elements. By selecting the top and bottom edges and specifying an even number of elements, the mesh was evenly divided, resulting in uniform element distribution. This structured mesh with five nodes along the part simplified the

application of boundary conditions, allowing for precise and consistent application of loads, constraints, and other boundary conditions, ultimately leading to more reliable simulation results.

The convergence analysis graph in Figure 3.25 shows that the load increased markedly as the number of nodes rose from 2.5 to 3.5, growing from around 2.7 kN to 5.3 kN. After this range, the load values began to level off, reaching approximately 5.8 kN at five nodes. This pattern demonstrates that the results had converged, as further increases in node count caused only minor changes in the load. Consequently, the model achieved convergence at five nodes, indicating that this mesh density was adequate for producing accurate and reliable simulation results.

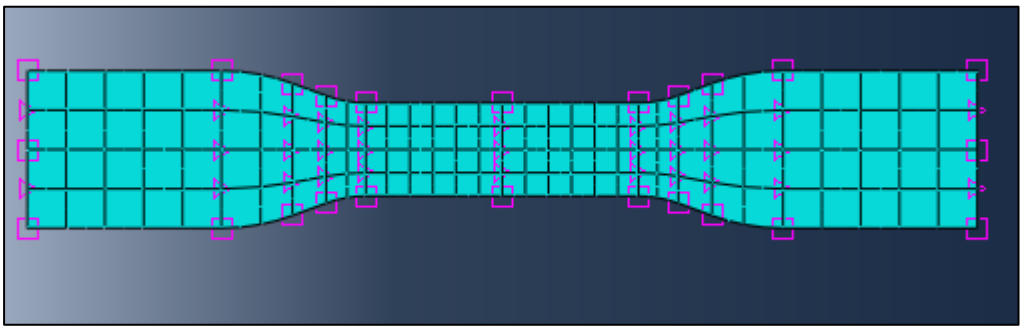

Figure 3.24 Meshing the part with 5 nodes

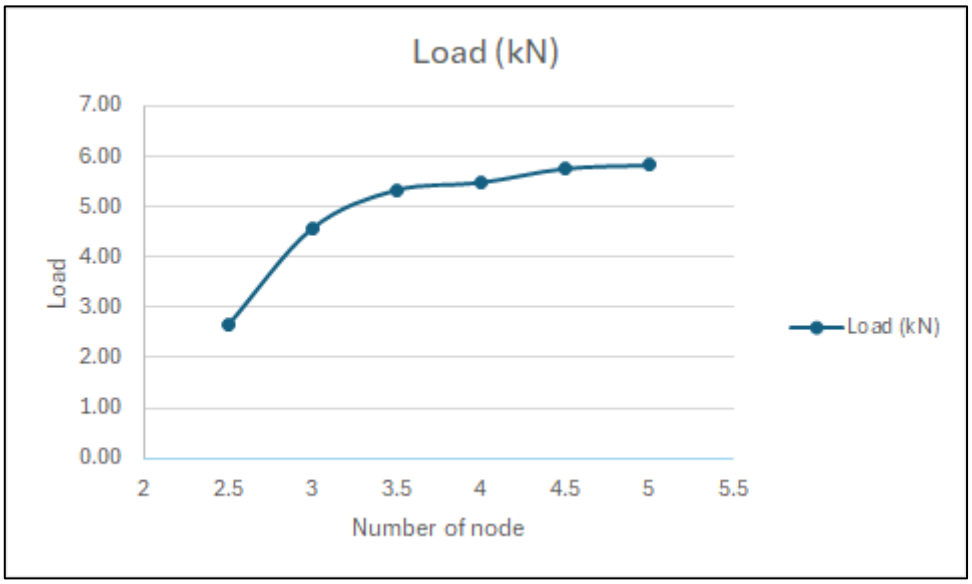

Figure 3.25 Convergence Analysis

3.3.8 Setting Boundary Condition (BCs)

The boundary conditions (BCs) were crucial for accurately modeling the physical test by specifying the constraints and displacements on the created part to closely match the physical test conditions.

Node sets were created at the top and bottom of the specimen, as illustrated in Figure 3.26. A displacement boundary condition was then applied to simulate the effect of a tensile force being exerted on the specimen, pulling it in the direction of the force.

This setup allowed for the accurate simulation of a tensile test, where the applied displacement at the top pulled the specimen, and the fixed bottom-maintained stability, ensuring that the stresses, strains, and deformation patterns observed in the simulation closely matched those in the actual physical test, thereby providing reliable and meaningful results.

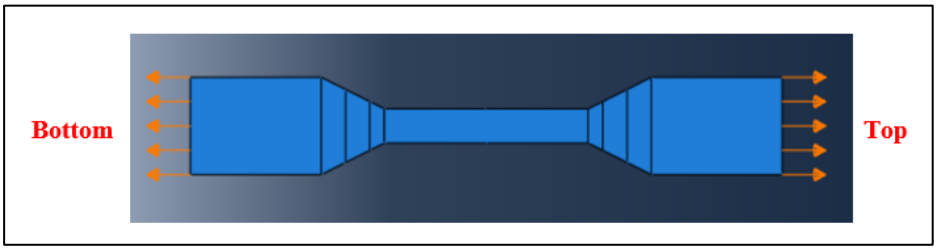

Figure 3.26 Boundary condition of part in Top and Botto

CHAPTER 4
RESULT AND DISCUSSION

4.1 Introduction

This topic addresses the results of simulations and experiments involving glass fiber and banana fiber with various configurations. By analyzing the tensile properties of these fibers under different configurations, the goal is to identify the optimal tensile properties. Finally, the tensile properties obtained from the simulation results are validated against the experimental results.

4.2 Finite Element Model Validation

Figure 4.1 to Figure 4.6 show the specimens that were subjected to a tensile test according to ASTM D-638. The tests were conducted at a controlled rate of 1 mm/min to ensure consistent loading conditions for all specimens.

In simulation the contour plot L1 (Figure 4.1(b)), L3 (Figure 4.3 (b)), L4 (Figure 4.3 (b)) and L6 (Figure 4.6 (b)) show the highest stress concentrations were observed in the middle sections of each specimen, likely due to their smallest cross-sectional areas. This was indicated by the color scale, with red representing the highest stress and blue the lowest. Such stress concentration is typical in tensile tests and highlights potential failure points under tensile loading. The color scale exhibited a linear gradient from the center towards the ends of the specimens, suggesting they were subjected to a uniform tensile load. This resulted in a consistent variation in stress along the length, with a uniform stress distribution across the cross-section at any given point, indicating that the tensile test was accurately simulated with evenly applied loads(Monzón et al., 2019).

When comparing the experimental specimens for configurations L1 (Figure 4.1 (a)), L3 (Figure 4.3(a)), L4 (Figure 4.4 (a)), and L6 (Figure 4.6 (a)), it was observed that even though the tensile test reached the maximum tensile load, the specimens did not completely fracture. Instead, they developed cracks, primarily because the stress was uniformly distributed across the middle section of the specimens(Monzón et al., 2019).

While the simulation L2 (Figure 4.2 (b)) and L5 (Figure 4.5 (b)), where banana fibers outnumber glass fibers significantly, the stress distribution shows a distinct pattern. The contour plot stress decreases from the center toward the edges, a phenomenon rooted in the distinct mechanical properties of the fibers. Glass fibers, known for their superior strength and stiffness, bear a larger portion of the load, resulting in higher stress concentrations in the central region of the specimen. As the load is transferred outward towards the edges, where banana fibers are more prevalent, the stress diminishes. This was due to banana fibers being less stiff and less strong, making them less effective at resisting the applied load. The adhesion loss between the fibers and the matrix led to the initiation of fiber breakage and pull-out (Reddy et al., 2020). Consequently, the material exhibits a stress gradient, with higher stress levels at the center and lower levels at the edges—a characteristic common in uniformly loaded composite materials, where stronger materials are positioned to handle more stress in the central regions, and weaker materials manage less stress towards the periphery.

In the experimental specimen L2, as depicted in Figure 4.2 (a), this stress distribution pattern leads to the formation of a crack, particularly at the top middle, indicating that the specimen is on the verge of failure at this location (Monzón et al., 2019), (Xin et al., 2017). This partial damage reflects the uneven distribution of stress and the material's varying resistance across different regions. On the other hand, in the experimental specimen L5 as shown in Figure 4.5 (a), the stress gradient and the material's inability to uniformly resist the applied load have resulted in complete failure, as evidenced by the specimen breaking apart entirely. This complete breakage in L5 highlighted the critical influence of fiber composition and distribution on the structural integrity of the composite material under stress.

This condition mirrors what might happened in an experiment as Figure 4.6 (a) where a specimen, after being subjected to maximum tensile stress, remained intact at its center but exhibited signs of laminate peeling at the edges(Monzón et al., 2019). This peeling or delamination at the edges could be attributed to the specific composition of the laminate, particularly the L6 configuration, which includes six layers of glass fiber and three layers of banana fiber.

In conclusion, the difference in mechanical properties between glass fiber and banana fiber can play a significant role. Glass fiber typically has higher tensile strength and stiffness compared to banana fiber. When these materials are combined in a laminate, the glass fibers bear a greater portion of the applied load, especially at higher

stress levels, while the banana fibers, being less stiff and strong, might not provide the same level of reinforcement. The glass fibers, being stiffer, could resist deformation, while the banana fibers might begin to separate, especially if the adhesive bond between layers is not strong enough to handle the differential strain (Jubair et al., 2021).

Therefore the analysis of simulated specimens with contour plots containing a higher proportion of glass fiber compared to banana fiber revealed the following stress values, arranged from highest to lowest: L1 in Figure 4.1(b) experienced the highest stress about 3.404 MPa, followed by L6 in Figure 4.6 (b) with approximately 2.27 MPa, L4 in Figure 4.4 (b) with about 1.033×10^{-1} MPa, L3 in Figure 4.3 (b) with around 2.756×10^{-2} MPa, L5 in Figure 4.5 (b) with approximately 1.449×10^{-2} MPa, and L2 in Figure 4.2 (b) with approximately 1.327×10^{-3} MPa.

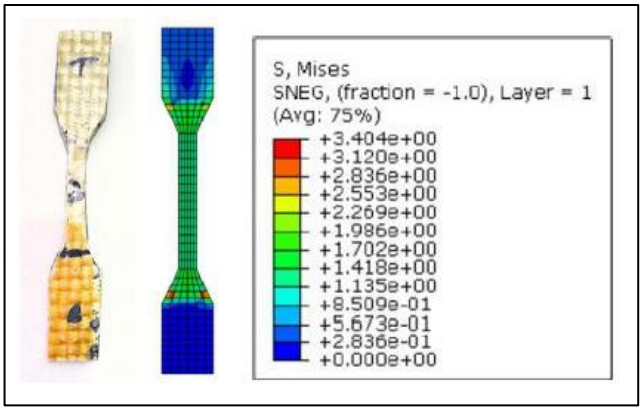

(a) (b)

Figure 4.1 Specimen L1 after tensile test (a) Experiment (b) Simulation

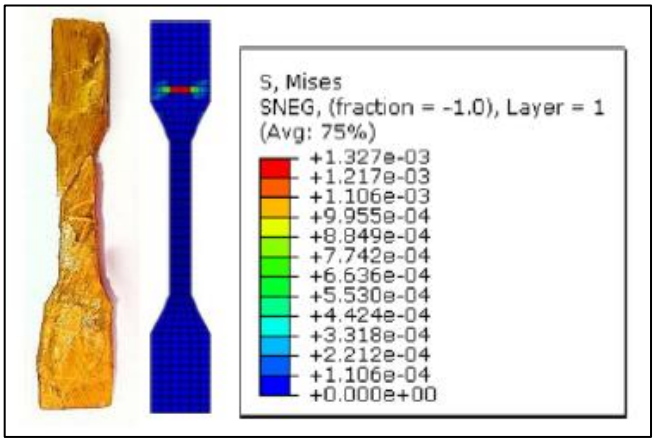

(a) (b)

Figure 4.2 Specimen L2 after tensile test (a) Experiment (b) Simulation

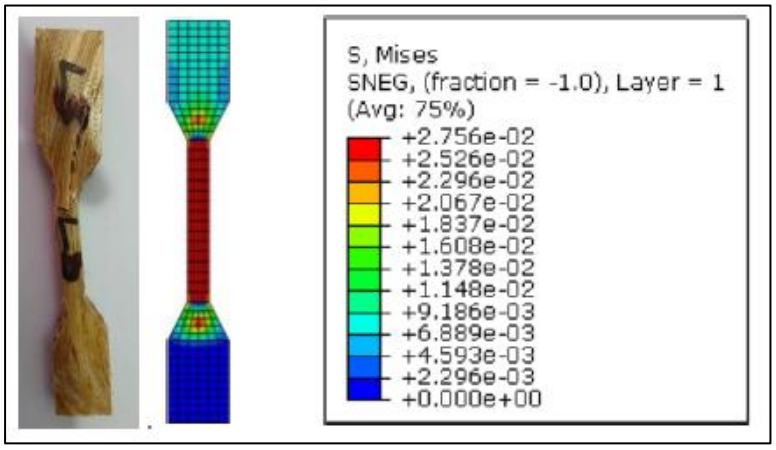

(a) (b)

Figure 4.3 Specimen L3 after tensile test (a) Experiment (b) Simulation

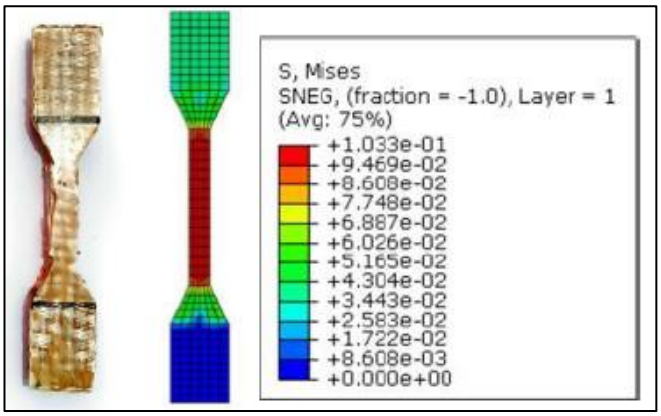

(a) (b)

Figure 4.4 Specimen L4 after tensile test (a) Experiment (b) Simulation

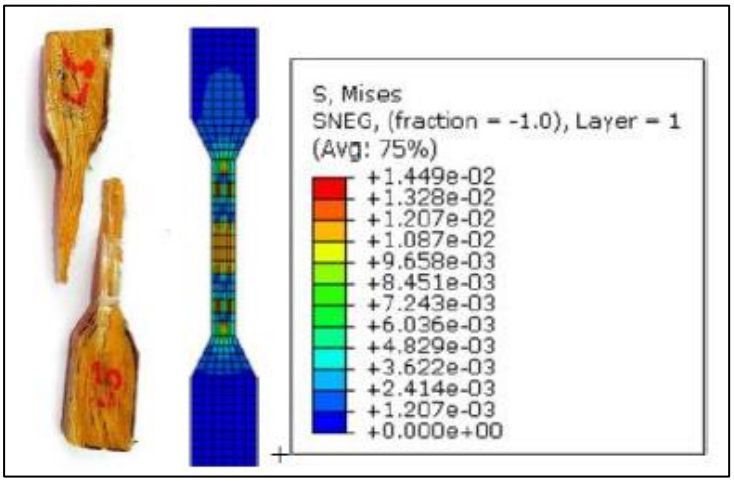

(a) (b)

Figure 4.5 Specimen L5 after tensile test (a) Experiment (b) Simulation

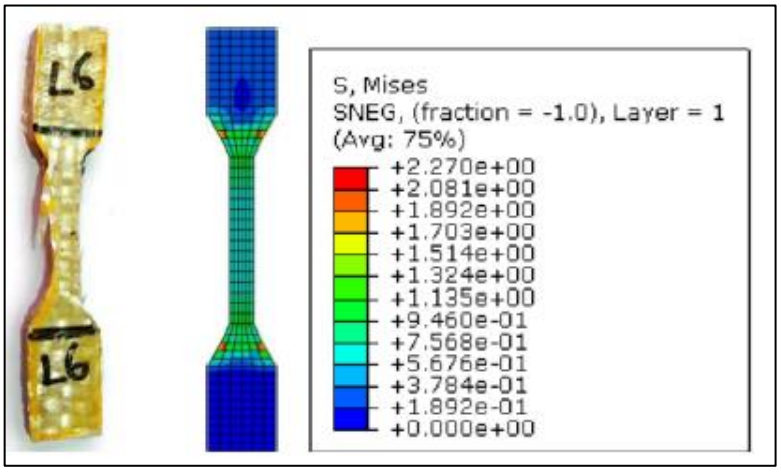

(a) (b)

Figure 4.6 Specimen L6 after tensile test (a) Experiment (b) Simulation

4.3 Volume Fraction Analysis

Table 4.1 shows the volume fraction of six different laminate configurations (L1 to L6), each composed of varying layers of glass fiber (GF), banana fiber (BF), and matrix material. A sample calculation of the fiber and matrix volume fractions is provided in Appendix A.

Laminate L1 was composed of nine layers of glass fiber without any banana fiber, resulting in the highest total fiber weight of 9.78 grams and a relatively low matrix weight of 7.682 grams. This configuration yielded the highest fiber volume fraction (V_f) of 35.9% and a matrix volume fraction (V_m) of 64.1%. The high fiber density of 22.5 g/cm³ contributed significantly to the total fiber weight, even with less matrix content. As a result, Laminate L1 exhibited the highest mechanical properties among all configurations, primarily due to its increased fiber volume fraction (M.R.M.Rejab, 2008).

In contrast, Laminate L2 used nine layers of banana fiber with no glass fiber. Due to the lower density of banana fiber (11.3 g/cm³), the total fiber weight was only 4.190 grams, while the matrix weight was significantly higher at 23.046 grams. This resulted in a low fiber volume fraction of 13.8% and a matrix volume fraction of 86.2%. From the calculation lower density of banana fiber directly impacted the weight contribution from the fiber portion, highlighting how density and layer count together influence the final weight distribution(Messiry, 2013).

Laminate L3 incorporated four layers of glass fiber and five layers of banana fiber. This hybrid arrangement resulted in a combined fiber density of 16.3 g/cm³,

contributing to a total fiber weight of 6.673 grams and a matrix weight of 16.217 grams. As a result, the fiber volume fraction was 20%, while the matrix volume fraction was 80%. In comparison, Laminate L4 consisted of five layers of glass fiber and four layers of banana fiber, yielding a higher combined fiber density of 17.5 g/cm³. This led to an increased fiber weight of 7.29 grams and a reduced matrix weight of 14.510 grams. Consequently, the fiber volume fraction increased slightly to 22.1%. The mechanical properties of the laminate improved in correlation with the increase in fiber volume fraction. (Ciprian et al., 2015).

Laminate L5, consisting of six layers of glass fiber and three layers of banana fiber, had a lower combined fiber density of 15 g/cm³. It recorded a total fiber weight of 6.052 grams and a matrix weight of 17.925 grams. In comparison to Laminate L2, which was made entirely of banana fiber, the fiber volume fraction in L5 was higher due to the incorporation of glass fibers alongside natural fibers. In addition to the notable improvement in mechanical properties, the presence of glass fiber helped reduce the variability (standard deviation) in those properties, which typically arises from the inconsistent structure of natural fibers (Kureemun et al., 2018).

Lastly, Laminate L6 featured a reversed hybrid layout with three layers of glass fiber and six layers of banana fiber, leading to the highest hybrid fiber density of 18.8 g/cm³ among the mixed configurations. It achieved a fiber weight of 7.92 grams and a matrix weight of 12.803 grams. Among the hybrid laminates, L6 had the highest fiber volume fraction at 24.6%, which is the lowest banana fiber weight and it has shown highest strength values compared with the other hybrid composite sample (Batu & Lemu, 2020).

Table 4.1

Volume of fraction fiber and matrix

Laminate		L1	L2	L3	L4	L5	L6
Layer	**Banana Fiber**	0	9	5	4	3	6
	Glass Fiber	9	0	4	5	6	3
Total Density (g/cm^3)	**Matrix**	9.9	9.9	9.9	9.9	9.9	9.9
	Fiber	22.5	11.3	16.3	17.5	15.0	18.8
Total Weight (g) GF+BF	**Matrix**	7.682	23.046	16.217	14.510	17.925	12.803
	Fiber	9.78	4.19	6.67	7.29	6.05	7.92
Volume Fraction (%)	**Matrix (V_m)**	64.1	86.2	80.0	77.9	81.8	75.4
	Fiber (V_f)	35.9	13.8	20.0	22.1	18.2	24.6

4.4 Strength Analysis of Different Configurations

Tensile testing was performed using a Universal Testing Machine (UTM) in the Civil Engineering Laboratory for Strength Testing at UiTM Pulau Pinang, Malaysia, where the machine recorded Load vs. Displacement and Stress vs. Strain data. These results were utilized to determine the optimal tensile properties of glass fiber and banana fiber in various configurations.

Similarly, finite element analysis (FEA) simulations in Abaqus produced corresponding Load vs. Displacement and Stress vs. Strain data. The experimental and simulation results were then compared to validate the tensile properties obtained from the simulations [7].

Figure 4.7 through Figure 4.18, which depict the Load vs. Displacement and Stress vs. Strain curves for Laminates 1 through 6, feature two data series where the orange line represents the actual experimental data, and the blue dashed line corresponds to the simulation results.

4.4.1 Laminate 1 (L1)

Figure 4.7 presents the experimental and simulation results of Load versus Displacement for L1. Initially, both curves exhibit a linear increase as the applied load increases, continuing this trend until reaching their respective peak loads. The experimental results show a peak load of 5.96 kN at a displacement of 6.42 mm, while the simulation results indicate a maximum load of 5.83 kN at 7.45 mm. These peak values represent the material's maximum load capacity, signifying the complete failure of the matrix material in the laminate. The remaining portion of the graph illustrates the progressive failure of the reinforcing material (Prem Chand et al., 2021).

This result is essential for verifying whether the experimental outcome meets the required specifications based on the selected method. To ensure accuracy, the experimental result was compared with data from Stanciu et al. (2021) (Stanciu et al., 2021), which reported a value of 5.738 kN. The calculated percentage error was approximately 3.83%, demonstrating that the experimental results fell within an acceptable range as detail in Section 2.6.

Additionally, the comparison between the experimental and simulation results reveals a close alignment in both load-displacement. The discrepancies are minimal,

with only a 2.18% variation in ultimate load (kN), where the experiment yielded 5.96 kN and the simulation produced 5.83 kN.

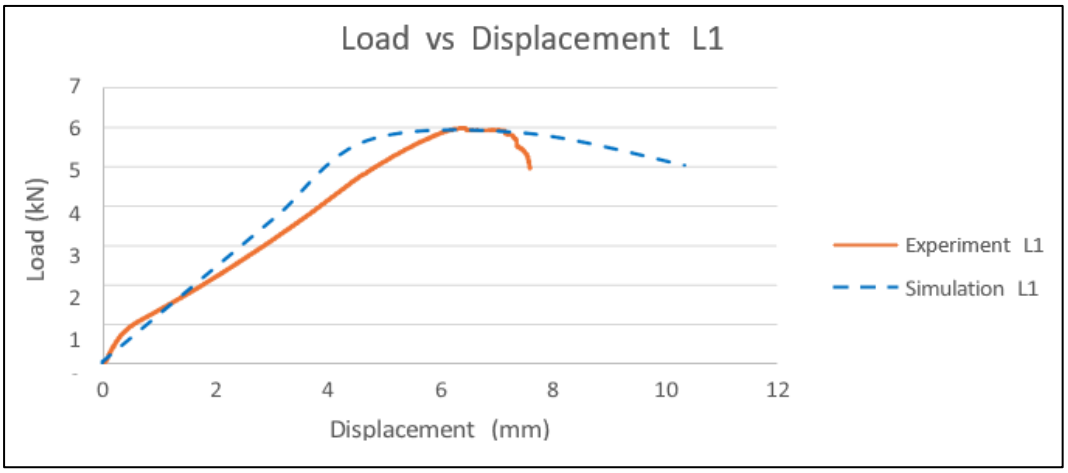

Figure 4.7 Load vs displacement curve for L1

Figure 4.8 presents the stress-strain curve for L1, comparing experimental and simulation results to provide key insights into its tensile behaviour. Initially, the curve follows a linear trend at low strain values. This linearity persists until the material reaches its ultimate tensile strength. The peak stress, representing the ultimate tensile strength, was recorded at 119.46 MPa with a strain of 10.94% in the experiment and 119.06 MPa with a strain of 13.55% in the simulation. This corresponds to a 0.33% variation in ultimate stress between the experimental and simulation results. Furthermore, the obtained values align with the reported range of ultimate stress from previous studies, such as 120 MPa by Prem Chand et al. (2021) (Prem Chand et al., 2021)and 228 MPa by Stanciu et al. (2021) (Stanciu et al., 2021), confirming that the results fall within an acceptable range, as detailed in Section 2.6.

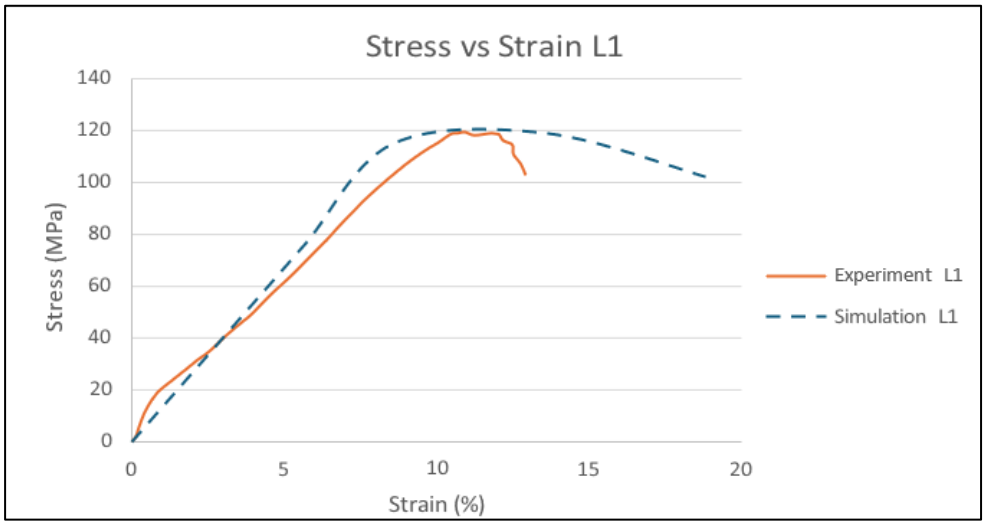

Figure 4.8 Stress vs strain curve for L1

4.4.2 Laminate 2 (L2)

The graph in Figure 4.9 illustrates the relationship between load and displacement, comparing experimental data with simulation data for L2. Both the experimental and simulation curves exhibit an upward trend, indicating that as displacement increases, the load required also increases(Sanjay et al., 2016). In the initial phase, both curves exhibit a relatively steep slope. In the mid-region, the curves become less steep, with the experimental curve reaching 1.13 kN at a displacement of 4.02 mm, while the other curve attains 1.11 kN at a displacement of 3.42 mm. Towards the final stage, the curves gradually flatten out. The peak load values are considered acceptable, as they fall within the acceptable range based on previous references, as detailed in Section 2.6 (Sanjay et al., 2016)(Monzón et al., 2019)(Sampath et al., 2021).

Moreover, the experimental and simulation curves show some similarities. The simulation curve generally lies above the experimental curve, indicating that the simulation predicts slightly higher load for a given displacement compared to the actual experiment [48]. The ultimate load recorded in the experiment is 1.13 kN, while the simulation predicts an ultimate load of 1.11 kN. This comparison indicates that the results for load displacement are closely aligned, with only a slight discrepancy of 1.77% in the ultimate load (kN).

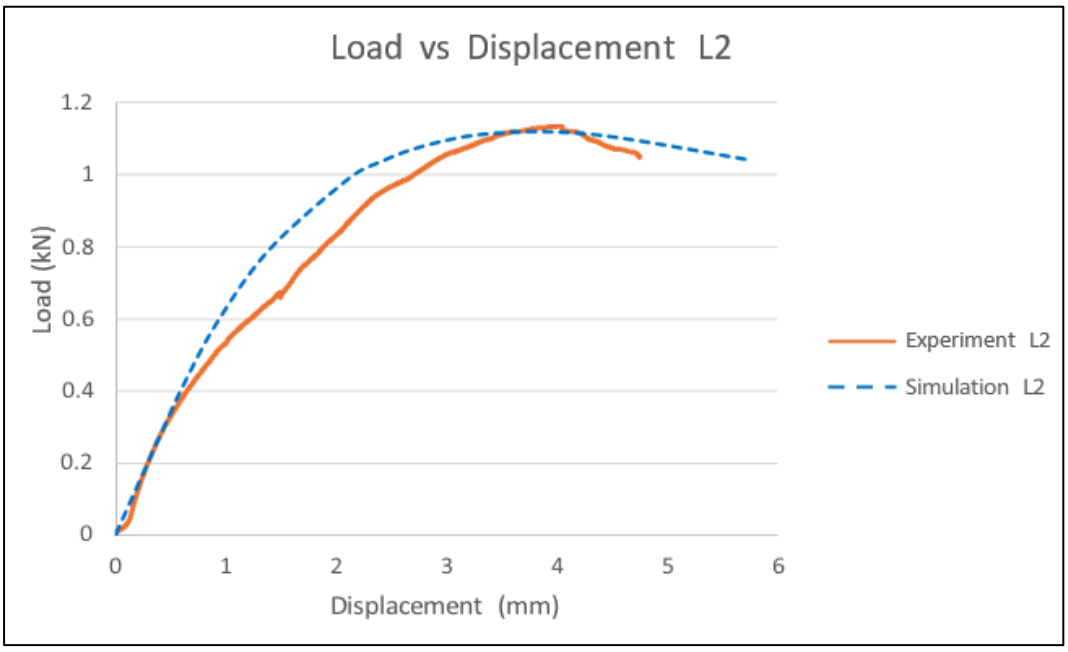

Figure 4.9 Load vs displacement curve for L2

Figure 4.10 illustrates a comparison of the stress-strain behaviour observed in Experiment L2 and Simulation L2, revealing several key differences between the two datasets. Both curves demonstrate an increase in stress as strain increases. However, Simulation L2 initially exhibits a steeper slope in comparison to Experiment L2 (Al Rashid et al., 2020). In terms of peak stress and strain, Simulation L2 reaches a maximum stress of approximately 9.84 MPa at a strain of 6.82%, while Experiment L2 achieves a higher peak stress of 10.17 MPa at a strain of 8.05%. These results are deemed acceptable as they align with the expected range outlined in previous references, as detailed in Section 2.6 (Sanjay et al., 2016)(Moon et al., 2024).

The ultimate stress recorded in experiment L2 is 10.17 MPa, whereas simulation L2 predicts an ultimate stress of 9.84 MPa. This comparison highlights that the results for stress-strain are closely aligned, with only a slight discrepancy of 3.24% in the Ultimate Stress. This minor difference underscores a generally good agreement between the experimental and simulated results, despite the observed variations. Additionally, the comparison between glass fiber and banana fiber reveals that while both materials exhibit similar trends, banana fiber has lower mechanical properties than glass fiber (Karthick et al., 2022).

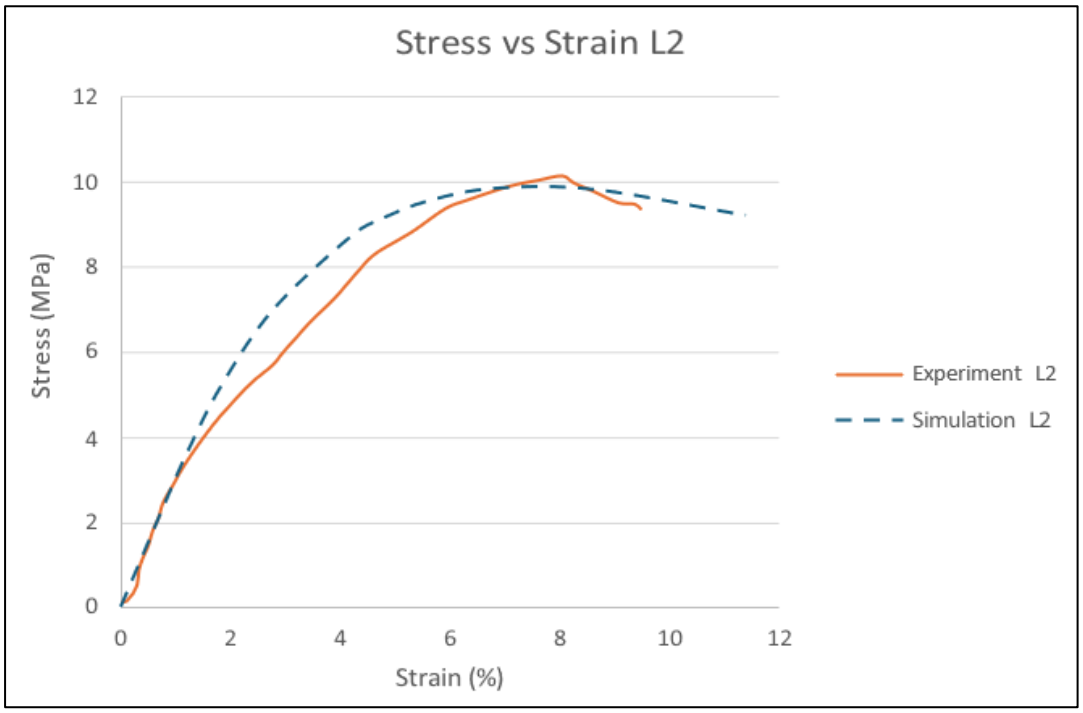

Figure 4.10 Stress vs strain curve for L2

4.4.3 Laminate 3 (L3)

The graph presented in Figure 4.11, is Load versus Displacement for experimental L3 and simulated data, illustrating the relationship between load and displacement. At the initial stage, both curves originate from the zero point then in the mid-region, the experimental curve exhibits a steeper slope compared to the simulation (Al Rashid et al., 2020), reaching a maximum load of 3.72 kN at a displacement of 6.92 mm, whereas the simulation records a maximum load of 3.78 kN at a displacement of 6.85 mm.

As a result, the ultimate load recorded in the experiment is 3.72 kN, while the simulation predicts a slightly higher ultimate load of 3.78 kN. The material failure in the laminate during the tensile test is attributed to fiber pull-out in the composite(Prem Chand et al., 2021). This comparison indicates a close agreement between the experimental and simulation load-displacement results, with only a minor discrepancy of 1.61% in the ultimate load.

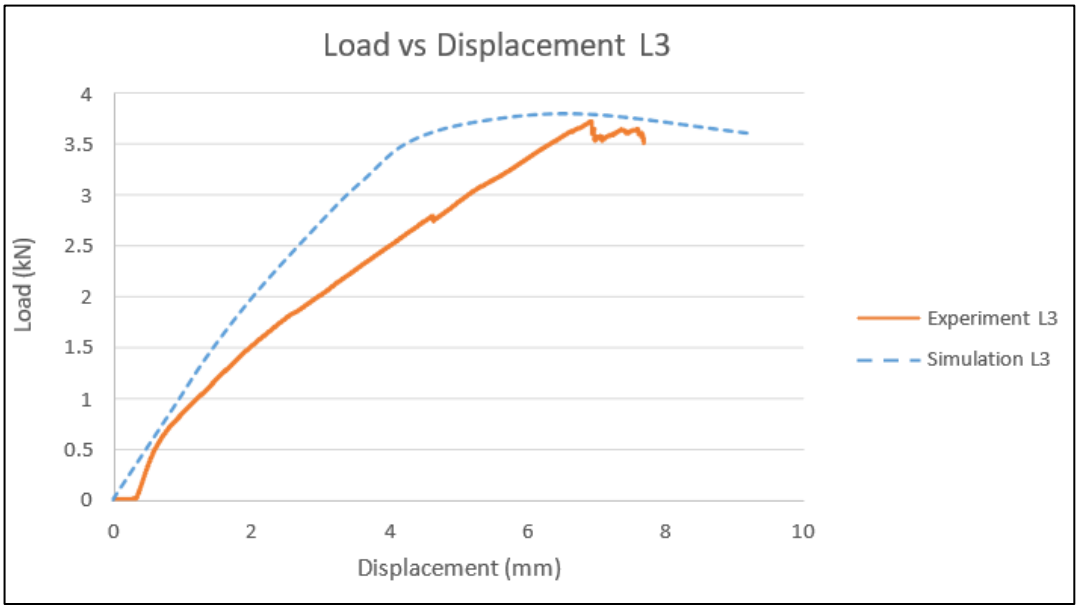

Figure 4.11 Load vs displacement curve for L3

Figure 4.12 presents a line graph showing the experimental and simulation Stress versus Strain curves for L3. Both the experimental and simulation curves follow a similar trend. Initially, stress increases almost linearly with strain, showing similar elastic behavior. The ultimate stress is reached at 36.57 MPa with a strain of 11.27% in the experiment, while in the simulation, it occurs at 36.77 MPa with a strain of 11.42%.

Both graph Load vs. Displacement and Stress-Strain curves, reveal a noticeable discrepancy in the slopes between the experimental and simulation results. This deviation arises due to factors such as void formation, uneven fiber distribution, and potential delamination of layers inherent in the hand layup technique. The FEA by used the ABAQUS software effectively captures the material's linear elastic behaviour across various stacking sequences. However, more advanced simulations are required to accurately model the plastic behaviour of composites, particularly for fatigue-related applications (Al Rashid et al., 2020).

The maximum stress, or strength, observed in the experiment is slightly higher than the simulation's prediction. For instance, the ultimate stress in experiment L3 is recorded at 36.57 MPa, compared to the 36.77 MPa predicted by simulation L3. This comparison reveals that the load displacement and stress-strain results are very close, with only a minimal difference of 0.55% in ultimate stress.

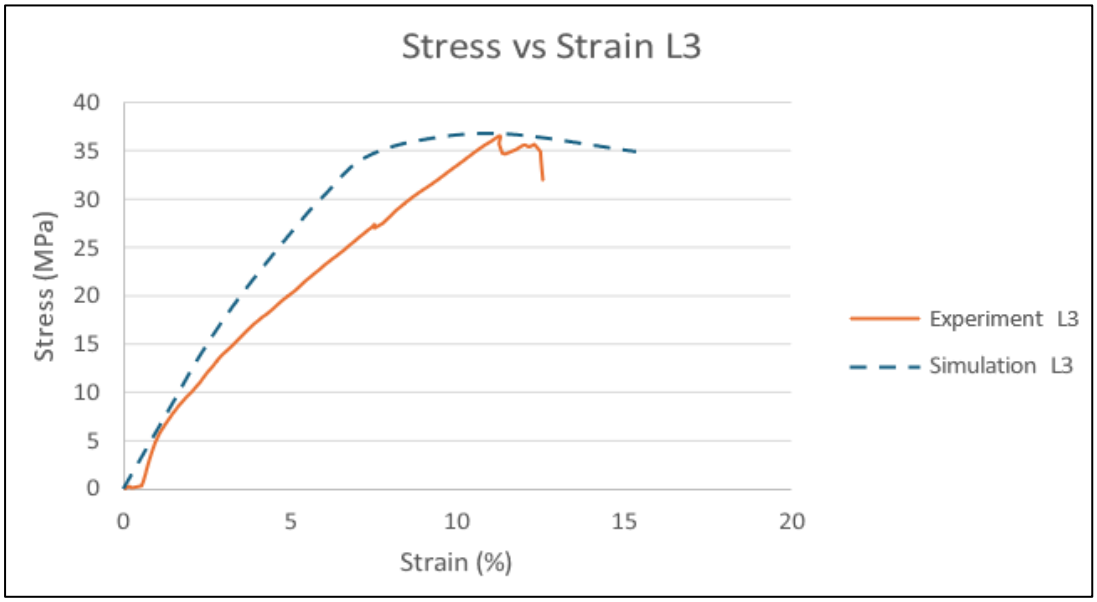

Figure 4.12 Simulation stress vs strain curve for L3

4.4.4 Laminate 4 (L4)

Figure 4.13 presents the Load versus Displacement results, where the experimental load graphs exhibit a general trend of increasing load and stress with displacement, progressing through distinct phases before reaching their peak values. Initially, the specimens follow a linear upward trend until they reach the maximum load stress (Moon

et al., 2024). The experimental results peaked at 4.23 kN at a displacement of 5.45 mm, while the simulation reached a slightly lower peak of 4.17 kN at 5.0 mm. Notably, after reaching the peak, the experimental data showed a load drop to 3.20 kN at 5.32 mm, whereas the simulation did not exhibit this immediate drop but instead gradually decreased to 3.61 kN at 7.80 mm. The comparison simulation and experiment of ultimate load shows a close match in the load-displacement results, with only a slight deviation of 1.42% in ultimate load (kN).

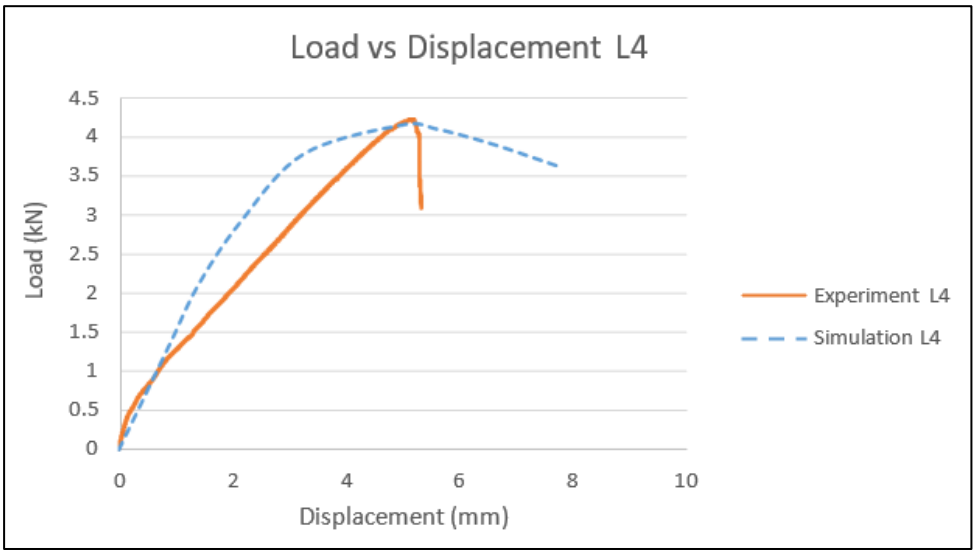

Figure 4.13 Load vs displacement curve for L4

Figure 4.14 illustrates the Stress versus Strain relationship, where both the experimental and simulated results followed a similar trend. The experimental peak stress was recorded at 52.46 MPa at 8.95% strain, while the simulation reached 52.08 MPa at 8.47% strain. Additionally, the ultimate stress in experiment L3 was recorded at 52.46 MPa, closely matching the 52.08 MPa predicted by simulation L4. The stress-strain results align closely, with just a minimal difference of 0.73% of simulation and experiment.

Both graph similar to L3, reveal a clear difference in slopes between the simulation and experiment, attributed to voids, uneven fiber distribution, and potential layer delamination in the hand layup process. While Abaqus effectively predicts the material's linear elastic behaviour, more advanced simulations are required to model plastic behaviour, particularly for fatigue applications (Al Rashid et al., 2020).

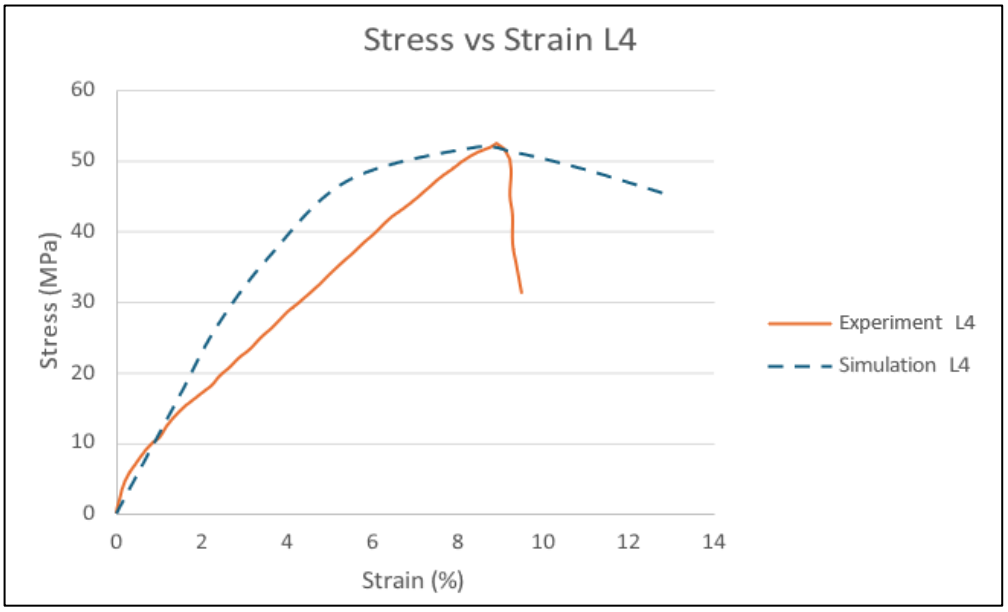

Figure 4.14 Stress vs strain curve for L4

4.4.5 Laminate 5 (L5)

Figure 4.15 depicts the Load-Displacement curve for L5, showing that both experimental and simulation results followed a similar trend. Initially, the load increased proportionally with displacement, reaching an ultimate load of 3.35 kN at a displacement of 14.55 mm in the experiment, while the simulation recorded an ultimate load of 3.26 kN at 16.68 mm displacement. This indicates the complete failure of the matrix material within the laminate (Prem Chand et al., 2021). The comparison further confirms that the load- displacement and stress-strain results are well-aligned, with only a minor deviation of 2.6% in the ultimate load (kN).

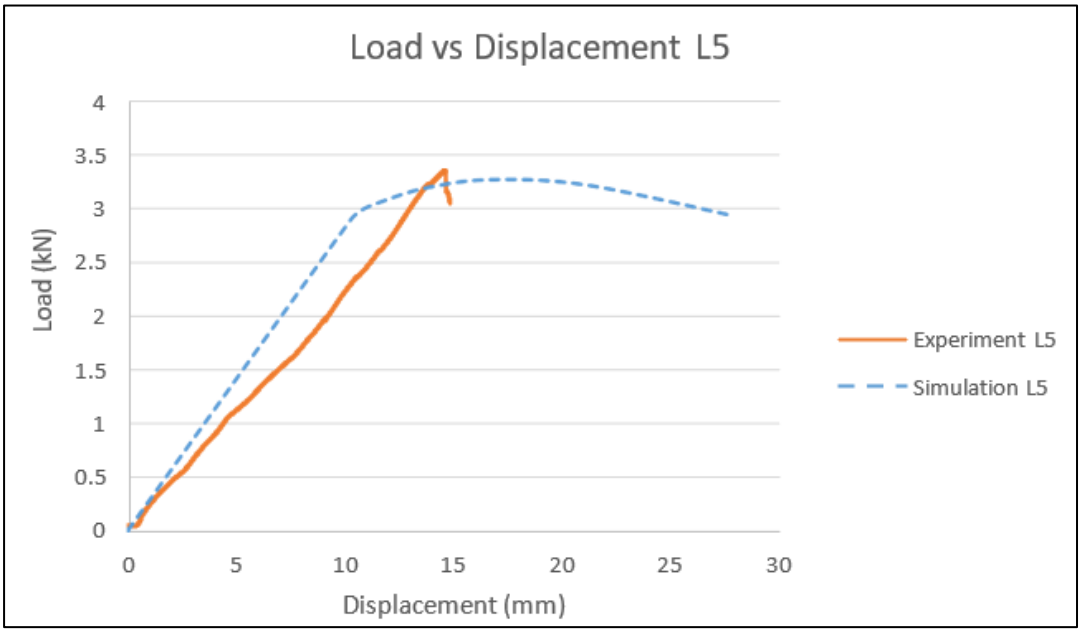

Figure 4.15 Load vs displacement curve L5

Figure 4.16 illustrates the Stress-Strain curve for L5, highlighting a significant nonlinear response up to approximately 20 MPa. Beyond this point, the stress exhibits a slight plateau before transitioning into a linear trend until reaching an ultimate stress of 30.03 MPa at a strain of 31.75%. In contrast, the simulation results indicate an ultimate stress of 30.19 MPa at a strain of 37.07%. During the linear phase, the applied load is evenly distributed between the fiber and the matrix. As the curve begins to decline, fiber pull-out occurs within the material. The bonding strength between the fiber and epoxy plays a crucial role in determining the overall tensile strength of the banana fiber and glass fiber laminate. (Prem Chand et al., 2021).

Thus, the ultimate stress in experiment L5 is measured at 30.03 MPa, compared to the 30.19 MPa predicted by simulation L5. This comparison shows that with only a slight difference of 0.53% in Ultimate Stress.

Similar to L3 and L4, both the Load-Displacement and Stress-Strain curve for L5 exhibit a distinct difference in slope between the experimental and simulation results. This variation is primarily attributed to the experimental process utilizing the hand layup technique, whereas the simulation effectively captures the material's linear elastic behaviour across different stacking sequences (Al Rashid et al., 2020).

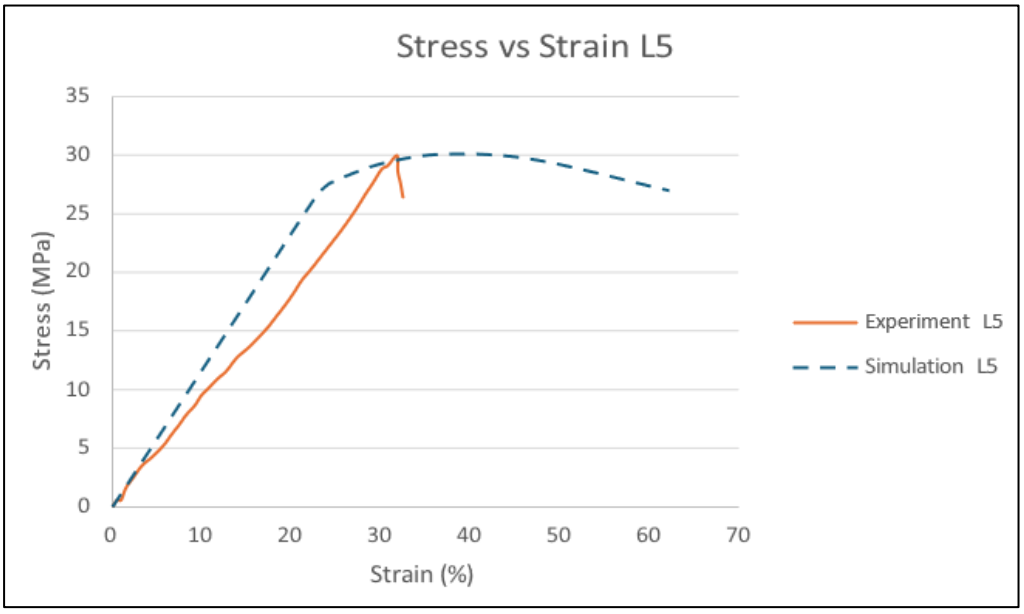

Figure 4.16 Stress vs strain curve for L5

4.4.6 Laminate 6 (L6)

Figure 4.17 presents a Load versus Displacement curve for experiment and simulation data of L6. The experiment L6 line begins with a steeper slope, indicating a more rapid initial increase in load compared to the simulation (Al Rashid et al., 2020). Around a displacement of 9-10 millimeters, the experimental curve levels off, forming a plateau where the load remains relatively constant until reaching an ultimate load of 5.34 kN at 9.54 mm displacement. In contrast, the Simulation L6 line demonstrates a more gradual and consistent increase in load throughout the entire displacement range, reaching 5.31 kN at 10.31 mm.

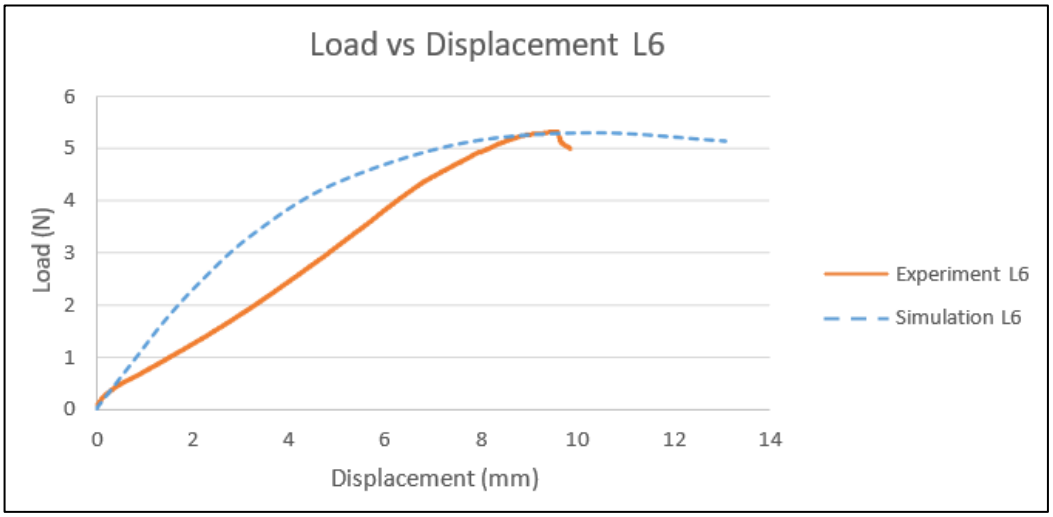

Figure 4.17 Load vs displacement curve for L6

The experiment and simulation of Stress versus Strain curve for Laminate 6, presented as Figure 4.18, shows that the maximum stress for L6 is nearly linear, indicating a direct proportionality between stress and strain (Sathishkumar et al., 2013). The maximum stress recorded for L6 is 72.52 MPa at approximately 17.81% strain, followed by a sharp decline. In contrast, the Simulation L6 curve consistently lies above the Experiment L6 curve, indicating that the simulated material experiences higher stress levels at the same strain compared to the experimental results. The simulation curve also shows a more noticeable deviation from linearity, with a steeper upward bend at a higher stress of 72.74 MPa at 18.71% strain. It is also found L6 is higher in ultimate load and ultimate stress to the other hybrid (L2-L5) due L6 have the high number of glass fiber compared to the banana fiber(Jubair et al., 2021).

Thus, the comparison between the experimental and simulation results indicates that the load-displacement behaviour is closely matched, with only a slight deviation of 2.6% in the ultimate load. Similarly, the ultimate stress comparison reveals a strong alignment between the stress-strain results, showing a minimal discrepancy of just 0.30% in ultimate stress.

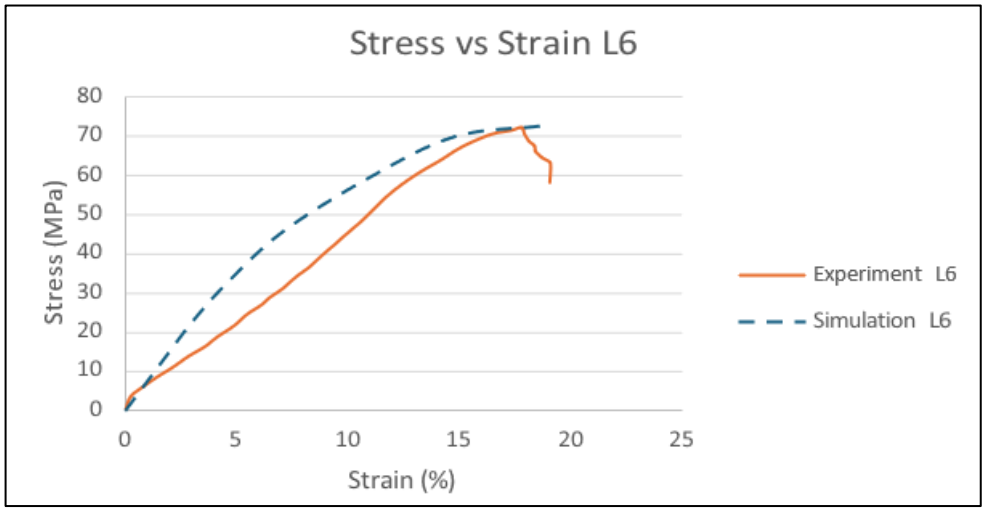

Figure 4.18 Stress vs strain L6

4.5 Comparison of the Composition Arrangement

The study conducted a comprehensive comparison of results obtained from both experimental tests and simulation models, focusing on two key parameters: Ultimate Load (kN) and Ultimate Stress (MPa). The Ultimate Load, representing the maximum load a material could withstand before failure during tensile tests, provided insights into the material's load-bearing capacity. Similarly, the Ultimate Stress, obtained from the ultimate load and the material's cross-sectional area, indicated the maximum stress the material could endure before failure, assessing its strength in terms of stress distribution.

As presented in Table 4.2, comparing these parameters between the experimental and simulation results was essential for validating the accuracy of the simulation models, which showed an average percentage error of 9% (Karthick et al., 2022). By analyzing the similarities and discrepancies in these values, the study assessed the reliability of the simulations. These findings were then utilized to evaluate the material's performance, ensuring that the simulation results corresponded accurately to the conducted experiments. This analysis was crucial for drawing informed conclusions and making recommendations in the thesis, thereby providing a solid foundation for future work

Table 4.2

Result experiment versus simulation

Laminate (specimen)	Source	Ultimate Load (kN)	Ultimate Stress (MPa)
L1 Composition: 9 GF	Experiment	5.96	119.46
	Simulation	5.83	119.06
	Error (%)	2.18	0.33
L2 Composition: 9 BF	Experiment	1.13	10.17
	Simulation	1.11	9.84
	Error (%)	1.77	3.24
L3 Composition: 5 BF and 4 GF	Experiment	3.72	36.57
	Simulation	3.78	36.77
	Error (%)	1.61	0.55
L4 Composition: 4 BF and 5 GF	Experiment	4.23	52.46
	Simulation	4.17	52.08
	Error (%)	1.42	0.73
L5 Composition: 6 BF and 3 GF	Experiment	3.35	30.03
	Simulation	3.26	30.19
	Error (%)	2.60	0.53
L6 Composition: 3 BF and 6 GF	Experiment	5.34	72.52
	Simulation	5.31	72.74
	Error (%)	0.56	0.30

Figure 4.19 presents a comparison of the ultimate load values for various laminate configurations, measured in kilo Newtons (kN). The x-axis represents different laminate configurations, ranging from L1 to L6, while the y-axis indicates the corresponding ultimate load values. In the graph, experimental data is depicted in blue, whereas simulation results are shown in orange with an x-pattern, facilitating a direct comparison between the two datasets. This figure provides valuable insights into the influence of laminate configurations on ultimate load capacity and highlights the level

of agreement between experimental and simulated results (Reddy et al., 2020).

The difference in experimental ultimate loads between L1 and L2 was 4.83 kN (L1 = 5.96 kN, L2 = 1.13 kN), corresponding to a percentage difference of approximately 81.67% relative to L1. Similarly, the difference in simulation results was 4.72 kN (L1 = 5.83 kN, L2 = 1.11 kN), yielding a percentage difference of approximately 81.03% relative to L1. These findings indicated that the ultimate load of L1 was 81.67% higher than that of L2 in the experimental results, and 81.03% higher in the simulation results. Among the laminates examined, L2 exhibited the most significant difference from L1, with an ultimate load approximately 81% lower in both experimental and simulation data. This suggests a substantial structural variation or inherent weakness in L2 compared to L1, which served as the reference point for comparison. From this comparison between L1 and L2, it can be concluded that the tensile strength of the glass fiber composite is superior to that of the banana fiber composite (Karthick et al., 2022).

In contrast, L6 exhibited the least variation compared to L1, with an ultimate load that was only 10–12% lower, indicating that L6 was the most structurally comparable laminate to L1. Moreover, L6 contained the lowest banana fiber content among the hybrid laminates, which contributed to improved strength performance compared with the other hybrid composite samples (Batu & Lemu, 2020). Meanwhile, L3, L4, and L5 showed moderate differences from L1, indicating varying levels of structural modifications or weaknesses relative to L1. Additionally, it was observed that composites incorporating glass fiber fabric at the outer layers demonstrated superior performance compared to other configurations (Santhanam et al., 2020).

Figure 4.20 presents the ultimate stress values for the same laminate configurations, measured in Mega Pascals (MPa). The x-axis represents the laminate configurations, while the y-axis displays the corresponding ultimate stress values. The graph compares experimental and simulation data, highlighting trends in stress performance across different laminates.

L1 demonstrated the highest ultimate stress, reaching approximately 120 MPa in both experimental and simulation results, making it the reference point for comparison. Among the laminates examined, L2 exhibited the most significant reduction in ultimate stress, decreasing by approximately 91.67% in the experiment and 93.33% in the simulation, indicating the greatest deviation in strength properties. The findings revealed that banana fiber had the lowest tensile strength, whereas glass fiber exhibited the highest tensile strength (Jubair et al., 2021).

The analysis of the data revealed the percentage differences in ultimate stress between L6 and L3, L4, and L5 for both experimental and simulation results. In the experimental results, L6 exhibited an ultimate stress 36 MPa higher than L3 (72 MPa vs. 36 MPa), which corresponded to a 50% increase. Similarly, in the simulation results, L6 recorded an ultimate stress 30 MPa higher than L3 (60 MPa vs. 30 MPa), also indicating a 50% increase. These findings demonstrated that L6 had 50% higher ultimate stress than L3 in both experimental and simulated conditions.

When comparing L6 and L4, the experimental results indicated that L6 had an ultimate stress that was 20 MPa higher than L4 (72 MPa vs. 52 MPa), representing a 27.78% increase. In the simulation results, L6 exhibited an ultimate stress 10 MPa higher than L4 (60 MPa vs. 50 MPa), corresponding to a 16.67% increase. These findings suggest that L6 experienced a moderate increase in ultimate stress compared to L4, with a slightly larger percentage difference observed in experimental results. Additionally, the tensile strength values of L6 and L4 were closer to each other compared to other laminates, indicating that variations in the stacking sequence had minimal impact on the tensile strength (Santhanam et al., 2020).

Regarding L6 and L5, the experimental results demonstrated that L6 had an ultimate stress 42 MPa higher than L5 (72 MPa vs. 30 MPa), translating to a 58.33% increase. Meanwhile, in the simulation results, L6 recorded an ultimate stress 36 MPa higher than L5 (60 MPa vs. 24 MPa), resulting in a 60% increase. This highlighted that L6 had the highest percentage increase in stress relative to L5, confirming its superior strength among the laminates.

L1 exhibited the highest ultimate load and ultimate stress, while L2 showed the lowest ultimate load and ultimate stress. This indicates that the tensile strength of the glass fiber composite is higher than that of the banana fiber composite. The difference is also influenced by the fiber volume fraction, where L1 had the highest total fiber volume fraction (Vf) of 35.9%, while L2 had the lowest fiber volume fraction of 13.8% as shown in Table 4.1. Among the hybrid composites, L6 exhibited the highest ultimate load and ultimate stress, which is associated with its relatively high fiber volume fraction of 24.6% compared to the other hybrid laminates(Messiry, 2013).

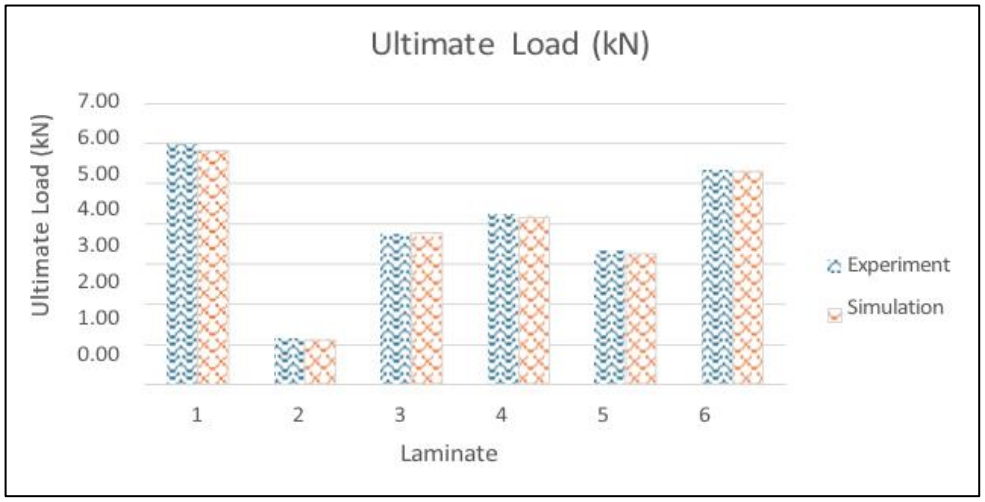

Figure 4.19: Comparison experiment and simulation: Ultimate Load (MPa)

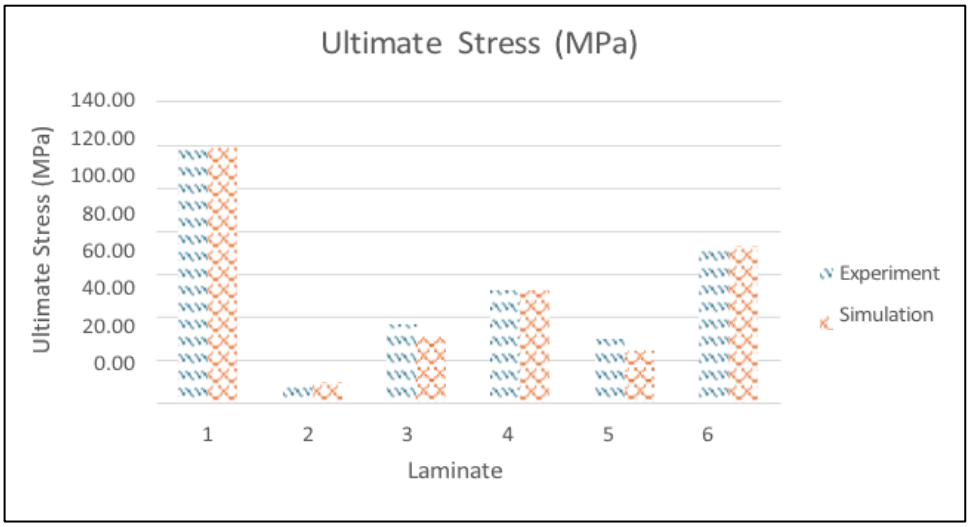

Figure 4.20: Comparison experiment and simulation: Ultimate Stress (MPa)

4.6 Finding summary

Overall, both experimental and simulation results consistently showed that Laminate L6 exhibited significantly higher ultimate stress compared to L3, L4, and L5. The percentage differences between experimental and simulated data remained relatively consistent, demonstrating a strong correlation between the two sets of results. Among all the hybrid laminates, L6 showed the most substantial increase in ultimate stress relative to L3, L4, and L5, confirming its superior performance. One possible reason for this improvement could be attributed to the layup configuration, where the arrangement of glass fiber layers between banana fiber layers helped enhance the load distribution and overall strength of the laminate (Jubair et al., 2021). This result further supports that the volume fraction and stacking sequence of glass fiber within the composite play a crucial role in improving the mechanical performance of the hybrid laminate (Batu & Lemu, 2020).

For the hybrid laminates (L3 to L6), the variation in the number of glass fiber and banana fiber layers affected the overall fiber volume fraction and mechanical behavior. As the proportion of glass fiber increased, the fiber volume fraction also increased, leading to better tensile performance. Conversely, when the banana fiber content increased, the matrix proportion became higher, and the tensile properties gradually decreased (Ciprian et al., 2015). Therefore, the results indicate that the volume fraction plays an important role in determining the mechanical properties of the composites, where a higher glass fiber proportion contributes significantly to improving tensile strength and impact energy, while higher banana fiber content tends to reduce these properties (Kureemun et al., 2018).

In conclusion, the volume fraction of fiber and matrix in each laminate configuration significantly influenced the tensile properties of the composites. Laminates with a higher glass fiber content produced a higher fiber volume fraction, which contributed to improved mechanical performance (Reddy et al., 2020). Laminate L1 exhibited the highest fiber volume fraction due to the presence of only glass fiber layers, resulting in superior tensile strength compared with the other configurations (M.R.M.Rejab, 2008). While, Laminate L2 showed the lowest fiber volume fraction because it consisted entirely of banana fiber with lower density, which increased the matrix content and consequently reduced the tensile strength (Messiry, 2013).

CHAPTER 5
CONCLUSION

5.1 Introduction

This chapter summarized the findings based on the established objectives, which were to determine the optimal tensile properties of glass fiber and banana fiber in various configurations and to validate the tensile properties from simulation results with experimental data. Additionally, recommendations for future research were offered.

5.2 Conclusion

The first objective, which involved validating the tensile properties obtained from simulation results against experimental results, was successfully achieved. The validation process confirmed that the simulation model accurately predicted the tensile properties of the composite materials, with a high degree of consistency between the experimental outcomes and simulated data, reinforcing the model's reliability. The comparison was conducted by modeling the specimens using finite element analysis (FEA) in Abaqus. The experimental graph patterns from Laminate 1 (L1) to Laminate 6 (L6) closely followed the simulation trends. Comparing the experimental and simulation results was crucial for validating the accuracy of the simulation models. An average percentage error of below 9% (Prem Chand et al., 2021) is referred as guideline when comparing Ultimate Load (kN) and Ultimate Stress (MPa). For Laminate 1 (L1), the ultimate load had a percentage error of 2.18%, and the ultimate stress had an error of 0.33%. For Laminate 2 (L2), the ultimate load error was 1.77%, and the ultimate stress error was 3.24%. Laminate 3 (L3) showed a percentage error of 1.61% for ultimate load and 0.55% for ultimate stress. Laminate 4 (L4) had errors of 1.42% for ultimate load and 0.73% for ultimate stress. For Laminate 5 (L5), the errors were 2.6% for ultimate load and 0.53% for ultimate stress. Finally, Laminate 6 (L6) exhibited the lowest errors, with 0.56% for ultimate load and 0.30% for ultimate stress.

The second objective was to determine the optimal tensile properties of glass fiber and banana fiber hybrid composites by varying the laminate configuration and fiber volume fraction. This objective was successfully achieved. Laminate 1 (L1), which

consisted entirely of glass fiber and had the highest fiber volume fraction, exhibited the highest tensile performance, achieving an ultimate load of 5.96 kN and an ultimate stress of 119.46 MPa. This was followed by Laminate 6 (L6), which consisted of six layers of glass fiber and three layers of banana fiber, with an ultimate load of 5.34 kN and an ultimate stress of 72.52 MPa. Laminate 4 (L4), containing five layers of glass fiber and four layers of banana fiber, recorded an ultimate load of 4.23 kN and an ultimate stress of 52.46 MPa. Laminate 3 (L3), with four layers of glass fiber and five layers of banana fiber, demonstrated an ultimate load of 3.72 kN and an ultimate stress of 36.57 MPa. Laminate 5 (L5), comprising three layers of glass fiber and six layers of banana fiber, exhibited an ultimate load of 3.35 kN and an ultimate stress of 30.03 MPa. Finally, Laminate 2 (L2), made entirely of nine layers of banana fiber and having the lowest fiber volume fraction, displayed the lowest tensile properties, with an ultimate load of 1.13 kN and an ultimate stress of 10.17 MPa. These results indicate that the fiber volume fraction significantly influenced the tensile properties of the composites, where laminates with higher glass fiber content produced a higher fiber volume fraction and consequently improved tensile performance (Reddy et al., 2020).

Overall, the comparison between the experimental and simulation results was essential to validate the accuracy of the simulation model. An average percentage error of less than 9% (Prem Chand et al., 2021) was used as a guideline when comparing the Ultimate Load (kN) and Ultimate Stress (MPa). Then the findings of this study demonstrated that the mechanical performance of hybrid composites is strongly influenced by the type of fiber, layer configuration, and the proportion of reinforcement within the laminate, particularly the fiber volume fraction. Laminates with a higher glass fiber content produced a higher fiber volume fraction, which contributed to improved tensile properties. Laminate 1 (L1), consisting of 100% glass fiber, achieved the highest tensile performance due to its highest fiber volume fraction and the superior mechanical properties of glass fiber reinforcement. The results also indicated that incorporating glass fiber significantly enhanced the tensile performance of the composite, while banana fiber provided a potential natural alternative that can be combined with synthetic fibers to form hybrid laminates. Among the hybrid configurations, Laminate 6 (L6) showed the best performance, achieving relatively high tensile properties and a higher fiber volume fraction compared with the other hybrid laminates. Therefore, this study confirms that an appropriate hybridization of glass fiber and banana fiber, together with an optimized fiber volume fraction and stacking

sequence, can produce composite materials with improved mechanical properties while also promoting the use of natural fibers in engineering applications (Reddy et al., 2020).

5.3 Recommendation

Future research should explore a broader range of laminate configurations with varying ratios and orientations of glass fiber and banana fiber layers, such as 45°, 90°, and 180°. These specific orientations may offer valuable insights into optimizing the mechanical properties of composites for targeted applications, particularly where directional strength or flexibility is crucial. By experimenting with these orientations, researchers can gain a deeper understanding of the anisotropic behavior of these materials, leading to more customized solutions for various engineering challenges.

In addition to exploring different fiber orientations, it is advisable to investigate composites that incorporate other natural and synthetic fibers. Natural fibers like cotton, flax, and jute can be combined with banana fiber to enhance certain mechanical or thermal properties while maintaining a focus on sustainability. On the other hand, synthetic fibers such as Rayon, Acrylic, Nylon, and Polyester could be utilized to create hybrid composites that combine the strengths of both natural and synthetic materials. This exploration could uncover new possibilities for achieving desired mechanical characteristics while addressing environmental sustainability and cost-efficiency.

Another important area for future research involves examining the effects of environmental factors on the tensile properties of these composites. Factors like humidity, temperature, and UV exposure can significantly impact the performance and durability of composite materials. By systematically studying how these variables affect tensile strength, stiffness, and failure modes, researchers could develop more resilient and adaptable materials suitable for a wider range of applications. This understanding is particularly important for use in harsh or fluctuating environmental conditions, where the longevity and reliability of materials are critical.

To deepen the understanding of composite material behavior, future studies should also integrate advanced simulation techniques, such as finite element analysis (FEA), with higher fidelity models. These models would enable more accurate predictions of how composite materials behave under complex loading conditions, including multiaxial stresses and varying strain rates. By incorporating detailed simulations that account for potential failure modes, such as cracking, delamination, or fiber pull-out,

researchers could gain valuable insights into the material's performance and safety margins.

Furthermore, conducting rupture and failure analysis through these advanced simulations could provide critical information on how and why certain materials fail under specific conditions. This knowledge could then be used to design composites that are not only stronger but also fail in a more predictable and controlled manner, thereby enhancing their safety and reliability in critical applications.

REFERENCE

Abaqus. (2006). *ABAQUS VERSION 6.6 DOCUMENTATION*. Abaqus. https://classes.engineering.wustl.edu/2009/spring/mase5513/abaqus/docs/v6.6/books/exa/default.htm?startat=ch01s04aex50.html

Al Rashid, A., Khalid, M. Y., Imran, R., Ali, U., & Koc, M. (2020). Utilization of banana fiber-reinforced hybrid composites in the sports industry. *Materials*, *13*(14). https://doi.org/10.3390/ma13143167

ASTM. (2014). D3039/D3039M Standard Test Method for Tensile Properties of Polymer Matrix Composite Materials. *Annual Book of ASTM Standards*, *15*, 1–13. http://scholar.google.com/scholar?hl=en&btnG=Search&q=intitle:Standard+Test+Method+for+Tensile+Properties+of+Polymer+Matrix+Composite+Materials#1

Batu, T., & Lemu, H. G. (2020). Investigation of mechanical properties of false banana/glass fiber reinforced hybrid composite materials. *Results in Materials*, *8*. https://doi.org/10.1016/j.rinma.2020.100152

Bisht, N., & Gope, P. (2015). Mechanical properties of rice husk flour reinforced epoxy bio- composite. *International Journal of Engineering Research and Applications*, *5*(6), 123–128. https://doi.org/10.13140/RG.2.1.3457.0323

By, E., & Sloan, J. (2020). *Composites 101: Fibers and resins*. 1–10.

Ciprian, L., Radu, P., & Ioana, E. (2015). The Effects of Fibre Volume Fraction on a Glass-Epoxy Composite Material. *INCAS BULLETIN*, *7*(3), 113–119. https://doi.org/10.13111/2066-8201.2015.7.3.10

Fiber-reinforced composites. (n.d.). Retrieved February 16, 2020, from https://fog.ccsf.edu/~wkaufmyn/ENGN45/Course Handouts/14_CompositeMaterials/03_Fiber-reinforcedComposites.html

Fibers, C., & Hodgkin, J. (2020). *Epoxy Resin*. 1–8.

Jubair, K., Islam, M. S., & Chakraborty, D. (2021). Investigation of Mechanical Properties of Banana-Glass Fiber Reinforced Hybrid Composites. *Journal of Engineering Advancements*, 175–179. https://doi.org/10.38032/jea.2021.04.002

Karthick, L., Sivakumar, S., Sasikumar, A., Prabhu, A., Senthil Kumar, J., & Vadivukarasi, L. (2022). A comparison and analysis of mechanical properties of glass fiber and banana fiber composite. *Materials Today: Proceedings*, *52*, 398–402. https://doi.org/10.1016/j.matpr.2021.09.073

Kisan, M., Sangathan, S., Nehru, J., & Pitroda, S. G. (2005). म ा नक.

Koloor, S. S. R., Karimzadeh, A., Yidris, N., Petrů, M., Ayatollahi, M. R., & Tamin, M. N. (2020). An energy-based concept for yielding of multidirectional FRP composite structures using a mesoscale lamina damage model. *Polymers*, *12*(1). https://doi.org/10.3390/polym12010157

Kotla Rachana, S. K. (2020). DEVELOPMENT AND TESTING OF GLASS FIBRE REINFORCED COMPOSITES. *International Journal of Engineering Applied Sciences and Technology*, *5*, 450–455. http://www.ijeast.com

Kureemun, U., Ravandi, M., Tran, L. Q. N., Teo, W. S., Tay, T. E., & Lee, H. P. (2018). Effects of hybridization and hybrid fibre dispersion on the mechanical properties of woven flax-carbon epoxy at low carbon fibre volume fractions. *Composites Part B: Engineering*, *134*, 28–38. https://doi.org/10.1016/j.compositesb.2017.09.035

Messiry, M. El. (2013). Theoretical analysis of natural fiber volume fraction of reinforced composites. *Alexandria Engineering Journal*, *52*(3), 301–306. https://doi.org/10.1016/j.aej.2013.01.006

Monzón, M. D., Paz, R., Verdaguer, M., Suárez, L., Badalló, P., Ortega, Z., & Diaz, N. (2019). Experimental analysis and simulation of novel technical textile reinforced composite of banana fibre. *Materials*, *12*(7), 1–23. https://doi.org/10.3390/ma12071134

Moon, M. K., Saha, S., Biswas, A., & Paul, A. A. (2024). Characteristics and Comparative Study of Sodium Hydroxide Treated Banana Fiber Reinforced Composite Material. *IOP Conference Series: Materials Science and Engineering*, *1305*(1), 012029. https://doi.org/10.1088/1757-899x/1305/1/012029

Morton, N. (2010). *Design and Manufacture of an Advanced Composite Acknowledgements :*

M.R.M.Rejab, C. W. T. M. M. R. M. M. N. and A. N. M. R. (2008). An_Investigation_into_the_Effects_of_Fibre_Volume_Fraction_on_GFRP_Plate_1 (1). *MUCET2008*.

Narayanan, P., Vijaya Kumar, D., Chandra Mouli, K., Pannirselvam Associate Professor, N., Vijaya Kumar, D., Valeswara Rao Assistant Professor, S., Pannirselvam, N., Anitha, V., & Valeswara Rao, S. (2019). Strength Studies on Banana Fibre Concrete with Metakaolin. *International Journal of Civil Engineering and Technology (IJCIET)*, *10*(2), 684–689.

http://www.iaeme.com/IJCIET/index.asp684http://www.iaeme.com/ijciet/issues.asp?JType=IJCIET&VType=10&IType=2http://www.iaeme.com/IJCIET/index.asp685http://www.iaeme.com/IJCIET/issues.asp?JType=IJCIET&VType=10&IType=2

Pandya, K. S., Veerraju, C., & Naik, N. K. (2011). Hybrid composites made of carbon and glass woven fabrics under quasi-static loading. *Materials and Design*, *32*(7), 4094–4099. https://doi.org/10.1016/j.matdes.2011.03.003

Pillai, K. M., Masoodi, R., Verhagen, M. A., Duelge, T., & Masoodi, R. (2009). A Study of Change in Properties of Polymer Composite after Replacement of Glass with Jute Fibers Investigation of the effect of micro structure on wicking on using Lattice Boltzmann Method View project Water Filtration View project A Study of Change in Properties of Polymer Composite after Replacement of Glass with Jute Fibers. *Laboratory for Flow and Transport Studies in Porous Media*, 1–8. https://www.researchgate.net/publication/265259881

Prabhu, L., Krishnaraj, V., Sathish, S., Gokulkumar, S., Karthi, N., Rajeshkumar, L., Balaji, D., Vigneshkumar, N., Elango, K. S., Karpagam, J., Vijayalakshmi, V. J., Gowarthan, E. R., & Jayakumar, H. (2021). Experimental investigation on mechanical properties of flax/banana/ industrial waste tea leaf fiber reinforced hybrid polymer composites. *Materials Today: Proceedings*, *45*, 8136–8143. https://doi.org/10.1016/j.matpr.2021.02.111

Prem Chand, R., Ravitej, Y. P., Chandrasekhar, K. M., Adarsha, H., Shivamani Kanta, J. V., Veerachari, M., Ravi Kumar, R., & Abhinandan. (2021). Characterization of banana and e glass fiber reinforced hybrid epoxy composites. *Materials Today: Proceedings*, *46*, 9119–9125. https://doi.org/10.1016/j.matpr.2021.05.402

Quilter, A. (2019, May 6). *What is Young's Modulus?* IHS. https://www.servicethread.com/blog/what-is-youngs-modulus

Raheem, Z. (2019). *Standard Test Method for Tensile Properties of Plastics 1 Standard Test Method for Tensile Properties of Plastics 1*. (January). https://doi.org/10.1520/D0638-14

Rajak, D. K., Pagar, D. D., Menezes, P. L., & Linul, E. (2019). Fiber-reinforced polymer composites: Manufacturing, properties, and applications. *Polymers*, *11*(10). https://doi.org/10.3390/polym11101667

Reddy, M. V. K., Lakshmi, R. V. S., Pragathi, Y., Devaraj, P., & Naresh, N. (2020). Evaluation of mechanical properties: Influence of glass fiber on banana fiber

reinforced with epoxy composite. *Materials Today: Proceedings*, *37*(Part 2), 1305–1312. https://doi.org/10.1016/j.matpr.2020.06.467

Rout, A. K., & Satapathy, A. (2012). Study on mechanical and tribo-performance of rice-husk filled glass-epoxy hybrid composites. *Materials and Design*, *41*, 131–141. https://doi.org/10.1016/j.matdes.2012.05.002

Sampath, B., Naveenkumar, N., Sampathkumar, P., Silambarasan, P., Venkadesh, A., & Sakthivel, M. (2021). Experimental comparative study of banana fiber composite with glass fiber composite material using Taguchi method. *Materials Today: Proceedings*, *49*, 1475–1480. https://doi.org/10.1016/j.matpr.2021.07.232

Sanjay, M. R., Arpitha, G. R., Laxmana Naik, L., Gopalakrishna, K., & Yogesha, B. (2016). Studies on mechanical properties of Banana/E-Glass fabrics reinforced polyester hybrid composites. *Journal of Materials and Environmental Science*, *7*(9), 3179–3192.

Santhanam, V., Dhanaraj, R., Chandrasekaran, M., Venkateshwaran, N., & Baskar, S. (2020). Experimental investigation on the mechanical properties of woven hybrid fiber reinforced epoxy composite. *Materials Today: Proceedings*, *37*(Part 2), 1850–1853. https://doi.org/10.1016/j.matpr.2020.07.444

Sathishkumar, T. P., Navaneethakrishnan, P., Shankar, S., & Kumar, J. (2013). Mechanical properties of randomly oriented snake grass fiber with banana and coir fiber-reinforced hybrid composites. *Journal of Composite Materials*, *47*(18), 2181–2191. https://doi.org/10.1177/0021998312454903

Sivaranjana, P., & Arumugaprabu, V. (2021). A brief review on mechanical and thermal properties of banana fiber based hybrid composites. In *SN Applied Sciences* (Vol. 3, Number 2). Springer Nature. https://doi.org/10.1007/s42452-021-04216-0

Stanciu, M. D., Drăghicescu, H. T., & Roșca, I. C. (2021). Mechanical properties of GFRPs exposed to tensile, compression and tensile—tensile cyclic tests. *Polymers*, *13*(6). https://doi.org/10.3390/polym13060898

Standard Test Method for Tensile Properties of Plastics 1. (n.d.). https://doi.org/10.1520/D0638-14

Standard Test Method for Tensile Properties of Polymer Matrix Composite Materials. (n.d.).

Started, G., & Edition, I. (n.d.). *Getting Started with Abaqus: Interactive Edition: 6.8* (6.8). Dassault Systèmes. Retrieved

http://www.simulia.com/about/locations.html.

William D. Callister, J. (2003). *Material Science And Engineering An Introduction* (Sixth Edit).

Xin, H., Liu, Y., Mosallam, A. S., He, J., & Du, A. (2017). Evaluation on material behaviors of pultruded glass fiber reinforced polymer (GFRP) laminates. *Composite Structures*, *182*, 283–300. https://doi.org/10.1016/j.compstruct.2017.09.006

APPENDICES

APPENDIX A

The calculation of the fiber volume fraction percentage presented in Table 4.1 was divided into several steps, including the calculation of the total fiber density as shown in Table 7.1, total matrix density as shown in Table 7.2, total fiber weight as shown in Table 7.3, and total matrix weight as shown in Table 7.4. Equations 3.1 and 3.2, along with the properties listed in Table 3.2, were used for the calculations.

Total Density of Fiber

Laminate 1

Total Density Glass Fiber

$= Density\ Glass\ Fiber\ \times\ Number\ Layer\ Glass\ Fiber$

$= 2.5 \times 9$

$= 22.5\ g/cm^3$

Total Density Banana Fiber

$= Density\ Banana\ Fiber\ \times\ Number\ Layer\ Banana\ Fiber$

$= 1.25 \times 0$

$= 0\ g/cm^3$

$Total\ Density\ of\ Fiber = Density\ glass\ fiber + Density\ Banana\ Fiber$

$= 22.5 + 0$

$= 22.5\ g/cm^3$

Laminate 2

Total Density Glass Fiber

$= Density\ Glass\ Fiber\ \times\ Number\ Layer\ Glass\ Fiber$

$= 2.5 \times 0$

$= 0\ g/cm^3$

Total Density Banana Fiber

$= Density\ Banana\ Fiber\ \times\ Number\ Layer\ Banana\ Fiber$

$= 1.25 \times 9$

$= 11.3\ g/cm^3$

$Total\ Density\ of\ Fiber = Density\ glass\ fiber + Density\ Banana\ Fiber$

$= 0 + 11.3$

$= 11.03\ g/cm^3$

Laminate 3

Total Density Glass Fiber

$= Density\ Glass\ Fiber\ \times\ Number\ Layer\ Glass\ Fiber$

$= 2.5 \times 4$

$= 10\ g/cm^3$

Total Density Banana Fiber

$= Density\ Banana\ Fiber\ \times\ Number\ Layer\ Banana\ Fiber$

$= 1.25 \times 5$

$= 6.3\ g/cm^3$

$Total\ Density\ of\ Fiber = Density\ glass\ fiber + Density\ Banana\ Fiber$

$= 10 + 6.3$

$= 16.3\ g/cm^3$

Laminate 4

Total Density Glass Fiber

$= Density\ Glass\ Fiber\ \times\ Number\ Layer\ Glass\ Fiber$

$= 2.5 \times 5$

$= 12.5\ g/cm^3$

Total Density Banana Fiber

$= Density\ Banana\ Fiber\ \times\ Number\ Layer\ Banana\ Fiber$

$= 1.25 \times 4$

$= 5\ g/cm^3$

$Total\ Density\ of\ Fiber = Density\ glass\ fiber + Density\ Banana\ Fiber$

$= 12.5 + 5$

$= 17.5\ g/cm^3$

Laminate 5

Total Density Glass Fiber

$= Density\ Glass\ Fiber\ \times\ Number\ Layer\ Glass\ Fiber$

$= 2.5 \times 3$

$= 7.5\ g/cm^3$

Total Density Banana Fiber

$= Density\ Banana\ Fiber\ \times\ Number\ Layer\ Banana\ Fiber$

$= 1.25 \times 6$

$= 7.5\ g/cm^3$

$Total\ Density\ of\ Fiber = Density\ glass\ fiber + Density\ Banana\ Fiber$

$= 7.5 + 7.5$

$= 15\ g/cm^3$

Laminate 6

Total Density Glass Fiber

$= Density\ Glass\ Fiber \times Number\ Layer\ Glass\ Fiber$

$= 2.5 \times 6$

$= 15.0\ g/cm^3$

Total Density Banana Fiber

$= Density\ Banana\ Fiber \times Number\ Layer\ Banana\ Fiber$

$= 1.25 \times 3$

$= 3.8\ g/cm^3$

$Total\ Density\ of\ Fiber = Density\ glass\ fiber + Density\ Banana\ Fiber$

$= 15 + 3.8$

$= 18.8\ g/cm^3$

Table 7.1

Summary of density of fiber

Laminate	Layer		Density of Fiber (g/cm^3)		Total
	Glass Fiber	Banana Fiber	Glass Fiber	Banana Fiber	
L1	9	0	22.5	0	22.5
L2	0	9	0	11.3	11.3
L3	4	5	10.0	6.3	16.3
L4	5	4	12.5	5.0	17.5
L5	3	6	7.5	7.5	15.0
L6	6	3	15.0	3.8	18.8

Total Density of Matrix

Laminate 1

Total Density Matrix in Glass Fiber

$= Density\ Matrix\ \times\ Number\ Layer\ Glass\ Fiber$

$= 1.1 \times 9$

$= 9.9\ g/cm^3$

Total Density Matrix in Banana Fiber

$= Density\ Matrix \times Number\ Layer\ Banana\ Fiber$

$= 1.1 \times 0$

$= 0\ g/cm^3$

$Total\ Density\ of\ Matrix = Density\ glass\ fiber + Density\ Banana\ Fiber$

$= 9.9 + 0$

$= 9.9\ g/cm^3$

Laminate 2

Total Density Matrix in Glass Fiber

$= Density\ Matrix \times Number\ Layer\ Glass\ Fiber$

$= 1.1 \times 0$

$= 0\ g/cm^3$

Total Density Matrix in Banana Fiber

$= Density\ Matrix \times Number\ Layer\ Banana\ Fiber$

$= 1.1 \times 9$

$= 9.9\ g/cm^3$

$Total\ Density\ of\ Matrix = Density\ glass\ fiber + Density\ Banana\ Fiber$

$= 0 + 9.9$

$= 9.9\ g/cm^3$

Laminate 3

Total Density Matrix in Glass Fiber

$= Density\ Matrix \times Number\ Layer\ Glass\ Fiber$

$= 1.1 \times 4$

$= 4.4\ g/cm^3$

Total Density Matrix in Banana Fiber

$= Density\ Matrix \times Number\ Layer\ Banana\ Fiber$

$= 1.1 \times 5$

$= 5.5\ g/cm^3$

$Total\ Density\ of\ Matrix = Density\ glass\ fiber + Density\ Banana\ Fiber$

$= 4.4 + 5.5$

$= 9.9\ g/cm^3$

Laminate 4

Total Density Matrix in Glass Fiber

$= Density\ Matrix \times Number\ Layer\ Glass\ Fiber$

$= 1.1 \times 5$

$= 5.5\ g/cm^3$

Total Density Matrix in Banana Fiber

$= Density\ Matrix \times Number\ Layer\ Banana\ Fiber$

$= 1.1 \times 4$

$= 4.4\ g/cm^3$

$Total\ Density\ of\ Matrix = Density\ glass\ fiber + Density\ Banana\ Fiber$

$= 5.5 + 4.4$

$= 9.9\ g/cm^3$

Laminate 5

Total Density Matrix in Glass Fiber

$= Density\ Matrix \times Number\ Layer\ Glass\ Fiber$

$= 1.1 \times 3$

$= 3.3\ g/cm^3$

Total Density Matrix in Banana Fiber

$= Density\ Matrix \times Number\ Layer\ Banana\ Fiber$

$= 1.1 \times 6$

$= 6.6\ g/cm^3$

$Total\ Density\ of\ Matrix = Density\ glass\ fiber + Density\ Banana\ Fiber$

$= 3.3 + 6.6$

$= 9.9\ g/cm^3$

Laminate 6

Total Density Matrix in Glass Fiber

$= Density\ Matrix \times Number\ Layer\ Glass\ Fiber$

$= 1.1 \times 6$

$= 6.6\ g/cm^3$

Total Density Matrix in Banana Fiber

$= Density\ Matrix \times Number\ Layer\ Banana\ Fiber$

$= 1.1 \times 3$

$= 3.3\ g/cm^3$

$Total\ Density\ of\ Matrix = Density\ glass\ fiber + Density\ Banana\ Fiber$

$= 6.6 + 3.3$

$= 9.9\ g/cm^3$

Table 7.2

Summary of density matrix

Laminate	Layer		Density Matrix		
	Glass Fiber	Banana Fiber	Glass Fiber	Banana Fiber	Total
L1	9	0	9.9	0.0	9.9
L2	0	9	0.0	9.9	9.9
L3	4	5	4.4	5.5	9.9
L4	5	4	5.5	4.4	9.9
L5	3	6	3.3	6.6	9.9
L6	6	3	6.6	3.3	9.9

Weight of Fiber

Laminate 1

Total Weight Glass Fiber

$= Weight\ Glass\ Fiber\ \times\ Number\ Layer\ Glass\ Fiber$

$= 1.086 \times 9$

$= 9.78\ g/cm^3$

Total Weight Banana Fiber

$= Weight\ Banana\ Fiber\ \times\ Number\ Layer\ Banana\ Fiber$

$= 0.466 \times 0$

$= 0\ g/cm^3$

$Total\ Weight\ of\ Fiber = Weight\ glass\ fiber + Weight\ Banana\ Fiber$

$= 9.78 + 0$

$= 9.78\ g/cm^3$

Laminate 2

Total Weight Glass Fiber

$= Weight\ Glass\ Fiber\ \times\ Number\ Layer\ Glass\ Fiber$

$= 1.086 \times 0$

$= 0\ g/cm^3$

Total Weight Banana Fiber

$= Weight\ Banana\ Fiber\ \times\ Number\ Layer\ Banana\ Fiber$

$= 0.466 \times 9$

$= 4.19\ g/cm^3$

$Total\ Weight\ of\ Fiber = Weight\ glass\ fiber + Weight\ Banana\ Fiber$

$= 4.19 + 0$

$= 4.19\ g/cm^3$

Laminate 3

Total Weight Glass Fiber

$= Weight\ Glass\ Fiber\ \times\ Number\ Layer\ Glass\ Fiber$

$= 1.086 \times 4$

$= 4.35\ g/cm^3$

Total Weight Banana Fiber

$= Weight\ Banana\ Fiber \times Number\ Layer\ Banana\ Fiber$

$= 0.466 \text{ x } 5$

$= 2.33\ g/cm^3$

$Total\ Weight\ of\ Fiber = Weight\ glass\ fiber + Weight\ Banana\ Fiber$

$= 4.35 + 2.33$

$= 6.67\ g/cm^3$

Laminate 4

Total Weight Glass Fiber

$= Weight\ Glass\ Fiber\ \times\ Number\ Layer\ Glass\ Fiber$

$= 1.086 \times 5$

$= 5.43\ g/cm^3$

Total Weight Banana Fiber

$= Weight\ Banana\ Fiber\ \times\ Number\ Layer\ Banana\ Fiber$

$= 0.466 \times 4$

$= 1.86\ g/cm^3$

$Total\ Weight\ of\ Fiber = Weight\ glass\ fiber + Weight\ Banana\ Fiber$

$= 5.43 + 1.86$

$= 7.29\ g/cm^3$

Laminate 4

Total Weight Glass Fiber

$= Weight\ Glass\ Fiber\ \times\ Number\ Layer\ Glass\ Fiber$

$= 1.086 \times 5$

$= 5.43\ g/cm^3$

Total Weight Banana Fiber

$= Weight\ Banana\ Fiber \times Number\ Layer\ Banana\ Fiber$

$= 0.466 \times 4$

$= 1.86\ g/cm^3$

$Total\ Weight\ of\ Fiber = Weight\ glass\ fiber + Weight\ Banana\ Fiber$

$= 5.43 + 1.86$

$= 7.29\ g/cm^3$

Laminate 5

Total Weight Glass Fiber

$= Weight\ Glass\ Fiber\ \times\ Number\ Layer\ Glass\ Fiber$

= 1.086 × 3

= 3.26 g/cm^3

Total Weight Banana Fiber

$= Weight\ Banana\ Fiber\ \times\ Number\ Layer\ Banana\ Fiber$

= 0.466 × 6

= 2.79 g/cm^3

$Total\ Weight\ of\ Fiber = Weight\ glass\ fiber + Weight\ Banana\ Fiber$

= 3.26 + 2.79

= 6.05 g/cm^3

Laminate 6

Total Weight Glass Fiber

$= Weight\ Glass\ Fiber\ \times\ Number\ Layer\ Glass\ Fiber$

= 1.086 × 6

= 6.52 g/cm^3

Total Weight Banana Fiber

$= Weight\ Banana\ Fiber\ \times\ Number\ Layer\ Banana\ Fiber$

= 0.466 × 3

= 1.40 g/cm^3

$Total\ Weight\ of\ Fiber = Weight\ glass\ fiber + Weight\ Banana\ FIber$

= 6.52 + 1.40

= 7.91 g/cm^3

Table 7.3

Summary of weight of fiber

Laminate	Layer		Weight (gram)		
	Glass Fiber	Banana Fiber	Glass Fiber	Banana Fiber	Total Fiber
L1	9	0	9.78	0.00	9.78
L2	0	9	0.00	4.19	4.19
L3	4	5	4.35	2.33	6.67
L4	5	4	5.43	1.86	7.29
L5	3	6	3.26	2.79	6.05
L6	6	3	6.52	1.40	7.91

Weight Matrix of Glass Fiber

Laminate 1

Total Weight Matrix Glass Fiber

$= Weight\ Glass\ Fiber\ \times\ Number\ Layer\ Glass\ Fiber$

$= 0.854 \times 9$

$= 7.68\ g/cm^3$

Total Weight Matrix Banana Fiber

$= Weight\ Matrix\ Banana\ Fiber\ \times\ Number\ Layer\ Banana\ Fiber$

$= 2.561 \times 0$

$= 0\ g/cm^3$

$Total\ Weight\ Matrix\ of\ Fiber = Weight\ Matrix\ glass\ fiber +$

$Weight\ Matrix\ Banana\ Fiber$

$= 7.68 + 0$

$= 7.68\ g/cm^3$

Laminate 2

Total Weight Matrix Glass Fiber

$= Weight\ Glass\ Fiber\ \times\ Number\ Layer\ Glass\ Fiber$

$= 0.854 \times 0$

$= 0\ g/cm^3$

Total Weight Matrix Banana Fiber

$= Weight\ Matrix\ Banana\ Fiber\ \times\ Number\ Layer\ Banana\ Fiber$

$= 2.561 \times 9$

$= 23.05\ g/cm^3$

$Total\ Weight\ Matrix\ of\ Fiber = Weight\ Matrix\ glass\ fiber +$

$Weight\ Matrix\ Banana\ Fiber$

$= 0 + 23.05$

$= 23.05\ g/cm^3$

Laminate 3

Total Weight Matrix Glass Fiber

$= Weight\ Glass\ Fiber\ \times\ Number\ Layer\ Glass\ Fiber$

$= 0.854 \times 4$

$= 3.41\ g/cm^3$

Total Weight Matrix Banana Fiber

$= Weight\ Matrix\ Banana\ Fiber\ \times\ Number\ Layer\ Banana\ Fiber$

$= 2.561 \times 5$

$= 12.80\ g/cm^3$

$Total\ Weight\ Matrix\ of\ Fiber = Weight\ Matrix\ glass\ fiber +$

$Weight\ Matrix\ Banana\ Fiber$

= 3.41 + 12.80

= 16.22 g/cm^3

Laminate 4

Total Weight Matrix Glass Fiber

= $Weight\ Glass\ Fiber\ \times\ Number\ Layer\ Glass\ Fiber$

= 0.854 × 5

= 4.27 g/cm^3

Total Weight Matrix Banana Fiber

= $Weight\ Matrix\ Banana\ Fiber\ \times\ Number\ Layer\ Banana\ Fiber$

= 2.561 × 4

= 10.24 g/cm^3

$Total\ Weight\ Matrix\ of\ Fiber = Weight\ Matrix\ glass\ fiber +$

$Weight\ Matrix\ Banana\ Fiber$

= 3.41 + 12.80

= 14.51 g/cm^3

Laminate 5

Tota Weight Matrix Glass Fiber

= $Weight\ Glass\ Fiber\ \times\ Number\ Layer\ Glass\ Fiber$

= 0.854 × 3

= 2.56 g/cm^3

Total Weight Matrix Banana Fiber

$= Weight\ Matrix\ Banana\ Fiber\ \times\ Number\ Layer\ Banana\ Fiber$

$= 2.561 \times 6$

$= 15.36\ g/cm^3$

$Total\ Weight\ Matrix\ of\ Fiber = Weight\ Matrix\ glass\ fiber +$

$Weight\ Matrix\ Banana\ Fiber$

$= 2.56 + 15.36$

$= 17.92\ g/cm^3$

Laminate 6

Total Weight Matrix Glass Fiber

$= Weight\ Glass\ Fiber\ \times\ Number\ Layer\ Glass\ Fiber$

$= 0.854 \times 6$

$= 5.12\ g/cm^3$

Total Weight Matrix Banana Fiber

$= Weight\ Matrix\ Banana\ Fiber\ \times\ Number\ Layer\ Banana\ Fiber$

$= 2.561 \times 3$

$= 7.68\ g/cm^3$

$Total\ Weight\ Matrix\ of\ Fiber = Weight\ Matrix\ glass\ fiber +$

$Weight\ Matrix\ Banana\ Fiber$

$= 5.12 + 7.68$

$= 12.80\ g/cm^3$

Table 7.4

Summary weight of matrix

Laminate	Layer		Weight (gram)		Total Matrix
	Glass Fiber	Banana Fiber	Matrix GF	Matrix BF	
L1	9	0	7.68	0.00	7.68
L2	0	9	0.00	23.05	23.05
L3	4	5	3.41	12.80	16.22
L4	5	4	4.27	10.24	14.51
L5	3	6	2.56	15.36	17.92
L6	6	3	5.12	7.68	12.80

Volume of Fraction Laminate 1 (L1):

Volume Fraction Glass Fiber V_f:

$V_f = [\rho_m \cdot w_f/(\rho_m \cdot w_f + \rho_f \cdot w_m)]$

$V_{gf} = [(9.9 \times 9.78)/(9.9 \times 9.78) + (22.5 \times 7.68)]$

$V_f = 0.359$

$V_f = 35.90\%$

Volume of Matrix Fraction V_m:

$V_m = [1 - V_f]$

$V_m = [1 - 0.359]$

$V_m = 0.641$

$V_m = 64.10\%$

Laminate 2 (L2):

Volume Fraction Glass Fiber V_f:

$V_f = [\rho_m \cdot w_f/(\rho_m \cdot w_f + \rho_f \cdot w_m)]$

$V_{gf} = [(9.9 \times 4.19)/ (9.9 \times 4.19) + (11.3 \times 23.05)]$

$V_f = 0.138$

$V_f = 13.80\%$

Volume of Matrix Fraction V_m:

$V_m = [1 - V_f]$

$V_m = [1 - 0.138]$

$V_m = 0.862$

$V_m = 86.20\%$

Laminate 3 (L3):

Volume Fraction Glass Fiber V_f:

$V_f = [\rho_m \cdot w_f/(\rho_m \cdot w_f + \rho_f \cdot w_m)]$

$V_{gf} = (9.9 \times 6.67) / (9.9 \times 6.67) + (16.3 \times 16.22)$

$V_f = 0.200$

$V_f = 20\%$

Volume of Matrix Fraction V_m:

$V_m = [1 - V_f]$

$V_m = [1 - 0.2]$

$V_m = 0.8$

$V_m = 80\%$

Laminate 4 (L4):

Volume Fraction Glass Fiber V_f:

$V_f = [\rho_m \cdot w_f/(\rho_m \cdot w_f + \rho_f \cdot w_m)]$

$V_{gf} = (9.9 \times 7.29) / (9.9 \times 7.29) + (17.5 \times 14.51)$

$V_f = 0.221$

$V_f = 22.10\%$

Volume of Matrix Fraction V_m:

$V_m = [1 - V_f]$

$V_m = [1 - 0.221]$

$V_m = 0.779$

$V_m = 77.90\%$

Laminate 5 (L5):

Volume Fraction Glass Fiber V_f:

$V_f = [\rho_m \cdot w_f/(\rho_m \cdot w_f + \rho_f \cdot w_m)]$

$V_{gf} = (9.9 \times 6.05) / (9.9 \times 6.05) + (15 \times 17.92)$

$V_f = 0.182$

$V_f = 18.20\%$

Volume of Matrix Fraction V_m:

$V_m = [1 - V_f]$

$V_m = [1 - 0.182]$

$V_m = 0.818$

$V_m = 81.80\%$

Laminate 6 (L6):

Volume Fraction Glass Fiber V_f:

$V_f = [\rho_m \cdot w_f/(\rho_m \cdot w_f + \rho_f \cdot w_m)]$

$V_{gf} = (9.9 \times 7.91) / (9.9 \times 7.91) + (18.8 \times 12.80)$

$V_f = 0.246$

$V_f = 24.60\%$

Volume of Matrix Fraction V_m:

$V_m = [1 - V_f]$

$V_m = [1 - 0.246]$

$V_m = 0.754$

$V_m = 75.40\%$

AUTHOR'S PROFILE



Mustafa Bin Nordin obtained Bachelor of Mechanical Engineering (Manufacturing) (Hons.) on 1st October 2019 from University Teknologi MARA Pulau Pinang. Possess experience as a Process Engineer at UWC Berhad, Pulau Pinang for approximately five years (2019–2024), and currently working at Dou Yee Technologies, Singapore since 2025.

LIST OF PUBLICATION

Nordin, M., Aziz, M. R., & Othman, R. (2025). Experimental and simulation study of tensile strength of banana and glass fibres and their hybrid epoxy composites. *Journal of Applied Engineering Design and Simulation, 5*(2), 139–157. https://doi.org/10.24191/jaeds.v5i2.134